

**MARINE OIL SPILL SIMULATION AND UNCERTAINTY ANALYSIS – A
CASE STUDY IN THE NEWFOUNDLAND OFFSHORE AREA**

By

©Xiao Zheng

A thesis submitted to the School of Graduate Studies
in partial fulfillment of the requirements for the
Degree of Master of Engineering

**Faculty of Engineering and Applied Science
Memorial University of Newfoundland**

October, 2017

Newfoundland and Labrador

St. John's

Canada

ABSTRACT

Oil spills have been regarded as one of the major contributors to marine pollution. With the rapidly changing environmental conditions and the diverse uncertainties in the data associated with the observation or meteorological and oceanographic data, the simulation of an oil spill is challenging to be accurate and reliable enough for supporting response management. Furthermore, with the different assumptions, structures and translations of various simulation models, results could significantly vary even with the same inputs. The objectives of this research are therefore 1) to compare three widely used models for offshore oil spill simulation and evaluate their capabilities under harsh environmental conditions; and 2) to develop a Design of Experiment (DOE) based approach for analyzing uncertainties associated with the spill modeling input and parameters to help improve offshore oil spill simulation.

In this research, the Terra Nova oil spill occurred on November 21, 2004, the largest oil spill in offshore Newfoundland, was chosen as a case study. The models, namely GNOME/ADIOS2 and OSCAR, were employed for the simulation of fate and transport of the spilled oil. During the simulation, ocean currents data from the Hybrid Coordinate Ocean Model (HYCOM) and surface wind data measured by the National Climate Data Center (NCDC) were used. The simulation results indicated that 43.7% of the spilled oil evaporated or dispersed in the first two days. With the model of OSCAR, 87.4% of the total spilled oil was evaporated or dispersed, while 10.8% was biodegraded. Only 1.6% of

oil remained on the sea surface after six days, which agreed well with the historical data. The results from GNOME showed a more reasonable match with the observations from the RADARSAT-1 satellite images regarding the spill plume, shape and location as compared to those from OSCAR. But on the other hand, OSCAR showed better performance in simulating weathering process.

To facilitate a better understanding of the oil fate and transport, and to improve simulation performance, a DOE aided method was developed for sensitivity analysis, parameter calibration and interaction analysis of key factors during spill simulation. The interactions between wind speed and direction, and the currents have been analyzed and the effects of their interactions have been studied. In this case study, the key factors “Windage” and “Wind speed scale” both had the negative effects on the modeling response, but their interaction showed positive effects. The “Along current uncertainty” and “Diffusion coefficient” caused the negative and positive effects, respectively, but leading to the positive effects by their interaction. The results indicated that when adjusting the primary factors in order to optimize the response, interactions between factors may lead an opposite way and missed the optimal solution. The validation through the case study showed consistency with high values of R^2 (e.g., 0.93 and 0.95 for deviations of coverage and distance between the observed and simulated spills respectively). The results indicated that this DOE aided parameterization method could potentially be a useful tool for the evaluation of the contribution of multiple parameters and be applied as a new calibration method for other oil spill simulation models.

ACKNOWLEDGMENTS

First and foremost, I would like to express my sincere thanks to Dr. Bing Chen for his excellent supervision and guidance during my research. Without his support and the confidence, this thesis would not have been possible. I am also very grateful to Dr. Baiyu Zhang for her help.

I also gratefully acknowledge the Faculty of Engineering and Applied Science at the Memorial University of Newfoundland (MUN) for the financial support.

I would also like to express my thanks to Dr. Hongjing Wu, Dr. Liang jing, Dr. Pu Li, Jisi Zheng, Zelin Li, Fuqiang Fan, Bo Liu, Qinhong Cai and Zhiwen Zhu for their help in the course of my research program. Also, I would like to thank my roommates Yongbin Geng, Jianxiang Xing, Zhaopeng Qu and Rufen Yu for their support.

Last but by no means least, I would like to offer my deepest appreciation to my mother Hongping Zhang, my father Dean Zheng for their love and encouragement.

TABLE OF CONTENTS

ABSTRACT.....	i
ACKNOWLEDGMENTS	iii
TABLE OF CONTENTS	iv
LIST OF TABLES	vii
LIST OF FIGURES	viii
LIST OF ABBREVIATIONS AND SYMBOLS	xii
CHAPTER 1: INTRODUCTION.....	1
1.1 Background.....	2
1.2 Challenges in marine oil spill simulation.....	4
1.3 Objectives	6
1.4 Structure of the thesis.....	7
CHAPTER 2: LITERATURE REVIEW	8
2.1 Marine Oil spills	9
2.1.1 <i>Background</i>	9
2.1.2 <i>Fate and transport of spilled oil</i>	11
2.1.3 <i>Marine oil spills in Newfoundland and Labrador</i>	18
2.2 Marine oil spill simulation	20
2.2.1 <i>Modeling inputs and preparation</i>	20
2.2.2 <i>Marine oil spill models</i>	24
2.3 Uncertainty analysis.....	30
2.4 Summary	33

**CHAPTER 3: SIMULATION OF MARINE OIL SPILLS AND MODELS
COMPARISON BY A CASE STUDY IN THE NEWFOUNDLAND OFFSHORE**

AREA	34
3.1 Introduction.....	35
3.2 Terra Nova oil spill	37
3.3 Modeling approach	41
3.3.1 <i>GNOME and ADIOS2</i>	41
3.3.2 <i>OSCAR</i>	41
3.3.3 <i>Comparisons of two models</i>	42
3.4 Data acquisition	45
3.4.1 <i>Wind and currents</i>	45
3.4.2 <i>SAR images</i>	52
3.5 Modeling settings.....	54
3.6 Results and discussion	54
3.7 Summary	61
CHAPTER 4: A DOE AIDED UNCERTAINTY ANALYSIS METHOD AND APPLICATION IN MARINE OIL SPILL MODELING.....	63
4.1 Introduction.....	64
4.2 A DOE aided uncertainty analysis method.....	66
4.3 Case study	70
4.3.1 <i>Parameter analysis</i>	70
4.3.2 <i>Response selection</i>	73
4.4 Results and discussion	77

4.4.1 <i>Modeling sensitivity</i>	77
4.4.2 <i>Calibration and validation</i>	110
4.5 Summary	117
CHAPTER 5: CONCLUSION AND RECOMMENDATIONS	120
5.1 Summary	121
5.2 Research contributions.....	124
5.3 Publications.....	125
5.4 Recommendations.....	127
References	128

LIST OF TABLES

Table 1	Key parameters and their upper and lower bound values	72
Table 2	ANOVA of minimum runs of design resolution V for response R1	78
Table 3	ANOVA of minimum runs of design resolution V for response R2	79
Table 4	ANOVA of minimum runs of design resolution V for response R3	80
Table 5	Coefficient list of the significant terms for response R1	112
Table 6	Coefficient list of the significant terms for response R2	113
Table 7	Coefficient list of the significant terms for response R3	114

LIST OF FIGURES

Figure 1 Diagram of basic oil in water processes related to spill trajectory modelling (after Drozdowski et al., 2011).	16
Figure 2 Study area: location of Terra Nova FPSO at Grand Banks, NL, Canada.....	40
Figure 3 Ocean currents derived from the HYCOM at 2004-11-21	47
Figure 4 (a) Wind field at 2004-11-21 06:00 (b) Wind field at 2004-11-23 00:00 (c) Wind field at 2004-11-25 12:00 (d)Wind field at 2004-11-26 18:00	51
Figure 5 Satellite images RADARSAT-1 image at 9:21 UTC on November 23 th , 2004 (derived from Environment Canada)	53
Figure 6 A combined figure with GNOME (blue), OSCAR (red), and Black solid lines represent the oil slick covered area by observation	55
Figure 7 Result from the GNOME compared with the SAR image	56
Figure 8 Result of oil weathering by AIDOS2 simulation	58
Figure 9 Result of oil weathering by OSCAR	59
Figure 10 The overall framework of the application of DOE aided method.....	69
Figure 11 A sample image from the GNOME simulation showing oil particles distribution in the case study.....	75
Figure 12 Half-normal probability plot for response R1	81
Figure 13 Normal probability plot for response R1	82
Figure 14 Diagnostic plots for assumption of ANOVA: normal probability of residuals for response R1	83
Figure 15 Diagnostic plots for assumption of ANOVA: residuals vs. predicted for	

response R1	84
Figure 16 Diagnostic plots for assumption of ANOVA: residuals vs. run for response R1	85
Figure 17 Diagnostic plots for assumption of ANOVA: predicted vs. actual for response R1	86
Figure 18 Half-normal probability plot for response R2	87
Figure 19 Normal probability plot for response R2.....	88
Figure 20 Diagnostic plots for assumption of ANOVA: normal probability of residuals for response R2	89
Figure 21 Diagnostic plots for assumption of ANOVA: residuals vs. predicted for response R2.....	90
Figure 22 Diagnostic plots for assumption of ANOVA: residuals vs. run for response R2	91
Figure 23 Diagnostic plots for assumption of ANOVA: actual vs. predicted for response R2.....	92
Figure 24 Diagnostic plots for assumption of ANOVA: residuals vs. windage for response R2.....	93
Figure 25 Diagnostic plots for assumption of ANOVA: normal probability of residuals for response R2	94
Figure 26 Half-normal probability plot for response R3	95
Figure 27 Normal probability plot for response R3.....	96
Figure 28 Diagnostic plots for assumption of ANOVA: residuals vs. predicted for response R3.....	97

Figure 29 Diagnostic plots for assumption of ANOVA: residuals vs. run for response R3	98
Figure 30 Diagnostic plots for assumption of ANOVA: actual vs. predicted for response R3	99
Figure 31 Diagnostic plots for assumption of ANOVA: residuals vs. windage for response R3	100
Figure 32 Three dimensional surface graph of interaction between factors B and F for response R1	103
Figure 33 Three dimensional surface graph of interaction between factors A and D for response R1	104
Figure 34 Three dimensional surface graph of interaction between factors E and D for response R1	105
Figure 35 Three dimensional surface graph of interaction between factors E and F for response R2	106
Figure 36 Three dimensional surface graph of interaction between factors E and D for response R3	107
Figure 37 three dimensional surface graph of interaction between factors B and F for response R3	108
Figure 38 Three dimensional surface graph of interaction between factors A and D for response R3	109

LIST OF ABBREVIATIONS AND SYMBOLS

τ	evaporative exposure parameter
θ	evaporative exposure
σ^2	the variance of the spilled oil locations
Δd	the range of droplet size.
(A)	windage
(B)	along current uncertainty
(C)	cross current uncertainty
(D)	wind speed scale
(E)	wind angle scale
(F)	diffusion coefficient
a	the spilled area
A	the area of slick
ADIOS	automated data inquiry for oil spills
ANOVA	analysis of variance
A_s	the oil slick area
A_{sim}	total covered cells of the simulated oil slick
ASA	applied science associates
C	the concentration of a material
c_{disp}	experimentally determined parameter
COZOIL	coastal zone oil spill model
d_0	the droplet size

D	the aforementioned diffusion coefficient
D_e	the dissipation of wave energy per unit surface area
D_0	the number of particles overlapped with the satellite image
DOE	design of experiment
f_{bw}	the fraction of breaking waves per wave period per unit
f_s	the surface fraction covered by oil
FPSO	floating production, storage and offloading
GIS	geographic information system
GNOME	general NOAA operational modeling environment
GODAE	global ocean data assimilation
h	the initial film thickness
HYCOM	hybrid coordinate ocean model
k	the mass transfer coefficient
K	the surface mass transfer coefficient
K_1	the dissolution mass transfer coefficient
MOTHY	French operational oil spill drift forecast system
NCDC	national climate data center
NL	Newfoundland and Labrador
NOPP	national ocean partnership program
NRC	national research council
OFAT	one-factor-at-a-time
OGCM	ocean general circulation model
OILMAP	oil spill model and response system

OSCAR	oil spill contingency and response
OSIS	oil spill identification system
OWM	oil weathering model
Q	volume of entrainment
S	the solubility in water and
S_0	the solubility of fresh oil
S_a	salinity
S_L	the sediment load
SAR	synthetic aperture radar
SCEM	complex evolution metropolis
t_1	time
T	the environmental temperature
T_0	initial boiling point
T_G	the slope of the boiling temperature curve
V_0	the initial volume of the spilled oil
V_{disp}	the volume of oil entrained per unit volume of water
V_m	the volume of spilled oil
V_{mean}	mean velocity
V_t	the local turbulent diffusion
Y	the fraction of water in oil
Y_{max}	the final fraction of water in oil

CHAPTER 1: INTRODUCTION

1.1 Background

An oil spill is often referred to an accidental release of liquid petroleum hydrocarbons into the environment. Spills may occur on land, in ocean or coaster waters. Due to natural reasons such as earthquakes and hurricane, or anthropogenic problems as equipment malfunctions and operational mistakes, oil spills can happen during oil and gas exploration, drilling, transportation, storage and utilization processes.

Many large-scale oil spills in the history resulted in the catastrophic impacts. In 1989, Exxon Valdez tanker hit a reef off the Alaskan coast, and released 11 million gallons of crude into the ocean. Oil washed onto 1,300 miles of coastline, resulting in carcasses of more than 250,000 birds and 2,800 sea otters (Piatt et al., 1990). In 1991, the Gulf War oil spill occurred in Kuwait was the largest oil spills in history, between 5 and 10 million barrels of oil poured into the Persian Gulf (Ross, 1991). In 2010, the Gulf of Mexico oil spill was officially the largest accidental spill in American history. It began when an oil well a mile below the surface of the Gulf blew out, causing an explosion on BP's Deepwater Horizon rig. Oil flowed possibly at a rate as high as 2.5 million gallons a day until capping the well. An estimated 206 million gallons of oil spilled and 572 miles of Gulf shoreline was oiled (Azwell et al., 2011). Totally, 1.82 million gallons of dispersant were used during this accident (Sumaila et al., 2012; Ruiz, 2013).

To deal with the potential oil spill accidents, accurate real-time observations and monitoring are critical considerations to the marine security agencies with data of climatology, meteorology, wind, currents and spilled oil (Marta-Almeida et al., 2013).

Remote sensing technologies, such as infrared sensors, visible sensors, microwave, laser fluorosensors, and ultraviolet sensors can be used as efficient tools to detect surface spills (Jha et al., 2008; Ferraro et al., 2009). Among the satellite sensors, Synthetic Aperture Radar (SAR) has been widely applied to provide precious synoptic imagery of the position, size, and shape of oil spills due to its considerable wide coverage and imaging capability under various circumstances (Singha et al., 2013; Li et al., 2014a). Many efforts have been undertaken to obtain statistical information on oil pollution from SAR images (Bern et al., 1993; Brekke et al., 2005; Cheng et al., 2011; Leifer et al., 2012; Li et al., 2013).

In addition to oil spill monitoring by satellite imagery, oil transport forecast models have been developed and used during the past 20 years (Reed et al., 1999). The purpose of oil spill modeling is to predict the movement of oil slicks through the data of ocean currents, winds, tides and other parameters (Drozdowski et al., 2011). Oil drifting models have frequently been utilized to predict oil slick and its fate (Huang, 1983; ASCE, 1996). Nowadays, some state-of-the-art oil drift models include OSCAR (Reed et al., 1995a), OILMAP (Howlett et al., 1993), GULFSPILL (Al-Rabeh et al., 2000), ADIOS (Lehr et al., 2002), , MOHID (Carracedo et al., 2006) , OD3D (Hackett et al., 2009), the Seatrack Web SMHI model (Ambjörn, 2006), MEDSLIK (Lardner et al., 1998; De Dominicis et al., 2013), GNOME (Beegle-Krause, 2001) and OILTRANS (Berry et al., 2012). These models are usually driven by a time series of ocean currents, ocean surface wind vectors, the temperature in sea depths, etc. In operational practice, the models can be run in near-real time for the prediction of oil spill trajectories after the oil spill data derives from SAR images or aircraft. The results of simulation could provide crucial, consultative advice to

the emergency response authorities to effectively predict or mitigate the negative impacts on the marine environment.

1.2 Challenges in marine oil spill simulation

The offshore oil and gas industry in Newfoundland and Labrador (NL) has maintained rapid growth during the past decade due to the energy demand and the new exploration of offshore oil fields as well as the technological advances in oil drilling and extraction even in deep waters. Growing association between offshore oil and gas development and economic growth resulted in the increase of maritime transit and storage activities, which poses increasing environmental risks and especially possibility of oil-related accidents. In offshore Newfoundland, more than 2700 barrels oil has been released into the ocean since 1997 due to 340 spill accidents (Li et al., 2014b). Development and implementation of a regional marine spill model for oil related accidental response is of great value but a significant challenge particularly in harsh environment prevailing in NL (Li et al., 2014a).

Simulation models are useful tools in supporting decision making on oil spill preparedness and response. However, The success of their application depends not only on how good weathering and trajectory formulations are chosen in the model, and also on how accurate and reliable the inputs can be provided by the models or observation (Sebastiao and Soares, 2006). Due to the errors in the wind, wave and currents data from the atmospheric and oceanographic modeling or monitoring which may affect the accuracy of oil spill simulation (Edwards et al., 2006; Price et al., 2006), parameter uncertainties should be

considered carefully when applying the oil spill models to the real situations. Significant differences between the simulated and actual buoy observations have been reported in many past spill events (Abascal et al., 2009; Kim et al., 2014). Therefore, parameterization and uncertainty and sensitivity analysis are essential to minimize the discrepancy between simulated and observed data and improve the accuracy and confidence of the oil spill modeling results.

Traditional sensitivity analysis methods adjust one parameter at a time while keeping other parameters fixed. The applications have been found in many previous studies conducted on various models (Lenhart et al., 2002; Holvoet et al., 2005; Jing and Chen, 2011). However, the limitation is the incapability of revealing the interactions between parameters. The potentially significant variables might be ignored (Saltelli, 1999; Montgomery, 2008; Peeters et al., 2014). As well known in the previous studies, there exists a close interdependence of oil spill weathering processes (Reed et al., 1999). Due to the incapability of revealing the interactions between parameters, traditional One-factor- at-a-time (OFAT) method could ignore the potentially significant variables and their interactive impacts. Therefore, a method to find the multiple optimal values of the parameters to minimize the differences between numerical and actual trajectories is needed.

To address this issue, design of experiment (DOE) aided method provides a parameterization option. DOE is a widely used statistical methodology, which can analysis the interactions between parameters and the corresponding responses (Czitrom, 1999; Park, 2007; Veličković et al., 2013; Sarikaya and Güllü, 2015). DOE was originally developed

to determine the relationship between factors affecting a process and guide the setup for physical experiments. In recent studies (Wu et al., 2012), DOE was used to conduct sensitivity analysis and parameterization for a hydrological model SLURP. With the optimization of the predicted regression equation, a greater goodness-of-fit value compared to the one achieved by the automatic calibration function was produced.

Though the effectiveness of parameterization and interaction analysis in the numerical models has been proven. DOE method has rarely been used in oil spill simulation models, in which uncertainties commonly exist and knowledge concerning interactions between each parameter is inadequate.

1.3 Objectives

The goals of this research are to find a better way to simulate oil spills with the rapidly changing weather conditions in the harsh environments given the varied capabilities of different simulation models, and to minimize the effects of the errors in the input data and the uncertainties with the modeling parameters. The key tasks of this research are 1) to apply three widely used models for offshore oil spill simulation and evaluate their capabilities under harsh environmental conditions; and 2) to develop and test a DOE based approach for analyzing uncertainties associated with the input and parameters during offshore oil spill simulation.

1.4 Structure of the thesis

The aims of this research are to facilitate a better understanding of the oil fate and transport, and to improve simulation performance with a DOE aided method for sensitivity analysis, parameter calibration and interaction analysis of key factors during spill simulation.

Chapter 2 provides a comprehensive review of the background of marine oil spills and marine oil spill simulation.

Chapter 3 presents the testing and comparison of three oil spill models, GNOME/ADIOS2 and OSCAR through a real case study.

Chapter 4 describes the DOE aided method for oil spill model calibration, sensitivity analysis, and interaction analysis along with a case demonstration.

Chapter 5 summarizes the achievements of the research and provides recommendations for the future work.

CHAPTER 2: LITERATURE REVIEW

2.1 Marine Oil spills

2.1.1 Background

An oil spill is defined as a discrete event in which oil is discharged caused by human errors, by accident, or with purposeful activities. Oil is defined as a petroleum-derived substance as defined in MARPOL Annex I, excluding liquefied natural or petroleum gas (Etkin, 2001). A significant amount of oil is spilled into the sea from operational discharge, collision, pipeline-breaks, blow-outs and human error (Tri et al., 2013). In the past decades, oil spills lead to a growing concern since they can cause long-term damage to the marine, coastal and estuarine ecosystem, beaches, coastal wetlands, fisheries and tourism, and threaten the health of humankind in the affected communities (Liu and Sheng, 2014).

Historical data shows that almost 60% of the total amount of spilled oil result from the large-scale accidents which account for 0.1% of the spilling incidents (Fingas, 2010). From 1978 to 1995, more than 4100 major oil spills had been recorded (Etkin and Welch, 1997). In all the spill events, only 5% of spills released more than 10,000 gallons which represent more than 90% of the total spilled amount (Etkin, 2001). Since the mid1980s, more than 60% of all large-scale (greater than 700 tons) oil spills in the past 40 years have occurred with the steadily increased seaborne oil transportation (Berry et al., 2012). Oil tankers and collisions are the leading causes of large oil spills which accounting for about two third of the total during 1970–2010 (Kim et al., 2014). Until the 1990s when large pipeline and facility spills occurred, tanker spills dominated the oil spill picture of 74 % world widely (Etkin, 2001). In the last two decades, close to half of the oil pollution in the oceans are

fuels and 29% are crude oil (Brekke and Solberg, 2005). Although the number of large oil spills has been decreasing, it is still a major problem for marine environmental conservation and sustainability.

Although the sources of oil input into the sea are diverse, OCEAN National Research Council (NRC) of Canada categorized them into four groups: natural seeps, petroleum extraction, petroleum transportation, and petroleum consumption (Board and Board, 2003). And based on some studies, an estimate of more than 1,300,000 metric tons (380,000,000 gallons) of oil entered the sea annually (Kvenvolden and Cooper, 2003; Council, 2003).

Large-scale oil spills happened in the history worldwide, and some of them had resulted in catastrophic impacts.

In 1989, Exxon Valdez tanker hit Bligh Reef in Prince William Sound off the Alaskan coast, dumping 11 million gallons of crude into the ocean. This incident was the largest tanker oil spill in the U.S. history at that time. Oil washed onto 1,300 miles of coastline, resulting in carcasses of more than 250,000 birds and 2,800 sea otters (Piatt et al., 1990).

Large-scale oil spill continued to occur, like the Torrey Canyon oil spill (36 million gallons, 1967 in UK), the Sea Star oil spill (35.3 million gallons, 1972 in Gulf of Oman), the Ekofisk blowout (1977 in Norway), Amoco Cadiz oil spill (69 million gallons, 1978 in France), Atlantic Empress oil spill (90 million gallons, 1979 in Trinidad and Tobago), Castillo de

Bellver oil spill (79 million gallons, 1983 in South Africa), and Gulf War oil spill (5-10 million barrels, 1991 in Arabian Gulf).

Particularly in 2010, the Deepwater Horizon oil spill (i.e., also known as the BP oil spill) (Bly, 2011) that occurred in the Gulf of Mexico. About 4.9 million barrels (approximately 486,000 tons) of crude oil (Ramseur, 2010) was released at a water depth of 1520 m (McNutt et al., 2011) resulting in impacts that can last for several decades. The spill is officially the largest accidental spill in America. It began when an oil well a mile below the surface of the Gulf blew out, causing an explosion on BP's Deepwater Horizon rig. Oil flowed possibly at a rate as high as 2.5 million gallons a day until the well was capped. An estimated pollution of 9900 km² of water surface (Wei et al., 2015) and 572 miles of Gulf shoreline was oiled. Totally, 1.82 million gallons of dispersant was used during this accident (Ruiz, 2013, Sumaila et al., 2012). The injection of chemical dispersants was successful in reducing the amount of oil that reached the surface, but it resulted in a large volume of oil drifting at depth (Beegle-Krause et al., 2006).

2.1.2 Fate and transport of spilled oil

Fate and transport of spilled oil are a series of processes which take place after an oil spill, including spreading, evaporation, emulsification, dispersion, advection, photo-oxidation, biodegradation, dissolution, and sedimentation (Reed et al., 1999; Spaulding, 1988; Yang et al., 2015). To understand and quantify the physical and chemical processes during oil spill, researchers have conducted many studies (Fay, 1971; Lehr et al., 1984; Mackay et al.,

1980; Stiver and Mackay, 1984; Delvigne, 1989; Berry et al., 2012; Goeury et al., 2014). Both experimental and modeling studies proved the oceanic and atmospheric physical variables and chemical and physical processes could affect the oil fate and transport significantly. (Reed et al., 1999; Hackett et al., 2006; Heydariha and Ghiassi, 2010; Liu et al., 2011; Marta-Almeida et al., 2013; Goeury et al., 2014).

Oil spreading is the process of the spilled volume of oil, under the influence of viscous, gravitational, buoyancy and, surface tension forces, spreading into a thin slick to cover a large area (Drozdowski et al., 2011). The process of oil spreading in still water is fairly well understood (Økland Gjøsteen et al., 2003). Several models of spreading have been developed over the last decades (Blokker, 1964; Fay, 1969; Hoult, 1972; Fannelop and Waldman, 1972; Di Pietro and Cox, 1979; Mackay et al., 1980; Aamo et al., 1997; Al-Rabeh et al., 2000; Beegle et al., 2001; Berry et al., 2012; De Dominicis et al., 2013). There are two dimensions to spreading: thickness of the oil while it spreads and the extension of the oil contaminated area (Venkatesh et al., 1990). Spreading of the oil slick is an important process in the early stages of oil slick transformation and also affected by the weathering processes. A general equation of the rate of change of area of spreading oil is given as eq. (2-1), which is developed by Mackey et al. (1980).

$$\frac{dA}{dt_1} = KA^{1/3}\{V_m/A\}^{4/3} \quad (2-1)$$

Where A is the area of slick, V_m is the volume of spilled oil, K is a constant and t_1 is the time.

Advection is the physical process involving the drifting of the surface oil slick and the subsurface oil which governing the location of oil (Økland Gjøsteen et al., 2003). The advection of surface oil is affected by surface current and wind drag on oil, considering that most oils are initially buoyant and float on the sea surface (Mackay et al., 1980). The advection of suspended oil is the movement of oil droplets in the water column affected by the water current. Advection velocity, V , can be calculated by the mean wind speed and currents, and local turbulent diffusion (Davidson et al., 2006), as shown in eq. (2-2).

$$V = V_m + V_t \quad (2-2)$$

Where V_{mean} is the mean velocity, and V_t is the local turbulent diffusion.

Evaporation is one of the most important characteristic changes in oil spilling. More than three fourth of light crudes and 40% of medium crudes can evaporate in several days after a spill. And only 10% of heavy or residual oils of its initial mass will be lost in the first few days due to evaporation (Aamo et al., 1997). Because of its significant impact on the spill mass balance, many spill models incorporate evaporation as a critical component. The rate of evaporation will differ drastically at where the spill accidents occur with the various sunshine periods and temperatures in a year. The remained oil at the surface will be less with surface slick exposing to more sunlight (Fingas et al., 2006). The volume fraction of evaporated oil is given in eq. (2-3) (Stiver and Mackey, 1984):

$$F_v = \ln \left[1 + B \left(\frac{T_G}{T} \right) \theta \exp \left(A - \frac{BT_0}{T} \right) \right] \left(\frac{T}{BT_G} \right) \quad (2-3)$$

$$\theta = \frac{kat}{V_0} \quad (2-4)$$

Where A and B are constants from the experimental data. T_0 is the initial boiling point. T_G is the slope of the boiling temperature curve. T is the environmental temperature. θ is the

evaporative exposure, where k is the mass transfer coefficient, V_0 is the initial volume of the spilled oil, a is the spilled area, t is the spilled time.

Dissolution is the process that separates molecules in the oil components going into the water phase. Stable oil can be dispersed and come into being smaller oil droplets and/or micelles (Berry et al., 2012). Usually, less than one percent of spilled oil on the water surface will be dissolved. Some numerical models do not consider dissolution because of the small effect on the mass balance. However, the dissolution can be of great importance considering the most soluble oil components are usually the most toxic, which could lead to serious effects on biological systems even with low concentrations. The rate of dissolution was calculated by Cohen et al. (1980) with eq. (2-5).

$$\frac{d_{Diss}}{dt} = K_1 f_s A_s S = S_0 e^{at} \quad (2-5)$$

Where K_1 is the dissolution mass transfer coefficient, f_s is the surface fraction covered by oil, A_s is the oil slick area, S is the solubility in water and S_0 is the solubility of fresh oil, a is a constant and t is the time after spill.

Dispersion is defined as the breakup of the oil slick on the surface into oil droplets, then spread and diffusion in the water column. The droplet sizes, droplet buoyancy, and the turbulence in the water are of particular interest. With the exposure to wind and waves, oil on the surface could disperse into oil droplets. Big size of droplets may disperse into the water column. Smaller droplets are unstable and could resurface to the water surface (Stiver and Mackay, 1984; Delvigne, 1989). The dispersion model proposed by Delvigne and

Sweeney (1988) has been used in the ADIOS, OSCAR and OILMAP models. It is shown in eq. (2-6).

$$Q = C_0 D_e^{0.57} d^{0.7} \Delta d d_0 \quad (2-6)$$

Where Q is the entrained mass of oil droplets, C_0 is a constant, D_e is the dissipating breaking wave energy per unit surface area, d_0 is the droplet size and Δd is the range of droplet size.

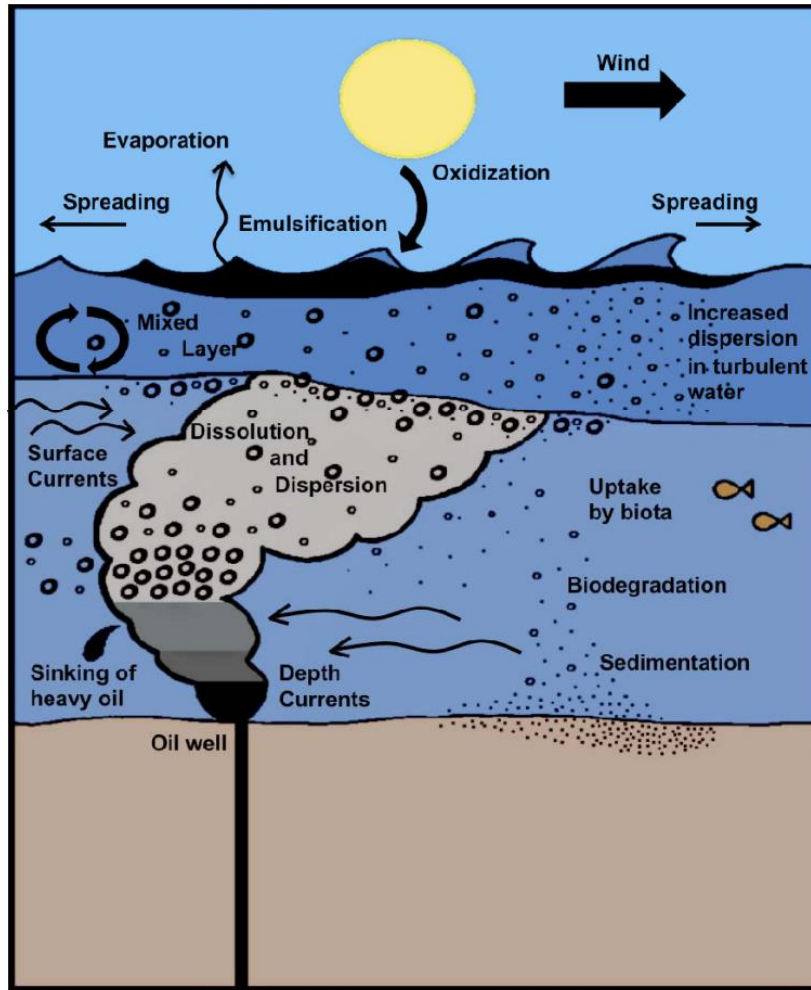


Figure 1 Diagram of basic oil in water processes related to spill trajectory modelling (after Drozdowski et al., 2011).

An oil emulsion is a dispersion of water droplets in oil. Based on water content and rheological measurements, oil emulsions are categorized into four distinct water-in-oil types: stable, meso-stable, entrained and unstable (Sunil et al., 2005). Because each type exhibits unique physical properties, when water-in-oil emulsions form, the physical properties of oil spills change significantly (Fingas, 2009). Mackey et al. (1980) developed eq. (2-7) to model the process of emulsification. This equation has been used in ADIOS and SINTEF.

$$\frac{dY}{dt} = KU^2 \left(1 - \frac{Y}{Y_{max}}\right) \quad (2-7)$$

Where K is a constant, Y is the fraction of water in oil and Y_{max} is the final fraction.

Sedimentation is the adhesion of oil to sediments and never back into water column (Anon, 2003). Some studies has been concentrated on the interactions between clay and oil stranded on the coastline. But it was found that oil attached to fine particles (clay) is more available for biodegradation (Anon, 2003). The rate of oil loss by sedimentation process is shown in eq. (2-8).

$$\frac{dA_d}{dt} = 1.4 * 10^{-12} S_L (1 - 0.023 S_a) \quad (2-8)$$

where S_L is the sediment load, S_a is the salinity (Korotenko et al., 2000).

Beside evaporation and dissolution, the dispersion is one of the most critical processes removing oil from the water surface.

2.1.3 Marine oil spills in Newfoundland and Labrador

In the offshore NL, the three active offshore oil fields, Hibernia, Terra Nova, and White Rose, produce about 0.27 million barrels of crude oil per day or 10% of Canada's total crude oil production (C-NLOPB, 2012). All three of these production operations locate at the Grand Banks. Hibernia produced more than 86 million barrels of oil in 2010, as the world's largest offshore oil platform. It is located 170 nautical miles east of St. John's, Newfoundland. Hibernia became operational in the 1997 and had produced 61% of all oil on the Grand Banks (Turner et al., 2010). The Terra Nova field is located 21 nautical miles southeast of Hibernia and operated from 2002. White Rose oil field is located 30 miles away from the Hibernia and operated from 2005. Until 2009, more than one billion barrels of oil has been produced from all three fields (Turner et al., 2010).

Oil spills in the NL offshore happened more often than environmental assessments predicted. In the typical harsh environment of offshore Newfoundland, 340 spills with more than 2,700 barrels of oil have been spilled into the ocean since 1997 (Li et al., 2014b). About 1,048 accidents were recorded from 1980 to 2005 in the South Coast of Newfoundland, Canada. The oil industry in Newfoundland maintained rapid growth due to the exploration of offshore oil fields, which increased environmental risks and brought a higher possibility of oil-related accidents.

A tragedy happened on the offshore drilling platforms of the Grand Banks region in 1982. 84 people were killed on a drill platform which was built for unrestricted open ocean

operations and designed to withstand 100-knot winds and 110-foot waves. In the harsh environment of the Grand Banks region, accidents could cause a significant oil spill and possibly a loss of life (McGrath, 2014).

In November 21st, 2004, two mechanical failures in produced water separation process caused more than 1,000 barrels of oil released into ocean. This accident happened at Terra Nova floating production, storage and offloading vessel (FPSO) resulted in more than 10,000 sea birds killing directly by the 793 km² oil slick coverage (Wilhelm et al., 2007). Based on the record of Petrocanada, two vessels were on the site and ready to deploy booms and skimmers on 22th. But cleanup operation was not started until 23rd because of terrible weather condition. (Martin, 2004). Large-scale oil spill has not been happened in offshore NL, but the booming oil industry could raise the risk of accident. Harsh environment in the NL might lead to a catastrophic damage to the marine ecosystem. The case study of Terra Nova can be helpful in prevention and response planning of oil spills in this area.

This region also happens to be one of the most dangerous shipping areas in the world (McGrath, 2014). The cold Labrador Current, originating off of the west coast of Greenland flowing north then back south, interacts with the warm Gulf Stream which flows north along the east shore of the United States, creating vast regions of fog with limited visibility. This limited visibility is a significant danger to shipping and a limitation to visual aerial reconnaissance in the event of an emergency at sea. With the opening of the Arctic Ocean and the increase in the shipping and offshore drilling in this area, a comprehensive plan must be developed before an internationally significant oil spill occurs.

2.2 Marine oil spill simulation

2.2.1 Modeling inputs and preparation

No matter where the spill occurs, we mainly use the spill trajectory models for the prediction of where the oil is most likely to go, based on information about the ocean currents, winds, and other environmental variables.

Ocean currents can be varied in time and space. Thus, information at one location or one instant in time is insufficient for tracking an oil spill in an extended period of time. For the accuracy of oil trajectory models, numerical ocean models that resolve the spatial and temporal variability of the ocean currents that have been validated against observations are required. Atmospheric conditions such as the wind, temperature, and precipitation, are necessary driving forces for ocean currents and oil behavior. The output from atmospheric models can provide wind data of nowcasts, forecasts for two to ten days or hindcasts that go back a few decades (Large and Yeager, 2004).

Unless the spill occurs in an area of stable mean or tidal currents, wind-induced drift is often the most important factor determining surface oil slick trajectories over timescales of a few days (Spaulding, 1988). Systematic measurements of drift currents below and of airflows above an air-water interface have been made under various wind conditions. The current near but not immediately below the water surface is found to follow a Kármán-Prandtl (logarithmic) velocity distribution. The current immediately below the water

surface varies linearly with depth. The transitions of the current boundary layer to various regimes appear to lag behind, or to occur at a higher wind velocity than, those of the airflow. The fraction of the wind stress supported by the wave drag seems to vary with the wind and wave conditions: a large fraction is obtained at low wind velocities with shorter waves and a small fraction is obtained at high wind velocities with longer waves. At the air-water interface, the wind-induced current is found to be proportional to the friction velocity of the wind. The Stokes mass transport, related to wave characteristics, is only a small component of the surface drift in laboratory tanks. However, in terms of the fraction of the wind velocity, the mass transport increases, while the wind drift decreases, as the fetch increases. The ratio between the total surface drift and the wind velocity decreases gradually as the fetch increases and approaches a constant value of about 3-5% at very long fetches. The currents are induced by the combination of wind stress, pressure gradients, density gradients, tidal forcing and wave induced (Stokes) drift.

Based on the past studies, oil at surface layer moves at a speed which is 2.5 to 4.4% of the wind speed (Spaulding, 1988; Reed et al., 1999) and at an angle of 0 to 25 degrees clockwise relative to the wind direction (Samuels et al., 1982; Spaulding, 1988). As a result of the underestimation of the surface current speeds, 1-3% of the wind speed is added to the trajectory model solution (Wang et al., 2007). The Hybrid Coordinate Ocean Model (HYCOM), is a generalized hybrid coordinate ocean model developed by the HYCOM Consortium, and have been used for supporting oil spill modeling. (Halliwell, 2004; Chassignet et al., 2006).

Remote sensing is a vulnerable tool for the observation of the distribution and fate of oil slicks on the ocean's surface (Kvenvolden and Cooper, 2003; Hu et al., 2009), and also plays a major role in oil spill trajectory monitoring. Remote sensing using airborne and space borne sensors is the most efficient technique for oil slick monitoring, oil slick movement forecasting, detection, identification and classification of oil covered regions as well as global scale (Nirchio et al., 2005; Migliaccio et al., 2007). Recently, a large number of airborne and space borne imagery have been acquired and analyzed for the 2007 Hebei Spirit oil spill in the Yellow Sea (Yim et al., 2012) and the aforementioned marine oil spill modeling and response, such as 2011 Deepwater Horizon oil spill (Leifer et al., 2012; Dietrich et al., 2012).

Among the satellite sensors, Synthetic Aperture Radar (SAR) can provide images during day and night and regardless of any weather conditions has been widely used to provide information about the location and size of oil spills (Migliaccio et al., 2012; Li et al., 2013). However, SAR images work best in limited wind regimes between 2 and 14 m/s (Brekke and Solberg, 2005), with best results for winds around 5–6 m/s. Low wind speeds below 2-3 m/s could produce false alarms with a high probability of oil slick look-alikes due to local wind variability, and at higher wind speeds, light oil is mixed and dispersed. Also, oil spill signatures appear distinguishable in SAR images only within a certain range of wind speeds between 3 and 10 m/s. Due to weathering and spreading processes, the thinner oil will be invisible (Brekke and Solberg, 2005; Solberg, 2012). At higher wind speeds only thick oil will be visible. The brightness of the image reflects of the microwave backscattering properties of the surface. Today, Two leading providers of satellite SAR

images for oil spill monitoring are RADARSAT-1 and ENVISAT (Brekke and Solberg, 2005; Migliaccio et al., 2012). RADARSAT-1 is Canada's first commercial Earth observation satellite. It utilized synthetic aperture radar (SAR) to obtain images of the Earth's surface to manage natural resources and monitor global climate change. As of March 2013, the satellite was declared non-operational and is no longer collecting data. Envisat ("Environmental Satellite") is a large inactive Earth-observing satellite which is still in orbit. Operated by the European Space Agency (ESA), it was the world's largest civilian Earth observation satellite.

The lifetime of an oil spill will depend on the type and amount of oil spilled, and weather conditions like sea temperature and wind and current conditions which affect the processes of evaporation, emulsification, and dispersion (Kotova and Espedal, 1998). Lighter components of oil will evaporate, and the rate of evaporation depends on oil type, thickness, wind speed, and sea temperature. Dispersion is a major factor in deciding the lifetime of an oil spill, and it is strongly dependent on the sea state. When monitoring an area on a daily basis, small spills of lighter oils are often not observed for several days, but larger oil spills are more persistent. During the Deepwater Horizon accident in the Gulf of Mexico, the oil was visible on satellite images for 70 days (Graber et al., 2006).

These types of observations could provide the input data for estimating the partitioning of the oil. In operational use, after the oil spill information is obtained from SAR images, trajectory models such as GNOME can be run in near-real time for the prediction of oil

spill trajectories. In this way, the simulation results can be used by the authorities to respond to decrease the pollution's impact on the marine environment within a short time.

2.2.2 Marine oil spill models

In the last three decades, the transport and fate processes of oil spills have been studied based on the trajectory method and mass balance approach, and various oil spill models have been developed (Mackay et al., 1980; Huang, 1983). Some detailed overview of oil spill models is given by Reed et al. (1999), Hackett et al. (2006) and Li et al. (2016). In general, commonly used operational oil spill models include GNOME, MOTHY, OSCAR, ADIOS, OILMAP and OSIS.

Six ocean models were used to predict oil spill trajectories in the Deepwater Horizon oil spill (Liu et al., 2011). Satellite-based observations were applied to reduce the errors in the trajectories simulation. Several oil spill models have been developed based on transport and weathering processes (Mackay et al., 1980; Huang, 1983). The Oil Weathering Model, OWM (Daling and Strøm, 1999) and the Oil Spill Contingency and Response model system, OSCAR (Aamo et al., 1997b) are used in simulation and prediction of oil spills, which have been tested extensively in laboratory and experimental field spills (Daling and Strøm, 1999; Daling et al., 2003).

Bergueiro López et al. (2007) used the EUROSPILL, OILMAP, GNOME and ADIOS models in simulating an oil spill at the Casablanca Platform (Tarragona, Spain) under a variety of environmental conditions (Bergueiro et al., 2007). OILBRICE oil spill spreading and drift model was developed by Environment Canada in the 1980's (El-Tahan and Warbanski, 1987) for the treatment of oil spilled in ice. Another spill model, Coastal Zone Oil Spill Model (COZOIL), was developed for near-shore interactions for use in Alaskan waters (Howlett and Jayko, 1998).

In general, there are two methods for modeling oil spills, the Eulerian, and the Lagrangian method. In classical field theory the Lagrangian specification of the field is a way of looking at fluid motion where the observer follows an individual fluid parcel as it moves through space and time. Plotting the position of an individual parcel through time gives the pathline of the parcel. This can be visualized as sitting in a boat and drifting down a river. The Eulerian specification of the flow field is a way of looking at fluid motion that focuses on specific locations in the space through which the fluid flows as time passes. This can be visualized by sitting on the bank of a river and watching the water pass the fixed location. The Lagrangian and Eulerian specifications of the flow field are sometimes loosely denoted as the Lagrangian and Eulerian frame of reference. However, in general both the Lagrangian and Eulerian specification of the flow field can be applied in any observer's frame of reference, and in any coordinate system used within the chosen frame of reference. The Eulerian approach treats the particle phase as a continuum while the Lagrangian method considers particles as a discrete phase and tracks the pathway of each particle (Maslo et al., 2014).

To avoid numerical diffusion which is often caused by the significant discrepancies in the Eulerian models, the majority of current oil spill models use the Lagrangian approach. Beside models based on the particle-tracking method (Coppini et al., 2011; De Dominicis et al., 2013), the smoothed particle hydrodynamics method has also been used (Violeau et al., 2007). However, with the increasing computer power and the implementation of the third order numerical schemes the use of Eulerian models is increasing again (Tkalich, 2006; Heydariha and Ghiassi, 2010).

From two-dimensional trajectory-type model to three-dimensional models (Cucco et al., 2012) including transport and weathering processes (Chao et al., 2003), accurate forecast of oil transport trajectories have resulted in the significant advancement during the last two decades (ASCE, 1996; Hackett et al. 2006; Li et al., 2016).

The Lagrangian models (Lonin, 1999; Zheng et al., 2003) represent the oil slick by a large set of hydrocarbon packets. Each packet is advected by the action of current and wind. However, to guarantee the calculation efficiency, the number of particles in these models must be restricted to limit the computational time. In Eulerian oil spill models (Tkalich et al., 2003; Papadimitrakis et al., 2006), the mass and momentum equations are solved for the oil slick. The main drawback of the Eulerian formulation is the problem of numerical dispersion, especially for small pollutant sources. Numerical dispersion is a difficulty with computer simulations of continua (such as fluids) wherein the simulated medium exhibits a higher dispersivity than the true medium. It occurs whenever the dispersion relation for

the finite difference approximation is nonlinear. Consequently, recently published numerical models couple Lagrangian and Eulerian approaches. Because hydrodynamics is already in a Eulerian framework, including advection and diffusion of tracers, it appeared very straightforward to treat dissolved oil in a Eulerian way, though numerical diffusion may seem as a drawback in the long run (Goeury et al., 2014).

Three methods have been developed to simulate the movement of oil in an ocean model: particle-tracking, tracers, and spilletts. For the particle-tracking method, oil is parameterized as a finite number of particles, each assigned a primary location and mass. Advection is provided for each particle independently from the ocean (or ice) velocity field. Random processes can be added (as random kicks) to simulate the dispersion (spreading, diffusion) of the oil, independent of ocean current. The distribution of particles represents the whole oil spill in a statistical fashion. The higher the resolution of the model and the longer the simulation, the more particles are required to achieve reasonable statistics over the resolved current structure and to account for the spreading of the particles over time. For the tracer method, the area where the oil spill to be tracked is represented by a fine-resolution grid. The spill occupies the cells that best represent its physical extent. At each time step, the oil field is advected from cell to cell using the local currents, in combination with imposed diffusion/spreading such that mass is conserved. Also, each cell sees its environment and interacts with the atmosphere, ocean accordingly. As a result, the computation takes longer than the other methods. Another disadvantage is the relative complexity of the formulation compared to the other methods. The spillet method is almost identical to the particle approach with the exception that the spillet has more degrees of

freedom than a particle. In essence, the total spill is represented by a some smaller spills, each with the ability to spread according to a spreading theory such as Fay's equation (Fay, 1969). The spilllet model can be regarded as a compromise between the particle and tracer methods (Økland Gjøsteen et al., 2003).

GNOME (Beegle-Krause, 2001; Beegle-Krause and O'Connor, 2005) is an oil spill trajectory model developed by the Emergency Response Division of National oceanic and Atmospheric Administration (NOAA)'s Office of Response and Restoration. GNOME requires, in general, fewer parameters than the majority of other oil spill models and can be applied to any region in the world with few inputs, in opposition to most of the available oil spill models. Wind and currents data from the implemented operational ocean modeling system can be easily converted to GNOME inputs (Marta-Almeida et al., 2013). The output from the model consists of graphics, movies, and data files for post-processing in a GIS system. GNOME has been validated against observations for many oil spill events, for example in the Gulf of Mexico (Klemas, 2010; Cheng et al., 2011), in the Persian Gulf (Farzinger et al., 2011), in the Rajaei Port of Bandar Abbas, Iran (Farzinger et al., 2011), in the Black Sea (Marta-Almeida et al., 2013) and Bosphorus Strait (Basar et al., 2006).

The "best estimate" solution shows the model result with all of the input data assumed to be correct. However, models, observations, and forecasts are rarely perfect. Consequently, we have incorporated in GNOME our understanding of the uncertainties (such as variations in the wind or currents) that can occur. This second solution allows the model to predict

other possible trajectories that are less likely to occur, but which may have higher associated risks. We call the trajectory that incorporates these uncertainties the “minimum regret” solution because it gives you information about areas that could be impacted if, for example, the wind blows from a somewhat different direction than you have specified, or if the currents in the area flow somewhat faster or slower than expected. In some cases, the areas within the minimum regret solutions might be especially valuable or sensitive to oiling.

Diagnostic Mode using realistic nowcasts and forecasts from oceanic and atmospheric numerical models. GNOME supports several types of pollutants and simple weathering algorithms. The oil spills are modeled as Lagrangian elements (spots) advected with the surface Eulerian current velocity field (Csanady, 2012). It can accurately predict both best guess trajectories and uncertainties (Bergueiro et al., 2007). Uncertainty on the input parameters and forcing fields can also be taken into account resulting in the Minimum Regret trajectories uncertainty bound.

ADIOS is NOAA's oil weathering model. A library of approximately one thousand oils is integrated into the ADIOS to help estimate the amount of time that spilled oil will remain in the marine environment, and to develop cleanup strategies. ADIOS calculations combine real-time environmental data, such as wind speed, with chemical and physical property information in its oil library. The program provides an output on oil weathering parameters such as evaporation, dispersion into the water column, and changes in oil density and viscosity.

OSCAR is a commercial model developed at SINTEF (Reed et al., 1995b; Aamo et al., 1997a). The oil spill contingency and response (OSCAR) model, which was specifically designed to support oil spill contingency and response decision-making, was used to simulate the behavior and fate of the hypothetical oil spill (Niu et al., 2014). OSCAR is a 3-dimensional particle-based model that simulates the evolution of oil on the water surface, along shorelines, and dispersed and dissolved oil concentrations in the water column. OSCAR includes a 3D advection model, data-based oil weathering, a chemical fates model, an oil spill combat model and a biological exposure model for fish and other species. The oil is modelled as particles. OSCAR addresses the following surface processes: surface spreading and advection, entrainment in the water column, emulsification (mousse formation), and volatilisation (dissolution). In the water column, horizontal and vertical advection and dispersion of entrained and dissolved hydrocarbons are simulated by random walk procedures. The algorithms used to simulate these processes controlling physical fates of substances are described by Aamo et. al. (1993) and Reed et al. (1994a, b; 1995a, b). OSCAR has been validated in considerable detail (Reed et al., 1996; Reed et al., 2000).

2.3 Uncertainty analysis

Uncertainties should be considered carefully when the numerical model applied to the real situations. Calibration and optimization, uncertainty and sensitivity analysis, are essential to be conducted to minimize the discrepancy between simulation and observation.

Parameter uncertainties have been extensively studied (Galt, 1997; Sebastiao and Soares, 2006; Abascal et al., 2009; Price et al., 2003; Xu et al., 2013) , particularly integrated with sensitivity analysis and model calibrations (Boufadel et al., 2014; Kim et al., 2014). The University of Amsterdam developed a model, Complex Evolution Metropolis (SCEM-UA), to obtain the optimal coefficients using the global optimization algorithm Shuffled (Vrugt et al., 2003). And a modified version has been developed by Duan et al. (1992). This method can find both the most likely parameter set in the feasible space and underlying posterior probability distribution (Abascal et al., 2009).

Kim et al. (2014) tried to use a varied wind drift factor instead of a fixed wind drift factor to improve the performance in the transport of oil slicks. The result suggested that, to some extent, wind drift factor was characterized with strong tidal currents.

One-factor-at-a-time (OFAT) is the most commonly used sensitivity analysis methods. This method simply adjusts one parameter at a time while keeping other parameters fixed. Its applications have been found in many previous studies conducted on various models (Holvoet et al., 2005; Lenhart et al., 2002; Jing and Chen, 2011). However, limitation of the OFAT is the incapability of revealing the interactions between parameters. The potentially significant variables might be ignored (Saltelli, 1999; Montgomery, 2008; Peeters et al., 2014). As well known in the previous studies, there exists a close interdependence of oil spill weathering processes (Reed et al., 1999). Therefore, a calibration method to find the multiple optimal values of the parameters to minimize the differences between numerical and actual trajectories is needed.

To address this issue, the design of experiment (DOE) provides a parameterization option. DOE is a widely used statistical methodology, which can analyze the interactions between parameters and the corresponding responses (Czitrom, 1999; Park, 2007; Veličković et al., 2013; Sarikaya and Güllü, 2015).

DOE was originally developed to determine the relationship between factors affecting a process and guide the setup for physical experiments. In recent studies (Wu et al., 2012), DOE was used to conduct sensitivity analysis and parameterization for a hydrological model SLURP. With the optimization of the predicted regression equation, a greater goodness-of-fit value compared to the one achieved by the automatic calibration function was produced.

Though the effectiveness of parameterization and interaction analysis in the numerical models has been proven. DOE method has rare application in oil spill modeling, in which uncertainties commonly exist, and knowledge concerning interactions between each parameter is inadequate.

2.4 Summary

In the past decades, oil spills led to a growing concern about the increasing contamination of water bodies and shoreline areas. With the rapid growth of the oil industry, the exploration of offshore oil fields, and maritime transit and storage activities, environmental risks and possibility of oil-related accidents are increasing. Many large-scale oil spills in the history resulted in the catastrophic impacts. To overcome this problem, the establishment of oil spill simulation and response systems is in great demand.

To fulfill the simulation of oil spill, researchers have conducted many studies to understand and qualify the physical and chemical processes during oil spills. Both experimental and modeling studies proved the oceanic and atmospheric physical variables and chemical and physical processes could affect the oil fate and transport significantly. The fate and transport processes of oil spills have been studied based on the trajectory method and mass balance approach, and various oil spill models have been developed.

Proper weathering and spreading formulations, and accurate inputs data, are two significant factors to make sure the success application of oil spill models in real cases. Uncertainties should be considered carefully with calibration and optimization, uncertainty and sensitivity analysis, to minimize the discrepancy between simulation and observation.

CHAPTER 3: SIMULATION OF MARINE OIL SPILLS AND MODELS COMPARISON BY A CASE STUDY IN THE NEWFOUNDLAND OFFSHORE AREA

The contents in the chapter are based on or will result in the following publications or potential publications:

1. **Zheng X.**, and Chen B. (2017). Simulation of marine oil spills and models comparison by a case study in the Newfoundland offshore area. *Marine Pollution Bulletin*. (Under preparation)
Role: I conducted case studies and drafted manuscript. Dr. Bing Chen is my M. Eng. Supervisor.
2. **Zheng X.**, Wu H.J., and Chen B. (2017). Design of Experiment Aided Uncertainty Analysis for Marine Oil Spill Modeling. In: *Proceedings of the 40th AMOP Technical Seminar on Environmental Contamination and Response*, June 6 to 8, 2017, Alberta, Canada. (Under review)
Role: I conducted case studies and drafted manuscript. Hongjing Wu conducted statistical analysis for results. Dr. Bing Chen is my M. Eng. Supervisor.
3. **Zheng X.**, Wu H.J., and Chen B. (2017). Marine oil spill simulation and uncertainty analysis- a case study in the Newfoundland offshore area. *Journal of Environmental Engineering*. (Under preparation)
Role: I conducted case studies and drafted manuscript. Hongjing Wu conducted DOE statistical analysis for results. Dr. Bing Chen is my M. Eng. Supervisor.

3.1 Introduction

Offshore oil spill is one of the major marine pollutions and can induce both social and environmental problems (Alpers and Espedal, 2004). Marine and coastal and estuarine environments can be negatively affected and significant damage can be produced to the associated marine ecosystem, coastal wetlands and nearby communities (Liu and Sheng, 2014).

Large-scale oil spills happened world-widely in the past decades. Such as Exxon Valdez spill in 1989 (Loughlin, 2013), Gulf of Mexico spill in 2010 (Azwell et al., 2011; McNutt et al., 2011; Wei et al., 2015). Historical data shows that almost 60% of the total amount of spilled oil was contributed by the large-scale accidents which account for only 0.1% of the total spilling incidents (Fingas, 2010). Exceed 1,300,000 metric tons of petroleum was released into the sea per year (Kvenvolden and Cooper, 2003; Council, 2003). Precise detection, tracking and prediction of spilled oil would favor aquatic life, seabirds, and resource monitoring and management, as well as the protection and preservation of the marine environment.

To deal with the oil spill disasters, accurate real time observations and monitoring are key considerations to the marine security agencies (Marta-Almeida et al., 2013). Synthetic aperture radar (SAR) is a form of radar that is used to create 2- or 3-dimensional images of objects, such as landscapes. SAR uses the motion of the radar antenna over a target region to provide finer spatial resolution than conventional beam-scanning radars. Remote sensing technologies, especially SAR are commonly used as efficient tool to detect the surface

spills to provide precious synoptic imagery of the position, size and shape of oil spills because of its considerable wide coverage and imaging capability under various circumstances (Jha et al., 2008; Ferraro et al., 2009; Cheng et al., 2011; Singha et al., 2013; Li et al., 2014a).

In addition to oil spill monitoring by satellite imagery, the demand of more accurate oil transport forecast models have been increased. Oil spill models are usually driven by a time series of ocean currents, ocean surface wind vectors, the temperature in sea depths, etc. Some of the most sophisticated Lagrangian operational models are OSCAR (Reed et al., 1995a), OILMAP (Howlett et al., 1993), GULFSPILL (Al-Rabeh et al., 2000), ADIOS (Lehr et al., 2002), , MOHID (Carracedo et al., 2006) , OD3D (Hackett et al., 2009), the Seatrack Web SMHI model (Ambjörn, 2006), MEDSLIK (De Dominicis et al., 2013, Lardner et al., 1998), GNOME (Beegle-Krause, 2001) and OILTRANS (Berry et al., 2012). The purpose of oil spill modeling is to predict and simulate the fate and transport of spilled oil through the input of ocean currents, winds, tides and other parameters (Drozdowski et al., 2011).

The oil industry in Newfoundland maintained rapid growth during the past decade with the exploration of offshore oil fields. Environmental risks increased and brought higher possibility of oil-related accidents. Since 1997, 340 spill accidents have been happened in the offshore Newfoundland, which have been impacted the marine ecosystem at a large scale (Li et al., 2014b). During the Terra Nova oil spill happened in 2004, which is the largest offshore oil spill in NL, more than 10,000 seabirds were killed directly by the covered oil slicks within 793 km² (Wilhelm, 2006, 2007). To overcome such disasters, the

establishment of a response system based on oil spill simulation and prediction is in high demand.

This chapter is organized in the following way: Section 2 introduced the target incident and the harsh environment in the region of the case study. Oil spill modeling approaches were described in Section 3. The acquired data for the model inputs was introduced in Section 4. The model validation was discussed in Section 5. Section 6 compared the oil spill simulation results from two models with detailed discussion and conclusions. Summary was given in Section 7.

3.2 Terra Nova oil spill

Newfoundland and Labrador (NL) produces about 0.27 million barrels of oil per day, accounting for 10% of Canada's total crude oil (Li et al., 2014b). The study area, Grand Bank, is located at 350 kilometres southeast of St. John's, Newfoundland, Canada. There are three operational oil production fields in the Grand Bank, including Hibernia, Terra Nova and White Rose. Among them, The Terra Nova field is located at 46° 28' N, 48° 27' W, and has been put into operation since 2002. The cold Labrador Current flows north then back south and introduces cold water to the region. Another warm Gulf Stream which flows north along the east coast of the United States. This interaction of cold and warm current creates extensive foggy regions with little visibility. Icebergs calved from Greenland's glaciers are also brought by the Labrador Current. With the increasing activities of offshore drilling and shipping in the area, a prediction and response plan is a must before an internationally-significant oil spill happens (McGrath, 2014).

In November 21st, 2004, two mechanical failures in produced water separation process caused more than 1,000 barrels or 160,000 liters of oil released into ocean. This accident happened at Terra Nova FPSO resulted in more than 10,000 sea birds killing directly by the 793 km² oil slick coverage (Wilhelm et al., 2007). Based on the record of Petrocanada, two vessels were on the site and ready to deploy booms and skimmers on 22nd. But cleanup operation was not started until 23rd because of terrible weather condition. (Martin, 2004). It remains the largest marine oil spill in the history of NL. Large-scale oil spill has not been happened in offshore NL, but the booming oil industry could raise the risk of accident. Harsh environment in the NL might lead to a catastrophic damage to the marine ecosystem. The case study of Terra Nova can be helpful in prevention and response planning of oil spills in this area.

The presence of sea ice, low temperature, limited visibility and strong wind are all existing harsh environment elements which affect oil spill recovery operations and effectiveness of oil recovery technologies such as booming, herding and skimming (Brandvik et al., 2006; Jing et al., 2012). Generally, oil spills in the regions with harsh weather conditions, fragile ecosystems and limited access to sea transport services are more challenging issue to deal with (Hung et al., 2010; Turner et al., 2010). And the damage is likely to be more significant without in time oil recoveries as a result of the restricted support from aircrafts, vessels and satellite remote sensing (Fingas, 2010). During the Terra Nova spill event in 2004, cleanup operations were not initiated until 23th (the third day) because of the harsh environment and weather conditions, and only about five percent of oil was recovered based on the record. According to the spill observation data, the domain oil slick was

determined as 6.1 litres and measured 1,500m by 100m by flight report on 27th (Welhelm, 2006).

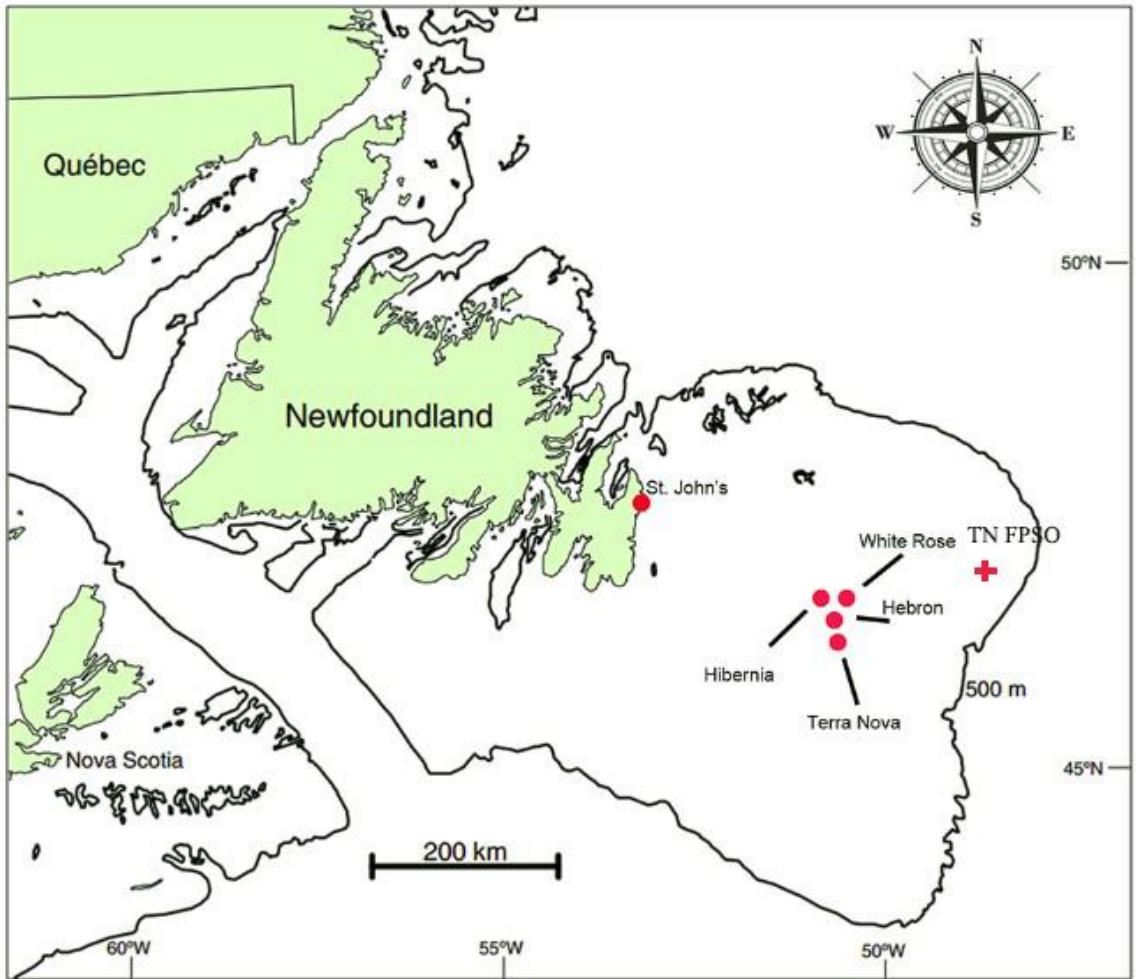


Figure 2 Study area: location of Terra Nova FPSO at Grand Banks, NL, Canada

3.3 Modeling approach

3.3.1 GNOME and ADIOS2

The GNOME is an oil spill trajectory model developed by the Emergency Response Division of NOAA's Office of Response and Restoration. Wind and currents data from the ocean models can be easily converted to GNOME inputs (Marta-Almeida et al., 2013). In the simulation of GNOME, The spilled oils are modeled as point masses as Lagrangian elements. It can simulate the fate and trajectory with the movers as the surface Eulerian current velocity field, the wind field and the diffusion as a random walk (Csanady, 2012). The Best Guess solution represents the most likely movement path and extension of the spill, whereas the Minimum Regret trajectory provides an uncertainty bound on the input parameters and forcing fields.

ADIOS2 is NOAA's oil weathering model. Since GNOME only includes several oil types, oil fate can derive from the ADIOS2. ADIOS2 has better evaporation and oil fate estimates with a library of more than one thousand types of oil, which can be helpful in developing cleanup and recovery strategies. Environmental data were combined with the chemical and physical property information in the oil library. Oil weathering parameters such as evaporation and dispersion can be calculated as an output.

3.3.2 OSCAR

The Oil Spill Contingency and Response (OSCAR) model (Reed et al., 1995a; Aamo et al., 1997a; Reed et al., 2004) was developed by SENTIF. It is a 3-dimensional particle-based

dynamic, simulation tool for contingency and response decision-making for oil spills. The behavior of fate and effects of released contaminant can be simulated on the water surface, along shorelines, in the water column and the ocean or shoreline sediments (Niu et al., 2014).

Oil characteristics database are key components of the system and provide chemical and toxicological parameters required by the model. An environmental database such as sea ice coverage and biological resource can be used as input to explore the results in a more complicated system; Response options database provide the results of different responses with skimmers or/with dispersant spread from air or subsurface. OSCAR employs surface spreading, advection, entrainment, emulsification to determine transport and fate at the surface. In the water column, horizontal and vertical advection and dispersion of entrained and dissolved hydrocarbons are simulated.

3.3.3 Comparisons of two models

GNOME and ADIOS2 can be applied to any region in the world with fewer inputs than most of the oil spill models (Marta-Almeida et al., 2013). It can be set up efficiently for real-time response and forecast simulations by providing a land-sea mask, ocean currents and climatological wind data (Samuels et al., 2013). GNOME can predict trajectories and uncertainties accurately and has been applied in many cases, which was implemented and validated successfully in many accidents (Bergueiro et al., 2007). The examples could be documented from cases in the Gulf of Mexico (Klemas, 2010; Cheng et al., 2011), Persian

Gulf (Farzingsohar et al., 2011), the Black Sea (Marta-Almeida et al., 2013), Bosphorus Strait (Basar et al., 2006) and Rajae Port of Bandar Abbas in Iran (Farzingsohar et al., 2011).

OSCAR couples weathering, surface trajectory, water column, and oil spill response components. The behavior of individual working groups, such as vessel-skimmer and helicopter dispersant systems, are simulated, each with an assigned strategy and work area. Environmental factors such as winds and waves, and available daylight relate functionally to effectiveness of mechanical cleanup. The application of chemical dispersants is simulated based on observations from field trials (Daling et al., 1995; Lewis et al., 1995). The weathering and transport algorithms of OSCAR has been tested and verified in accidents and experiments (Daling and Strøm, 1999; Reed et al., 2000; Daling et al., 2003).

In GNOME, ADIOS2 and OSCAR, the evaporation equation was developed by Stiver and Mackey (1984), in which an evaporative exposure parameter τ was introduced. For constant wind speed, the evaporative exposure parameter may be expressed as eq. (3-1).

$$\tau = Kt/h \tag{3-1}$$

For cases with variable wind with eq. (3-2).

$$\tau = \int (K/h) dt \tag{3-2}$$

Where K is the surface mass transfer coefficient, h is the initial film thickness and t is the exposure time.

In ADIOS and SINTEF, the dispersion equation (3-3) was used, which was developed by Delvigne and Sweeney (1988). The number and size distribution of oil droplets driven into the water column by breaking waves was measured as the volume of entrainment Q ,

$$Q = c_{disp} D_e^{0.57} f_{bw} V_{disp} \quad (3-3)$$

Where D_e is the dissipation of wave energy per unit surface area, c_{disp} is an experimentally determined parameter, f_{bw} is the fraction of breaking waves per wave period per unit, V_{disp} is the volume of oil entrained per unit volume of water.

In GNOME diffusion and spreading are treated as stochastic process. A stochastic or random process is a mathematical object usually defined as a collection of random variables. Classical diffusion as given in eq. (3-4).

$$\partial C / \partial t = D \nabla^2 C \quad (3-4)$$

Where C is the concentration of a material and D is the diffusion coefficient which recognized the characteristics of oil spills as they move with water and wind.

The method of calculating spreading is very similar to the method used to compute diffusion, except the spreading happens only in the direction of the wind.

$$d\sigma^2 / dt = S(t) \quad (3-5)$$

Where σ^2 is the variance of the spilled oil locations. $S(t)$ is a spreading parameter that is a function of time because the wind velocity is a function of time.

In OSCAR, spreading is calculated according to eq. (3-6) developed by Mackay et al. (1980):

$$dA / dt = Kh^{1.33} A^{0.33} \quad (3-6)$$

Where A is the area of the slick, h is the thickness of the slick, t is time, K is an empirical constant. In the model, spreading stops when the slick reached a minimum thickness.

Although both the GNOME/ADIOS2 and OSCAR have been applied in many oil spill cases worldwide, which have shown good performance in most of the accidents, neither of them have been used in the NL region. As one of the most common used tools in the oil spill response, the capability in the harsh environment of NL offshore is still unknown. With the same equations of evaporation and dispersion, the simulation results can be different in the two models. GNOME is good at the spreading simulation, especially compared with two other models in the case of Gulf of Mexico (Cheng et al., 2011). OSCAR derived its oil weathering data with field tests in the cold environment around Norway (Reed et al., 2000), which is similar to the environment at offshore NL. Their abilities of simulating spreading and weathering processes can be compared during this case.

3.4 Data acquisition

3.4.1 Wind and currents

For any model, reliable environmental observations and predictions are the basis for an accurate prediction of the oil spill trajectory. The data collected provide an overall picture of meteorological and oceanographic conditions. To simulate the movement of the oil spill detected in the SAR images, ocean wind, and current inputs were required to force the

models. The accessibility to high-quality information on ocean circumstances dominating factor to monitor and predict marine oil spills in the model (Hackett et al., 2009). In this study, ocean currents in the Grand Banks were obtained from the HYCOM model, with the spatial resolution $1/8^\circ$ (Fig. 3), which is developed by the National Ocean Partnership Program (NOPP), as part of the U.S. Global Ocean Data Assimilation Experiment (GODAE). As an ocean general circulation model (OGCM), HYCOM (Halliwell, 2004; Chassignet et al., 2006) can (a) retain its water mass characteristics for centuries, (b) have high vertical resolution in the surface mixed layer for proper representation of thermodynamical processes, (c) maintain sufficient vertical resolution in unstratified or weakly-stratified regions of the ocean, and (d) have high vertical resolution in coastal areas.

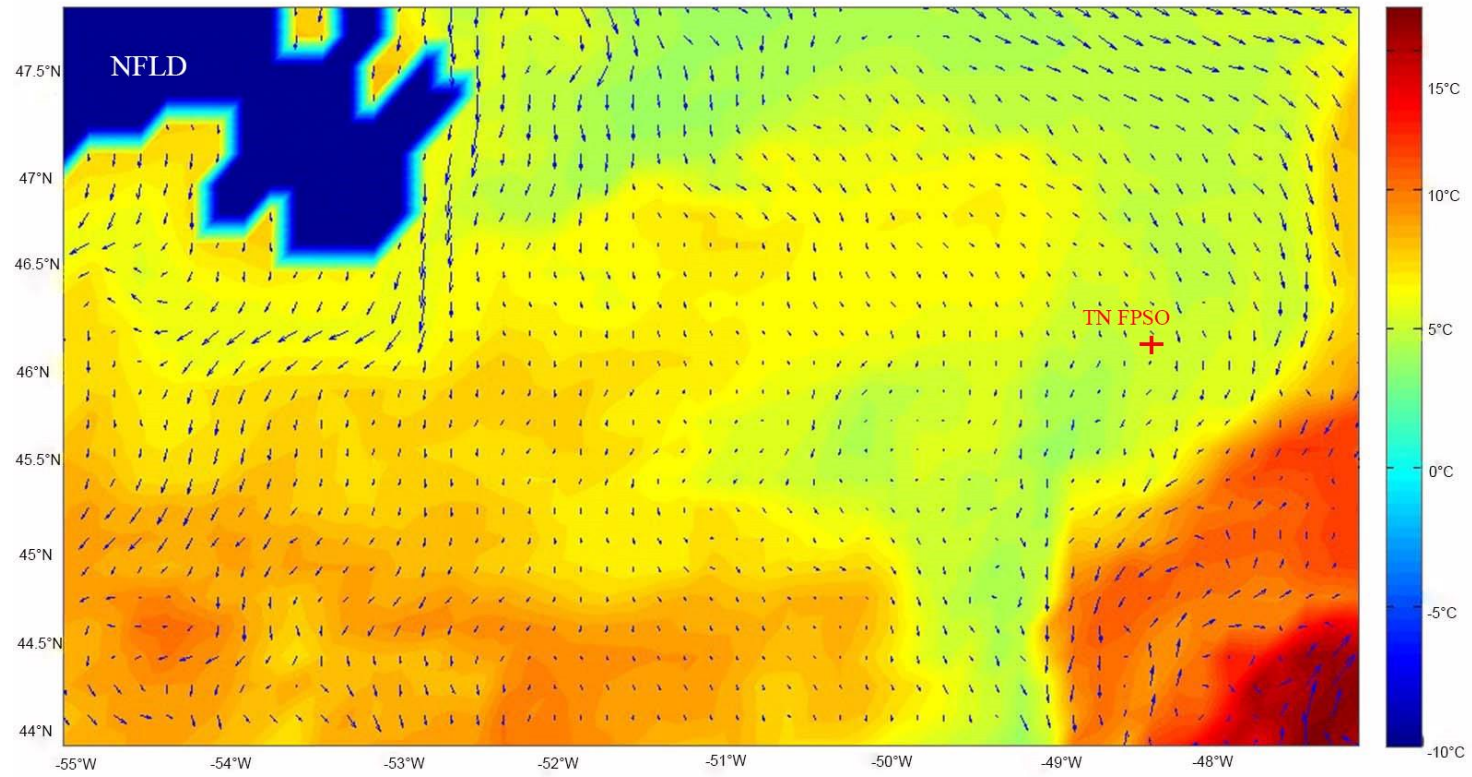
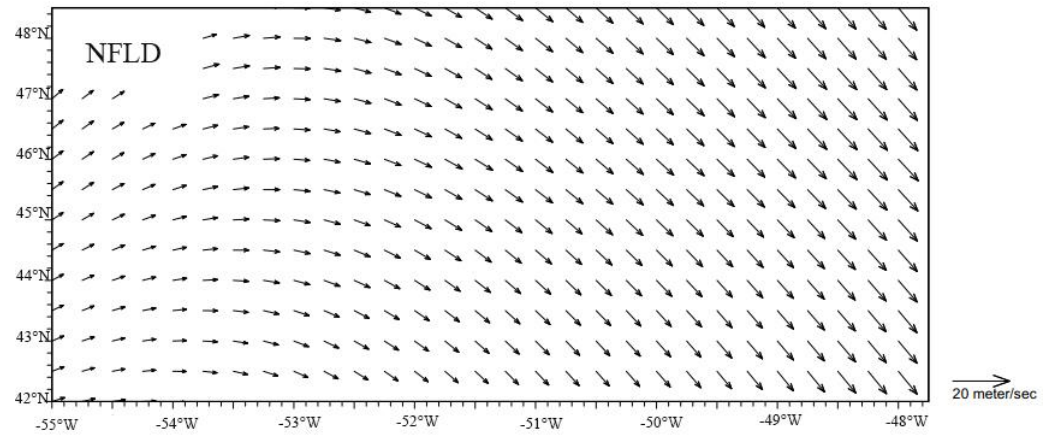
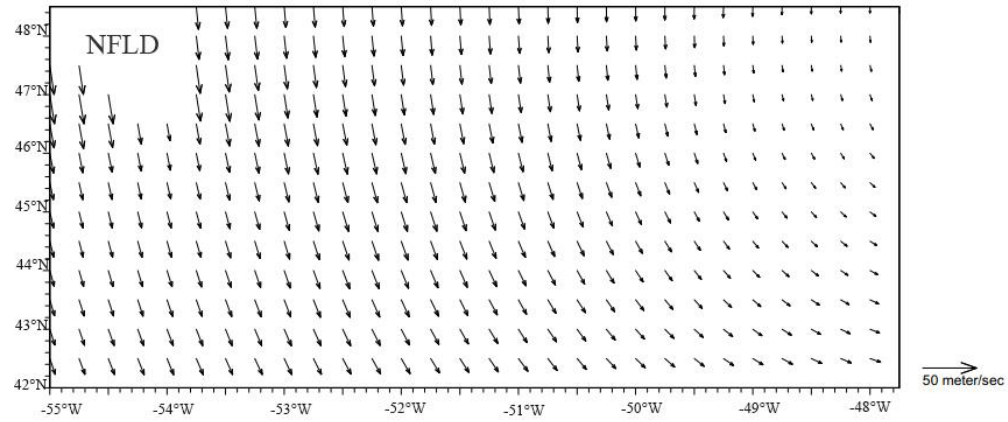


Figure 3 Ocean currents derived from the HYCOM at 2004-11-21

The fig. 3 shows the circulation of ocean current with the spatial resolution $1/8^\circ$ and the temporal resolution 3h. The cold Labrador Current, originating off of the west coast of Greenland flowing north then back south, interacts with the warm Gulf Stream which flows north along the east shore of the United States in this area. Continental shelf separate the ocean current into two part. Ocean current from south with water temperature can be as warm as 10-15 degrees centigrade. Cold Labrador Current is dominant in the Grand Banks area, with cold temperature as 5 degrees centigrade from north. The meeting of two currents creates vast regions of fog with limited visibility. This limited visibility is a significant danger to shipping and a limitation to visual aerial reconnaissance in the event of an emergency at sea. Also, a higher evaporation rate can be noticed under this circumstance, which can affect the simulation of weathering process of spilled oil.

In addition to ocean currents, surface wind is another important input parameter for the drift models (Cucco et al., 2012). In open water, unless the spill accident occurs in tidal currents, wind-induced drift (Stokes drift) is the most important factor in the simulation of oil slick trajectories (Spaulding, 1988). In the oil trajectory modeling, 1-3% of the wind speed was commonly added as a result of the underestimation of surface current speeds (Wang et al., 2007). Some researchers proved that surface layer of oil moves at a speed which is 2.5 to 4.4% of the wind speed (Spaulding, 1988; Reed et al., 1999) and at an angle of 0 to 25 degrees clockwise relative to the wind direction (Samuels et al., 1982; Spaulding, 1988). In this study, the hourly 10-m wind measurements from NCDC (National Climate Data Center) are used to force the models. In this study, the sea surface wind field is obtained from near real-time blended ocean winds with six-hour aggregation with a spatial

resolution of $0.25^\circ * 0.25^\circ$. As shown in Fig. 4, from November 21st to November 25th, 2004, the winds are strong, blowing toward the southeast with speeds more than 12 m/s, and on November 26, the wind direction changed toward the north. Overall, the oil slick traveled south, almost reaching the continental shelf edge, and then traveled back north on 26th in response to changes in wind direction (Wilhelm et al., 2007), which fits good with the wind data. According to the simulation results, when the wind direction was consistent with the current, oil slick moved faster to south during 21th and 25th. This might be caused by the current direction, as shown in Fig.3. When the current has a reverse direction with wind after 25th, the oil slick moved much slower. The movement of oil slick is determined mainly by wind and current at the same time. Wind with speeds higher than 7.7 m/s can break the surface oil film that the weathering process of spilled oil in Terra Nova case was faster than usual (Cheng et al., 2011).



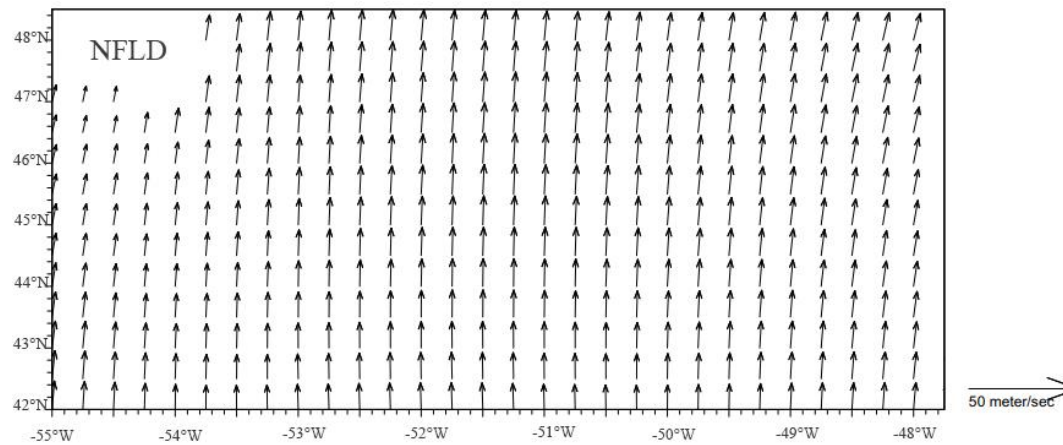
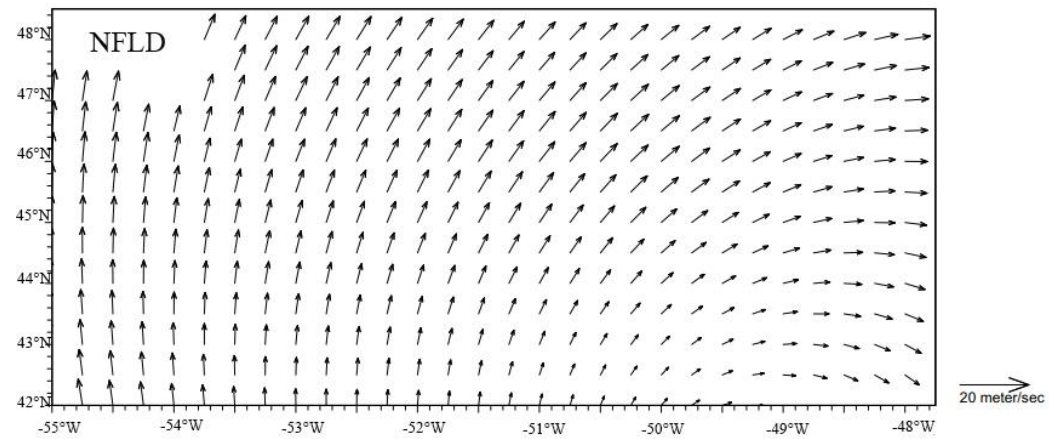


Figure 4 (a) Wind field at 2004-11-21 06:00 (b) Wind field at 2004-11-23 00:00 (c) Wind field at 2004-11-25 12:00 (d) Wind field at 2004-11-26 18:00

3.4.2 SAR images

Remote sensing technology plays a key role in oil spill trajectory monitoring and important in the observation of oil slick fate and distribution on the ocean surface (Kvenvolden and Cooper, 2003; Hu et al., 2009). Among the satellite sensors, SAR with wide coverage has been widely used to provide images during day and night (Migliaccio et al., 2012; Li et al., 2013) and regardless of any weather conditions. Today, RADARSAT-1 and ENVISAT are the two main providers of satellite SAR images for oil spill monitoring (Brekke and Solberg, 2005). Oil slick can be effectively observed from RADARSAT (Peterson et al., 2008). The observed information could provide the data support for modeling the fate and transport of the spilled.

The RADARSAT-1 satellite was launched in November 1995. Equipped with a powerful SAR, it is capable of acquiring images with different incidence angles, dual polarization and wide swath coverage. Users have access to a variety of beam selections that can image with resolutions from 20 to 150 m. In this study, the RADARSAT-1 was used to detect oil spill information. Fig. 5 shows the oil slick observed on 23rd November, 2004. The SAR image was derived from Environment Canada, which was taken on 09:21 UTC (5:51 AM local time), 23th November, 2004.

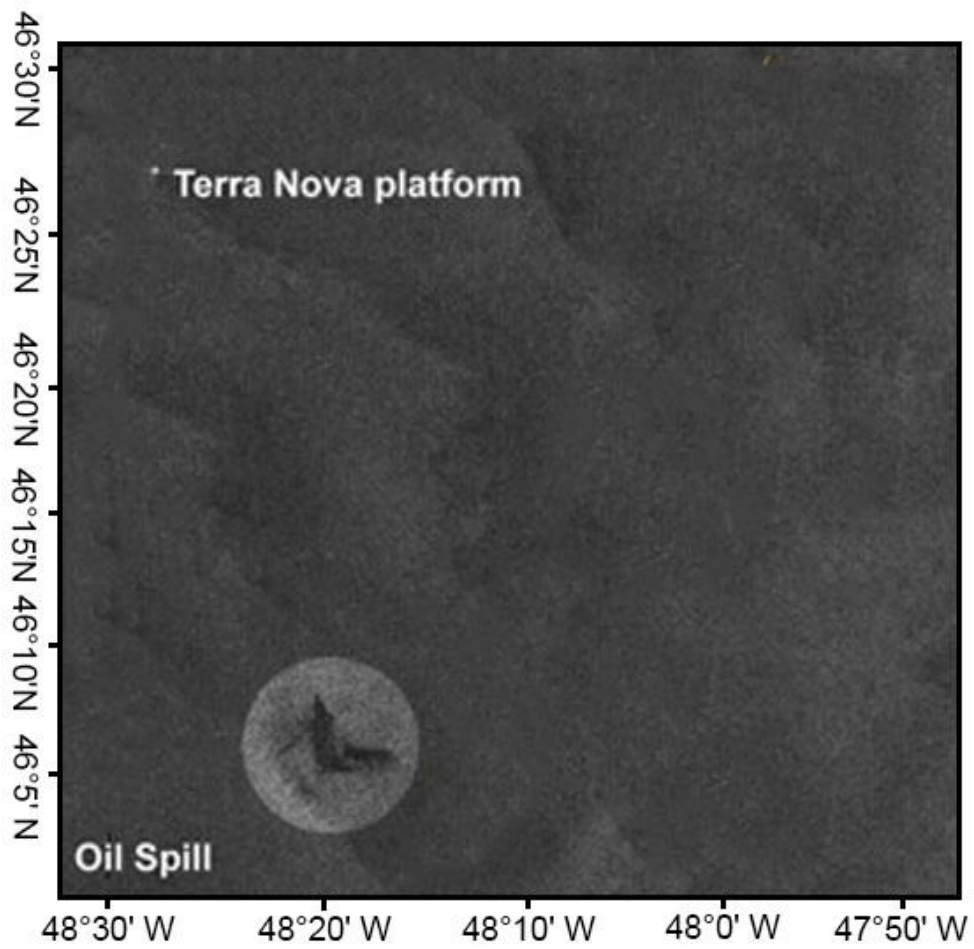


Figure 5 Satellite images RADARSAT-1 image at 9:21 UTC on November 23th, 2004 (derived from Environment Canada)

3.5 Modeling settings

In this study, we set the amount of oil spilled as 1000 barrels which were released in the Terra Nova spill in 2004 and the spill zone (modeling domain) shape from the SAR images. As described in Section 3.3, a time series of HYCOM current fields and the winds data from NCDC were input to the GNOME and OSCAR models to perform the simulation. GNOME allows users to select different types of weathering or non-weathering for various kinds of spills, i.e., gasoline, diesel, medium crude and fuel oil. GNOME defines the oil type as “medium crude” which fits the terra nova with medium density, low sulphur crude oil. In the ADIOS2 and OSCAR, the oil type can be found as “Terra Nova” in their oil library.

If the current data, wind data, diffusion parameters and windage (i.e., how much force the wind exerts on the oil to move it in the direction that the wind is blowing) are accurate, good simulation results will be produced. To compare the capabilities of two models with the same input, we assumed that there was no errors in both the current and wind data. Based on the manual, considering the high waves and complicated weather condition during the oil spill case, we set the windage as 1.5–3% and the minimum uncertainty error of both along-current and cross-current directions as 10% in magnitude, the diffusion coefficient and its uncertainty factor are set as $100,000 \text{ cm}^2/\text{s}$ and 2, respectively.

3.6 Results and discussion

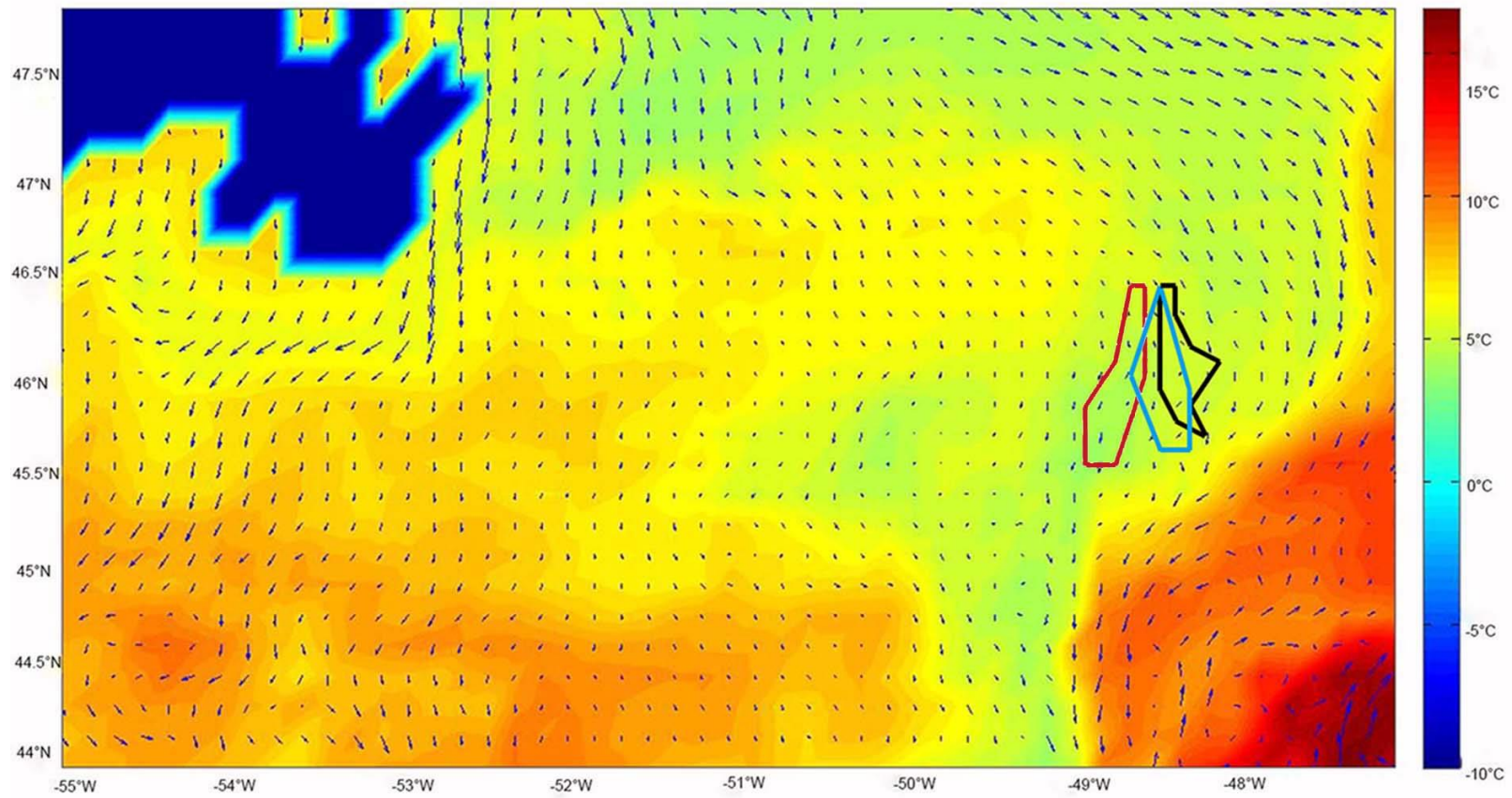


Figure 6 A combined figure with GNOME (blue), OSCAR (red), and Black solid lines represent the oil slick covered area by observation

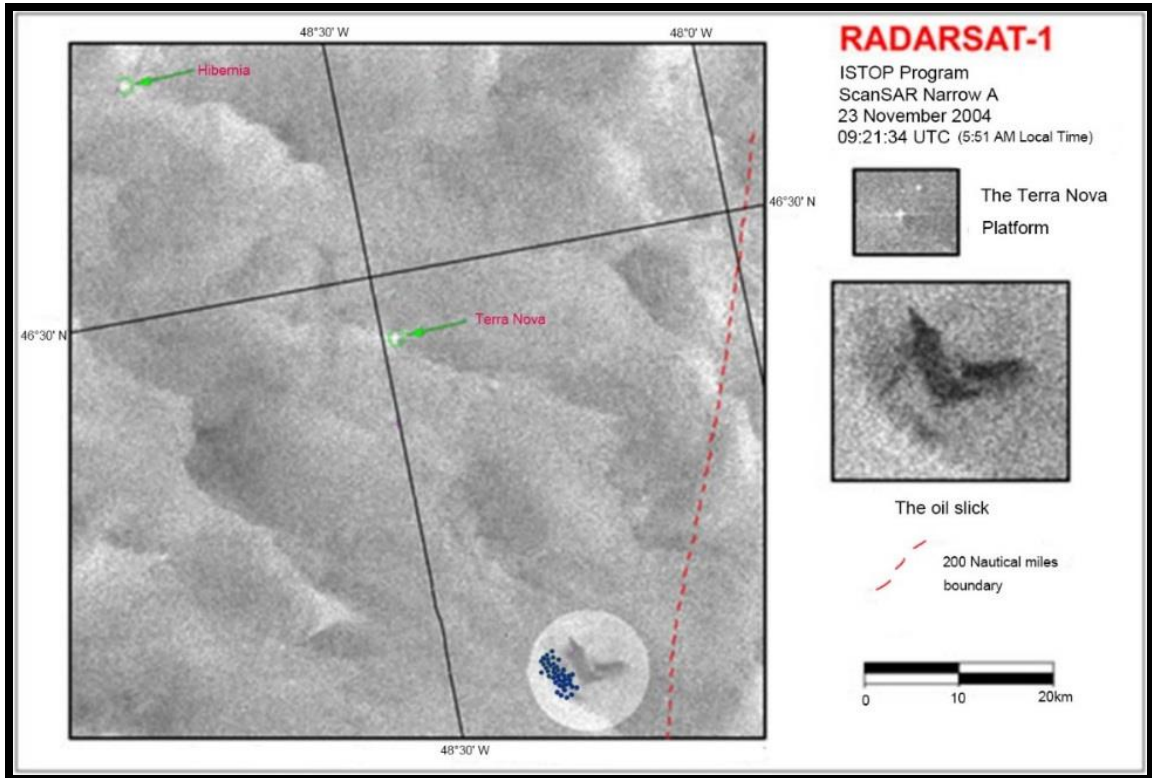


Figure 7 Result from the GNOME compared with the SAR image

Fig. 6 shows the modeling results by both modeling systems (i.e. GNOME and OSCAR) in comparison with the observation. There were shifts between observed and simulated oil slicks. The result of GNOME shows a 3-minute (about 5.5 km distance) deviation compared with the satellite image. Wind speed and direction were changing rapidly, and the high waves were promoting slick breakup during the extreme weather in the first two days. In general, compared with the actual spill observation, after 7 days run of the model, the simulated oil polluted area of GNOME coincides with the observation data and SAR image better in terms of shape and location than the OSCAR. Compared with the observation reported in Wilhelm et al. (2007), shown the estimated impacted area derived from aerial surveillance and information provided by the East Coast Response Center (ECRC), OSCAR has a worse performance. As we notice that different equations of spreading were applied in the two models, which might lead to the shifts in the simulation results. The effects of the two equations will be further studied in the future work.

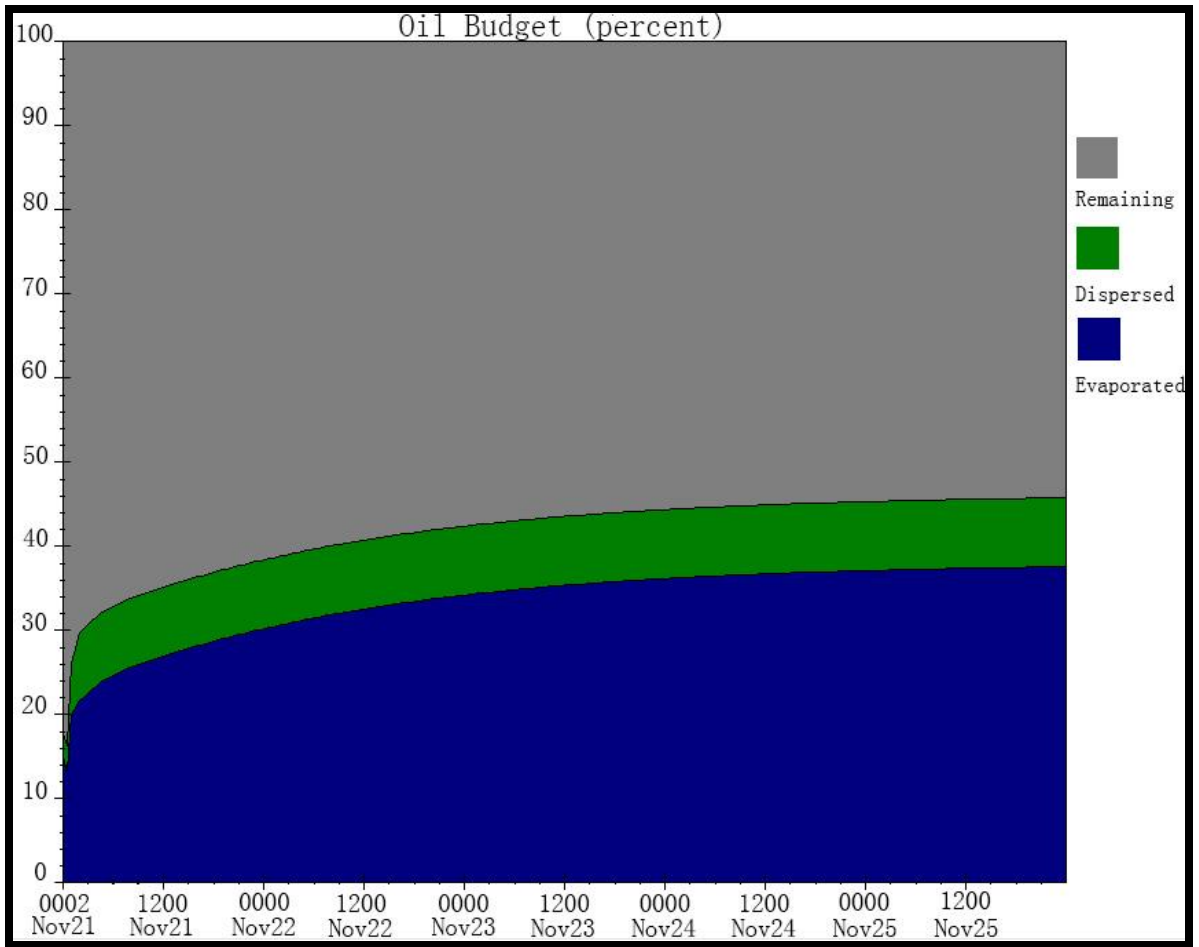


Figure 8 Result of oil weathering by AIDOS2 simulation

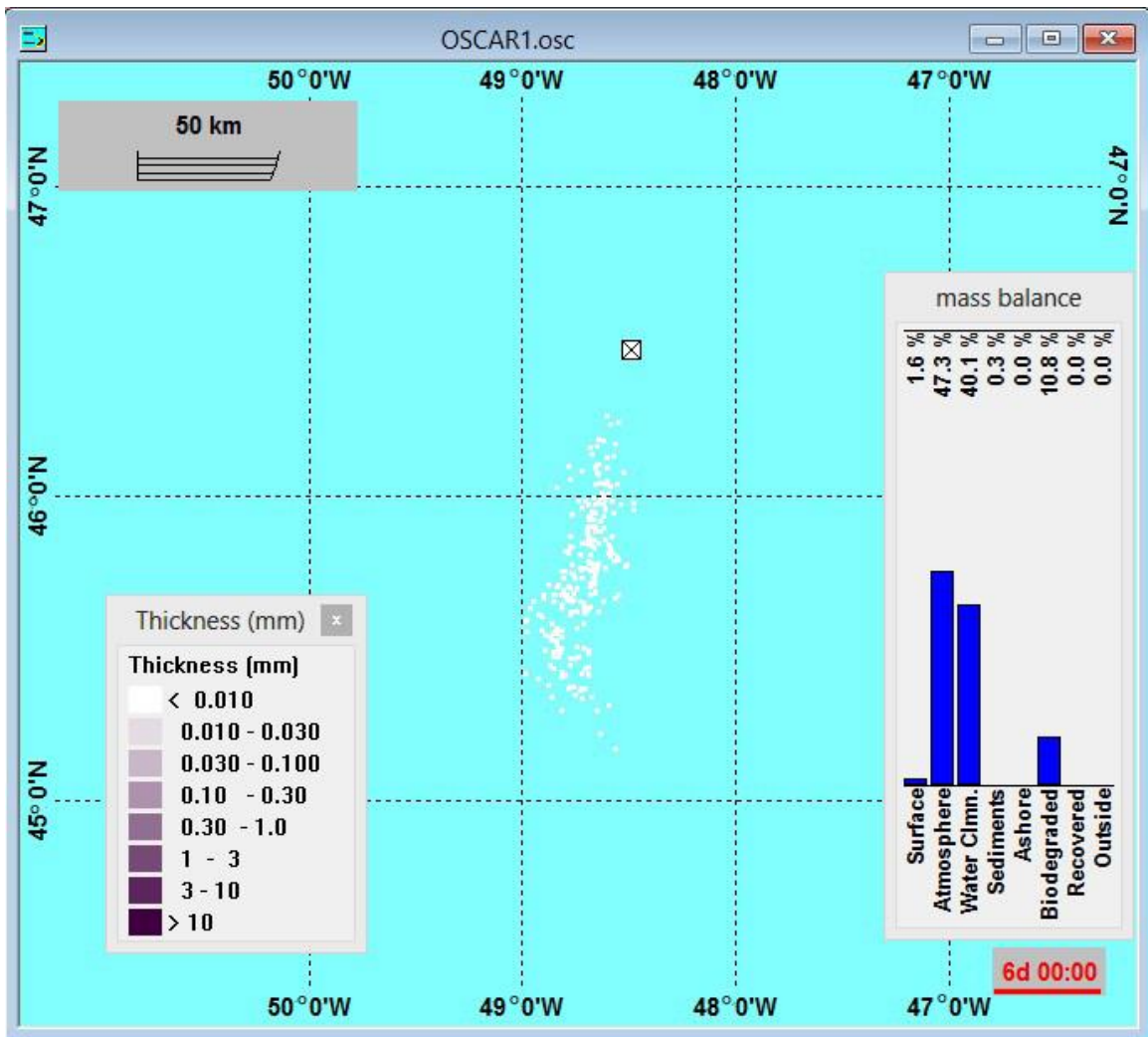


Figure 9 Result of oil weathering by OSCAR

In the Fig. 8, the simulation results indicated that 43.7% of the oil was evaporated and dispersed in the first two days. In the Fig. 9, with the model of OSCAR, 87.4% of total spilled oil was evaporated and dispersed, 10.8% was biodegraded and 0.3% were settled to the sea bed. Only 1.6% of oil floated on the sea surface after six days, which is more consistent with the observed data. Note that in this study, only evaporation and dispersion were considered as weathering processes in the ADIOS2 due to the model limitation. In the OSCAR, sediment and biodegradation were also taken into account.

Although the same equations of dispersion and evaporation processes were applied in the two modeling systems, the results of evaporation and dispersion processes simulations were quite different as shown in Figs. 8 and 9, especially the dispersion results. This might be caused by the difficulty in calculating De and f_{bw} . De is the dissipation of wave energy per unit surface area, and f_{bw} is the fraction of breaking waves per wave period per unit. Anyway, the comparison indicated that the simulation results could be different even with the same simulation equations in these two models.

In the harsh environment conditions, wind field plays a major role in driving the movement of the spilled oil. High waves can enhance the breakup of the oil slick and dispersion process. Strong winds and associated high waves can affect the spreading, evaporation and dispersion processes. Lacking of sunlight could reduce the oxidization, biodegradation and evaporation along with low temperature.

According to the spill observation data, only about five percent of oil was recovered, the domain oil slick was determined as 6.1 litres on 27th (Welhelm, 2006). When comparing with the historical record, more oil was evaporated and dispersed than those of the simulation result from the GNOME/ADIOS2. In this case, OSCAR showed a better performance on weathering process simulation than that of GNOME/ADIOS2. The shift of oil affected area between the observed and simulated results might be caused by the high waves which can promote weathering processes and oil slick breakup, especially in the first two days after the spill and the rapid change of wind direction.

3.7 Summary

In this chapter, an oil spill event from the Terra Nova FPSO in the Grand Banks in November 2004 was used as a real case to evaluate the capabilities of the two model systems. Furthermore, two model systems, GNOME/ADIOS2, and OSCAR, were discussed and compared. The ocean current fields from HYCOM and wind data from NCDC were obtained and prepared to force the models. The result comparison showed a better performance of oil slick location simulation by GNOME. On the other hand, better weathering simulation result derived from the OSCAR in this case. Two systems could show different results even with the same input data due to their adoption of different equations and associated assumptions in the weathering and spreading simulation. Even with the same equations for some weathering processes such as dispersion and evaporation, results from different simulation models could still be varied. In the harsh marine conditions, wind field played a major role in driving the movement of the spilled oil.

In the harsh environments such as those prevailing in the Grand Banks region, a similar accident as the Terra Nova spill in the future could cause more significant ecosystem impact and possibly a loss of life if with strong winds and higher waves. Finding a more accurate and reliable way to simulate oil spills with the rapidly changing conditions in the harsh environments by evaluating and understanding of the capabilities and limitations of spill simulation models is significantly meaningful and necessary.

CHAPTER 4: A DOE AIDED UNCERTAINTY ANALYSIS METHOD AND APPLICATION IN MARINE OIL SPILL MODELING

The contents in the chapter are based on or will result in the following publications or potential publications:

1. **Zheng X.**, and Chen B. (2017). Simulation of marine oil spills and models comparison by a case study in the Newfoundland offshore area. *Marine Pollution Bulletin*. (Under preparation)
Role: I conducted case studies and drafted manuscript. Dr. Bing Chen is my M. Eng. Supervisor.
2. **Zheng X.**, Wu H.J., and Chen B. (2017). Design of Experiment Aided Uncertainty Analysis for Marine Oil Spill Modeling. In: *Proceedings of the 40th AMOP Technical Seminar on Environmental Contamination and Response*, June 6 to 8, 2017, Alberta, Canada. (Under review)
Role: I conducted case studies and drafted manuscript. Hongjing Wu conducted statistical analysis for results. Dr. Bing Chen is my M. Eng. Supervisor.
3. **Zheng X.**, Wu H.J., and Chen B. (2017). Marine oil spill simulation and uncertainty analysis- a case study in the Newfoundland offshore area. *Journal of Environmental Engineering*. (Under preparation)
Role: I conducted case studies and drafted manuscript. Hongjing Wu conducted DOE statistical analysis for results. Dr. Bing Chen is my M. Eng. Supervisor.

4.1 Introduction

The oil spill is always defined as the release of liquid petroleum hydrocarbon into the marine. Large-scale oil spills occurred in the world history, and some of them had resulted in catastrophic impacts. (Piatt et al., 1990; Sumaila et al., 2012; Ruiz, 2013). To deal with the oil spill accidents, oil spill model has been generally accepted as a useful tool in spill simulation, and further be used to support decision making of spill response. However, The success of its application depends not only on the weathering and spreading formulations, and also on the accurate input data and model parameters (Sebastiao and Soares, 2006). Therefore, in marine oil spill modeling, parameter calibration and optimization, uncertainty and sensitivity analysis, are essential to help minimize the discrepancy between simulated and observed data.

Sensitivity analysis is to obtain all the information flowing in or out of a model, often refers to one or a series of procedures to determine how much total model uncertainty can be attributed to the uncertainty associated with each individual model factors. Sensitivity analysis is paramount in model validation where attempts are made to compare the simulation results to the observed results, which can help to improve the simulation performance with a method to determine the significant parameters and their importance.

Uncertainty refers to lack of knowledge or incomplete information about specific factor, parameters, model structure, input/output, or measurement errors. The environment may appear more complex than imply (e.g., wind and temperature can both contribute to the

evaporation process, also with the interaction between the wind and current). Oil spill simulation models always suffer from a number of model uncertainties, especially in the prediction of calibration process. Possible sources of uncertainties in the oil spill modeling are from the model inputs, and model parameters. Input uncertainty, results from bias and errors in the input data, always influence final responses significantly. Uncertainties of model parameters exist because of the empirical estimation of value obtaining. The interactions between the parameters also cause uncertainties. Parameter uncertainty is need to be controlled and quantified, because of the immeasurable parameters and errors in the data used for parameter calibration. Normally, hydro-meteorological data are the most widely used model input data for oil spill modeling, and model outputs are sensitive to input data. In this study, the uncertainties of input data (wind speed and direction, current speed and direction) have been considered with the range of possibility. The influence of input data has been minimized with the calibration. Parameters, such as windage (also known as wind reduced-drift) and diffusion coefficient can be varied in a large scale in different places and change with the continuous changing of wind and current.

Parameter uncertainties have been extensively studied (Galt, 1997; Sebastiao and Soares, 2006; Abascal et al., 2009; Price et al., 2003; Xu et al., 2013) , particularly integrated with sensitivity analysis and model calibrations (Boufadel et al., 2014; Kim et al., 2014). Traditional sensitivity analysis methods (e.g. One-factor-at-a-time) have been found in extensive studies involved modeling processes (Lenhart et al., 2002; Holvoet et al., 2005; Jing and Chen, 2011). However, the key limitation of this method is the incapability of revealing the interactions between parameters. The potentially significant variables might

be ignored (Saltelli, 1999; Montgomery, 2008; Peeters et al., 2014). As well known in the previous studies, there exist close interdependence of oil spill weathering processes (Reed et al., 1999). Therefore, a calibration method to find the multiple optimal values of the parameters to minimize the differences between modeled and actual data is needed. Due to the incapability of revealing the interactions between parameters, traditional One-factor-at-a-time (OFAT) method could ignore the potentially significant variables and their interactive impacts. To address this issue, the DOE provides an alternative option. DOE is a widely used statistical methodology, which can effectively analyze the interactions between parameters and the corresponding responses (Czitrom, 1999; Park, 2007; Veličković et al., 2013; Sarikaya and Güllü, 2015). In recent studies (Wu et al., 2012; Li et al., 2016), DOE was used to conduct sensitivity analysis and parameterization for a hydrological model SLURP, and improve simulation performance of a groundwater modeling BioF&T 3D. A greater goodness-of-fit value can be achieved by optimization of the predicted regression equations.

Though the advantages in parameterization and the capability of interaction analysis in the numerical models has been proven, DOE method has rarely been used in oil spill modeling, in which uncertainties commonly exist, and knowledge concerning interactions between each parameter is inadequate.

4.2 A DOE aided uncertainty analysis method

A factorial design is one of the most widely applied approaches in the DOE methodologies (Gruending et al., 2009; Karimi et al., 2010). Factorial design can be used in determining the influence of multiple factors in a system, which is proven satisfactory in dealing with linear problems. If the relationship between the parameters and responses can be adequately represented and the optimal values of the responses captured, the factorial design will be one of the most efficient methods for optimization (Wu et al., 2012). Otherwise, in which interacting effects between parameters with clear curvatures, a nonlinear method should be applied. Minimum run resolution V, as one of the most widely-used factorial design method, was implemented in this study. While linear optimization could be used for the linear DOE model, which was obtained by fractional factorial design, to predict the optimal values.

The overall framework of the DOE aided parameterization method is as illustrated in Fig.10. This process can be fulfilled by the following steps:

- 1) Choose the most relevant input parameters in oil spill model. The effects of the parameters can usually be found in the model's manual and literature. The parameters can be chosen based on traditional sensitivity analysis method.
- 2) Determine the upper and lower bounds of the chosen parameters based on the measurements, manuals, or suggested values from the experts and previous studies. The boundary can also determine based on the trial tests by running the numerical model, in comparison with the observed data or literature.

- 3) Select and calculate the responses which can represent the goodness-of-fit between observation and numerical simulation.
- 4) Analyze the relationships between responses and the corresponding parameter combinations using the DOE method.
- 5) Analyze the sensitivity and interactions between the responses and the corresponding parameters using the DOE method. The regression equations for the predicted responses can be produced.
- 6) Apply the minimum resolution V method to optimize the DOE predicted responses. The optimal parameters set can be obtained and then input into the numerical model to achieve the actual responses.
- 7) Compare the actual responses with the predicted optimized responses, and check if the optimized responses sufficiently close to the actual ones. If yes, go to step 8. Otherwise, go to step 4 or reselect DOE method.
- 8) The optimal response and the corresponding parameter combinations can be determined.
- 9) Verify the oil spill model for potential predictions.

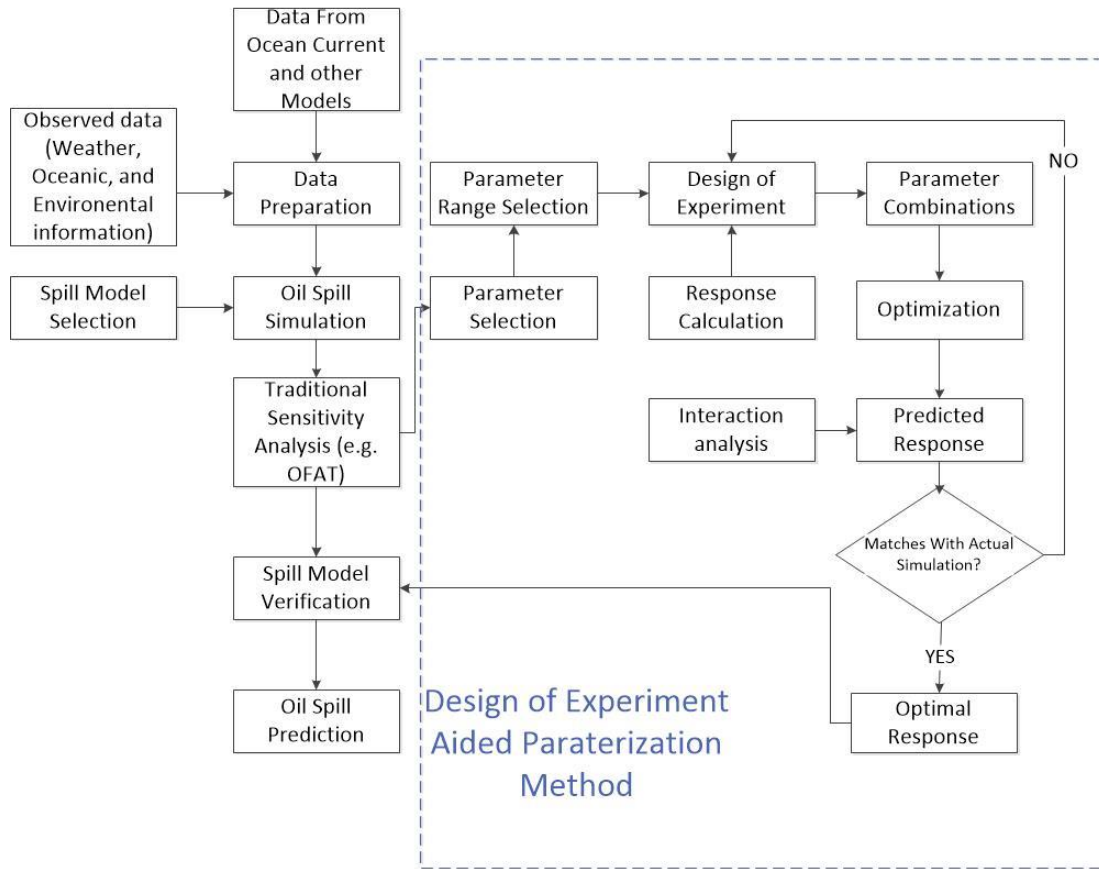


Figure 10 The overall framework of the application of DOE aided method

4.3 Case study

The study area, Grand Bank, is located at 350 kilometres southeast of St. John's, Newfoundland, Canada. The Terra Nova field is located at 46° 28' N, 48°27' W, and has been put into operation since 2002. In November 21st, 2004, more than 1,000 barrels of oil released into ocean. This accident happened at Terra Nova FPSO resulted in more than 10,000 sea birds killing directly by the 793 km² oil slick coverage (Wilhelm et al., 2007). It remains the largest marine oil spill in the history of NL. The case study of Terra Nova can be helpful in prevention and response planning of oil spills in this area. The GNOME is an oil spill trajectory model developed by the Emergency Response Division of NOAA's Office of Response and Restoration. With its Minimum Regret trajectory mode, parameter uncertainties should be determined to obtain a better performance in oil spill simulation. To have a better understanding of the Terra Nova spill case, and to explore the interactions between parameters in the GNOME, a DOE aided parameterization method is needed.

4.3.1 Parameter analysis

In the oil spill simulation models, the important parameters and their effects are usually provided in the model's manuals. For the GNOME model, it has been applied in many case studies, through the literature, the suggestions of local experts, and the trial tests, the upper and lower bounds for each parameter can be determined. Six parameters are considered to be important in the calibration method and described as follows:

- (1) Windage, A, is the movement of oil by the wind. It is typically about 3% of the wind speed based on analytical derivation and empirical observation that oil tends to spread out in the direction of the wind (Stolzenbach et al., 1977). Experience and observation have led us to use a factor in the range 1-4%, possibly adjusted based on overflight reports (Lehr and Simecek-Beatty, 2000).
- (2) Along current uncertainty, B, means forward and backward percentages of the velocity.
- (3) Cross current uncertainty, C, means left and right percentages of the velocity, that are used in the direction perpendicular to the velocity to make up the cross-current uncertainty range.
- (4) Wind speed scale, D, is related to how much the wind speeds are likely to be in error.
- (5) Angle scale (radians), E, is related to how much the wind forecast directions will be off.
- (6) Random spreading, i.e. diffusion, F, is done by a simple random walk with a square unit probability. Following the GNOME Technical Documentation, a low value of F would be 1,000 cm²/s, and a high value would be between 100,000 to 1,000,000 cm²/s. The chosen values of the upper and lower bounds are shown in Table 1.

Table 1 Key parameters and their upper and lower bound values

Factor (parameter)	Lower bound	Upper bound value
A: windage (%)	1.2	1.5
B: along current uncertainty (%)	5	50
C: cross current uncertainty (%)	5	50
D: wind speed scale	1	5
E: wind direction scale (radians)	0.2	0.8
F: Diffusion coefficient (cm ² /s)	100000	150000

4.3.2 Response selection

When using a SAR image to calibrate the result from the trajectory models, coverage between the oil slicks from SAR image and the simulated result from the models could be one of the most significant response for consideration. As the uncertainty ranges are considered in the parameter analysis, the spreading area, slick location and the distribution of the oil particles (each particle represents certain volume of spilled oil) will change at a large scale. To calculate the coverage value from the different sets of parameters, a consistent method should be considered. One method is to count the number of cells in the simulated binary image occupied oil particles that overlap with the grid cells with oil in the satellite image, then to calculate the matching rate in terms of the number of overlapping cells and partially covered cells (Kim et al., 2014). This method can be useful if without considering the uncertainty in the simulation model. Different scenarios of parameter values could result in various oil particles distribution. Some may cause a high density in the slick center but very few and scattered in the outer edge, or output as hypodispersion. Various distribution may lead to a cell that overlapped with both but only a few particles inside, which should not be regarded as fully covered. Particularly in the models like GNOME and OSCAR, more than a thousand of particle number could be set as initial particles. The difference of covered number can be significant. In this study, a modified method was developed. As shown in Fig. 11, to avoid the overestimated coverage, this study assumed that five or more particles in on cell can be considered as 100% covered. One particle in the cell was calculated as 20% coverage. The size of cells can be varied in different cases. Response R1 is shown in eq. (4-1).

$$R1 = D_o / A_{sim} \quad (4-1)$$

Where A_{sim} is the number of total covered cells by the simulated oil slick, and D_o is the number of particles overlapped with the observed coverage in satellite images.

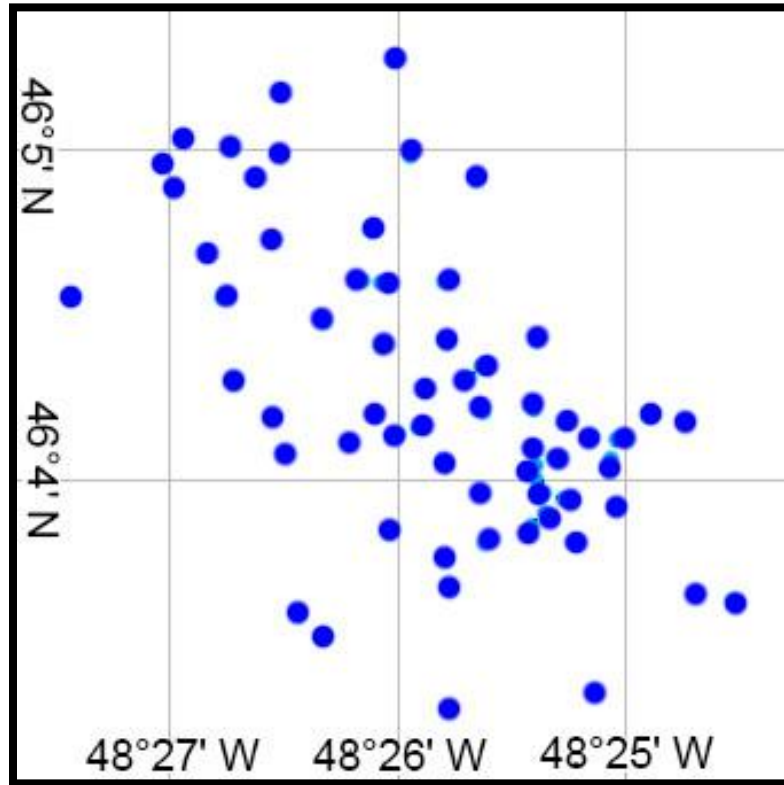


Figure 11 A sample image from the GNOME simulation showing oil particles distribution in the case study

The distance between the simulated and the observed location of oil slicks can also represent the goodness-of-fit in trajectory models. Response R2 derived from the distance between the central locations of the simulated oil slick and the observed oil-covered area. The central locations P were calculated as shown in eq. (4-2).

$$P = (P_1 + P_2 + \dots + P_i) / i \quad (4-2)$$

Where P_i is the geographic coordinate values of latitudes and longitudes.

Although the covered area R1 and the distance R2 can both represent the goodness-of-fit, in some cases, considering the diffusion and advection of oil slicks, while the covered area is large enough, the distance between the simulated location and observed oil slick could be far away. It should be taken into account with a new response which can reflect the R1 and R2 at the same time. Ideally, when the simulated result has the best matches the observed one, the distance should also be the closest approaching to zero. A response R3 was proposed in this study to represent the interaction between R1 and R2 as shown in eq. (4-3).

$$R3 = R1 / R2 \quad (4-3)$$

Where R1 is the coverage between the simulated and observed oil slicks, and R2 is the distance between the central locations of the simulated and observed oil slicks. To obtain good simulation results, maximum value of R1, R3 and minimum R2 would be acquired with optimization.

4.4 Results and discussion

4.4.1 Modeling sensitivity

Totally 23 groups of simulation runs were conducted by the spill model with different combinations of parameters. The sequence of simulations was randomly generated by using the minimum run resolution V factorial design. In this study, Design Expert 7.1® was used to analyze the effects of different parameters. The analysis of variance (ANOVA) for the three responses (R1-R3) are shown in Tables 2-4. The half-normal and normal probability plots of response R1 are shown in Figs. 12 and 13. The result indicated that factors A (Windage), D (Wind speed scale), E (Wind direction scale), AD (interaction between windage and wind speed), BF (interaction between along current and diffusion), and DE (interaction between wind speed and direction) stood as significant to the model. Factors B and F on their own were not significant. However, their interaction, BF, was significant. Hence for the hierarchical reasons, these two factors were included for further analysis. There was no significant curvature measured by the difference between the average of center points and the average of the factorial points in the design space. There were four main diagnostic plots to check the assumptions of ANOVA, including “normal probability plot of residuals”, “residuals vs. predicted”, “residuals vs. run”, and “predicted vs. actual” (Figs. 14-17). With R2 as response, A and EF were significant factors. With R3 as response, factors A, D, E, AD, BE, and DE are significant model terms. Similarly, the analysis results and the associated diagnostic plots for R2 and R3 are provided in Figs. 18–27.

Table 2 ANOVA of minimum runs of design resolution V for response R1

Source	Sum	of	df	Mean	F	p-value
Model	0.076		8	9.9495E-	23.70	<0.0001*
A:Windage	0.018		1	0.018	45.40	<0.0001*
B:Along	1.134E-003		1	1.134E-	2.83	0.1163
D: Wind speed	2.248E-003		1	2.248E-	5.61	0.0340*
E: Wind	0.028		1	0.028	68.92	<0.0001*
F: Diffusion	2.006E-005		1	2.006E-	0.050	0.8264
AD	3.869E-003		1	3.869E-	9.66	0.0083*
BF	2.839E-003		1	2.839E-	7.09	0.0196*
DE	4.055E-003		1	4.055E-	10.12	0.0072*
Curvature	7.137E-005		1	7.137E-	0.18	0.6799
Residual	5.209E-003		13	4.007E-		
Cor Total	0.081		22			
Std. Dev.	0.020		R ²	0.9358		
Mean	0.10		Adi R ²	0.8963		
C. V. %	19.32		Pred R ²	N/A		
Press	N/A		Adeq	16.162		

*means significant

Table 3 ANOVA of minimum runs of design resolution V for response R2

Source	Sum	of	df	Mean	F	p-value
Model	174.23		4	43.56	88.47	<0.0001*
A:Windage	149.10		1	149.10	302.8	<0.0001*
E: Wind	0.080		1	0.080	0.16	0.6911
F: Diffusion	0.56		1	0.56	1.14	0.3007
EF	4.47		1	4.47	9.09	0.0078*
Curvature	8535E-003		1	8.535E-	0.017	0.8968
Residual	8.37		17	0.49		
Cor Total	182.61		22			
Std. Dev.	0.70		R ²	0.9542		
Mean	25.87		Adi R ²	0.9434		
C. V. %	2.71		Pred R ²	N/A		
Press	N/A		Adeq	18.362		

*means significant

Table 4 ANOVA of minimum runs of design resolution V for response R3

Source	Sum	of	df	Mean	F	p-value
Model	8.651E-005		8	1.081E-	21.24	<0.0001*
A:Windage	1.109E-005		1	1.109E-	21.79	0.0004*
B:Along	1.208E-006		1	1.208E-	2.37	0.1474
D: Wind speed	1.963E-006		1	1.963E-	3.86	0.0713
E: Wind	4.044E-005		1	4.044E-	79.42	<0.0001*
F: Diffusion	1.114E-008		1	1.114E-	0.022	0.8847
AD	5.266E-006		1	5.266E-	10.34	0.0068*
BF	3.549E-006		1	3.549E-	6.97	0.0204*
DE	4.686E-006		1	4.686E-	9.20	0.0096*
Curvature	1.796E-007		1	1.796E-	0.35	0.5627
Residual	6.619E-006		13	5.091E-		
Cor Total	9.331E-005		22			
Std. Dev.	7.135E-004		R ²	0.9289		
Mean	3.898E-003		Adi R ²	0.8852		
C. V. %	18.30		Pred R ²	N/A		
Press	N/A		Adeq	15.185		

*means significant

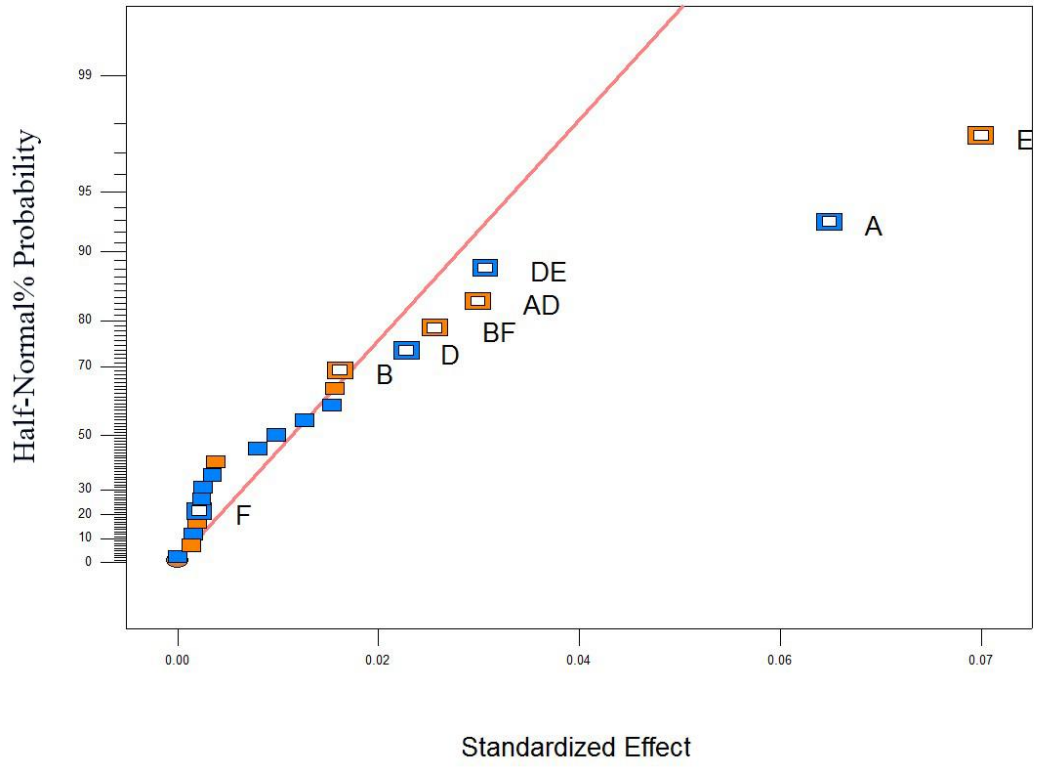


Figure 12 Half-normal probability plot for response R1

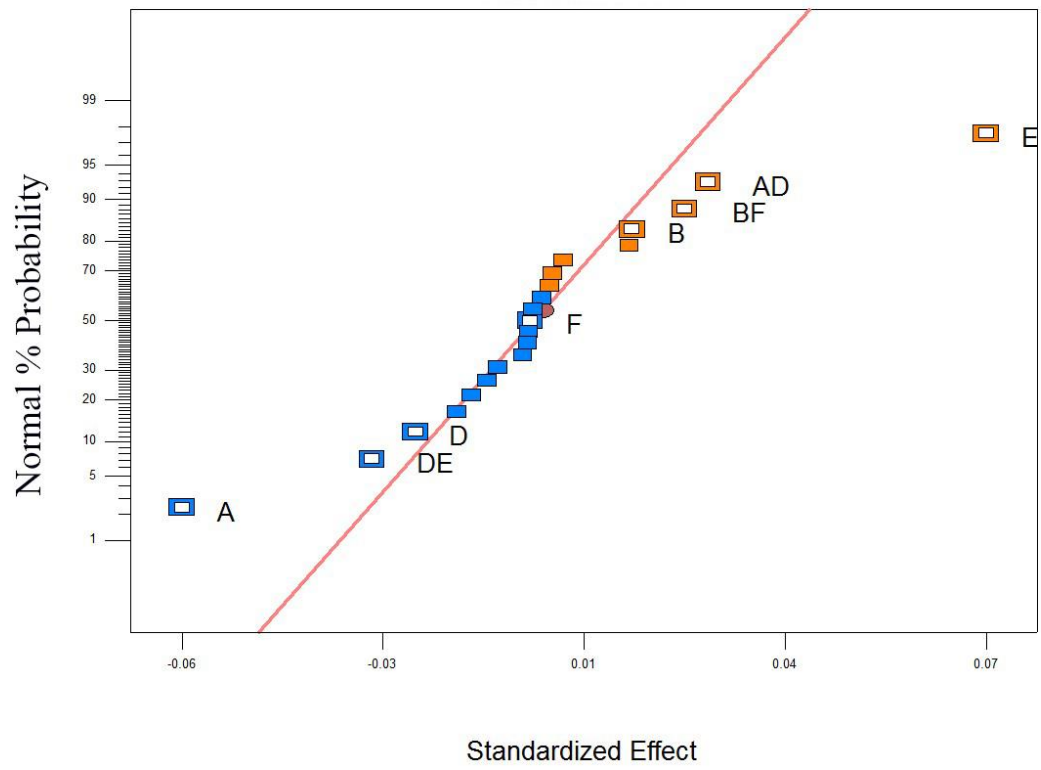


Figure 13 Normal probability plot for response R1

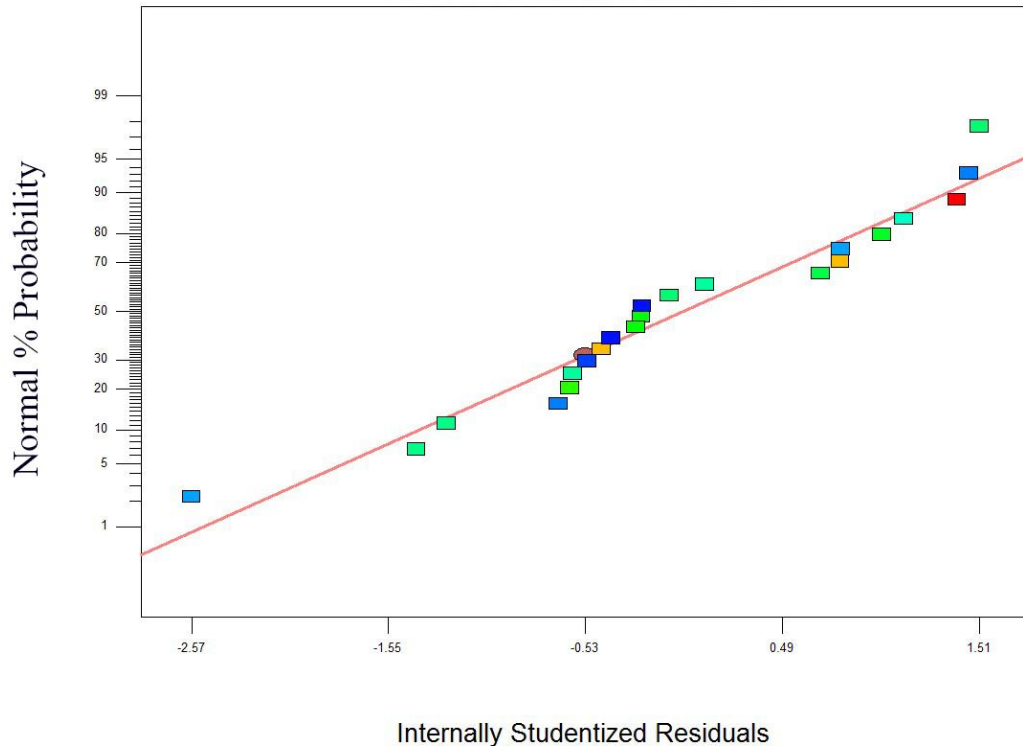


Figure 14 Diagnostic plots for assumption of ANOVA: normal probability of residuals for response

R1

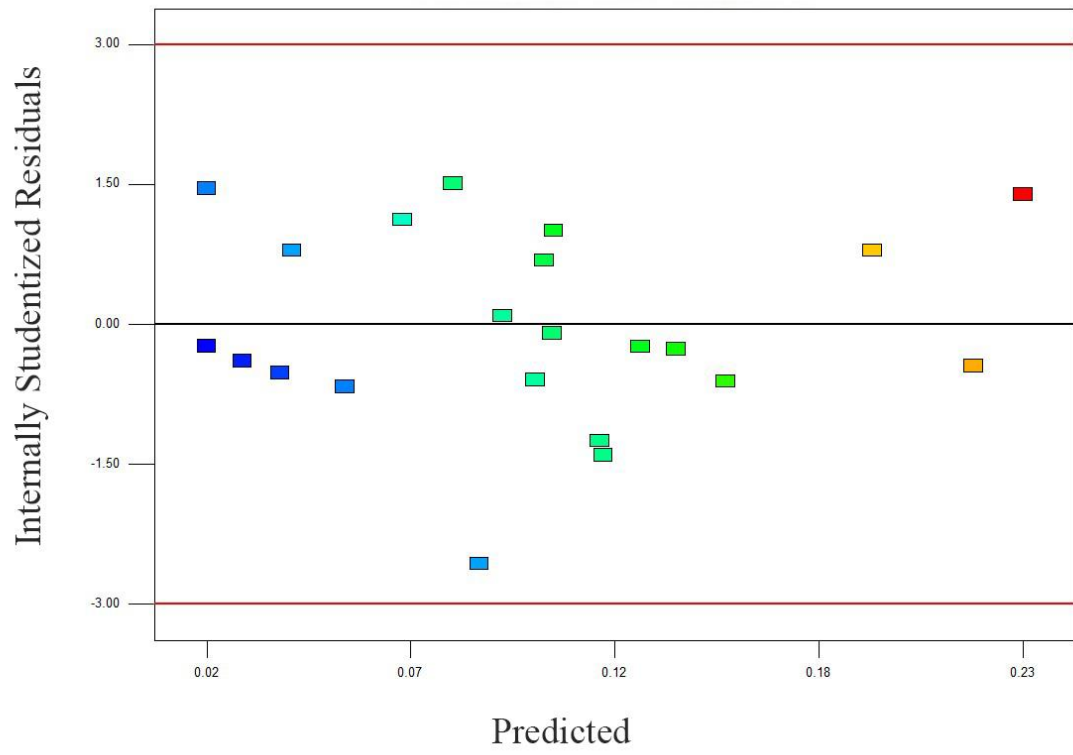


Figure 15 Diagnostic plots for assumption of ANOVA: residuals vs. predicted for response R1

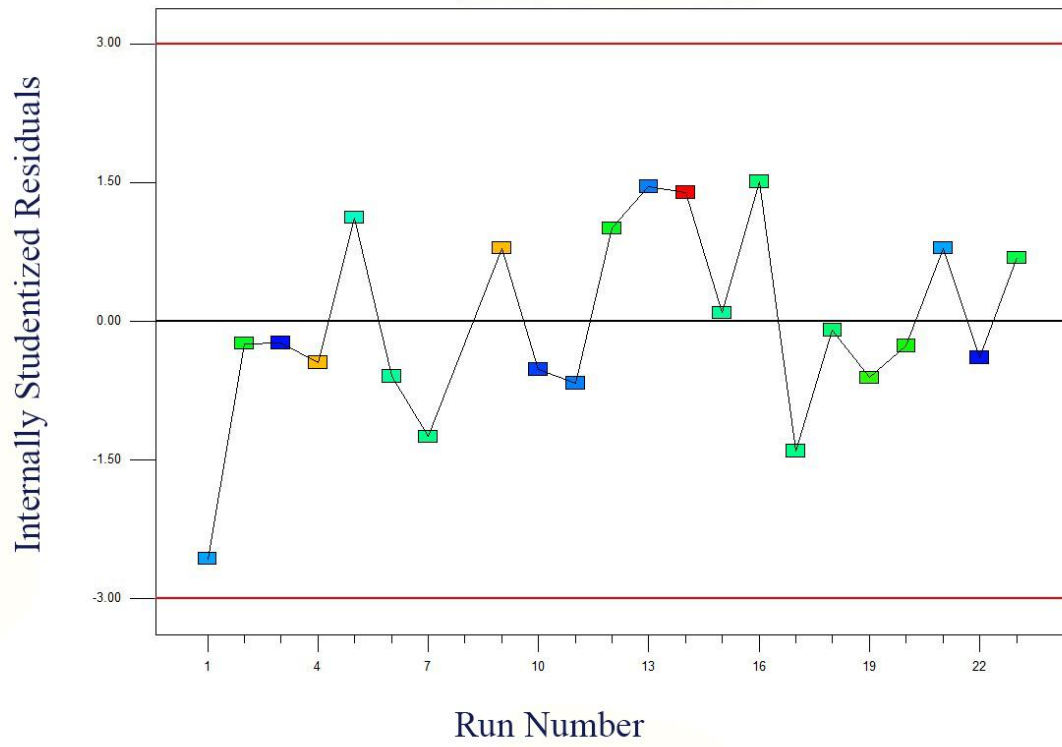


Figure 16 Diagnostic plots for assumption of ANOVA: residuals vs. run for response R1

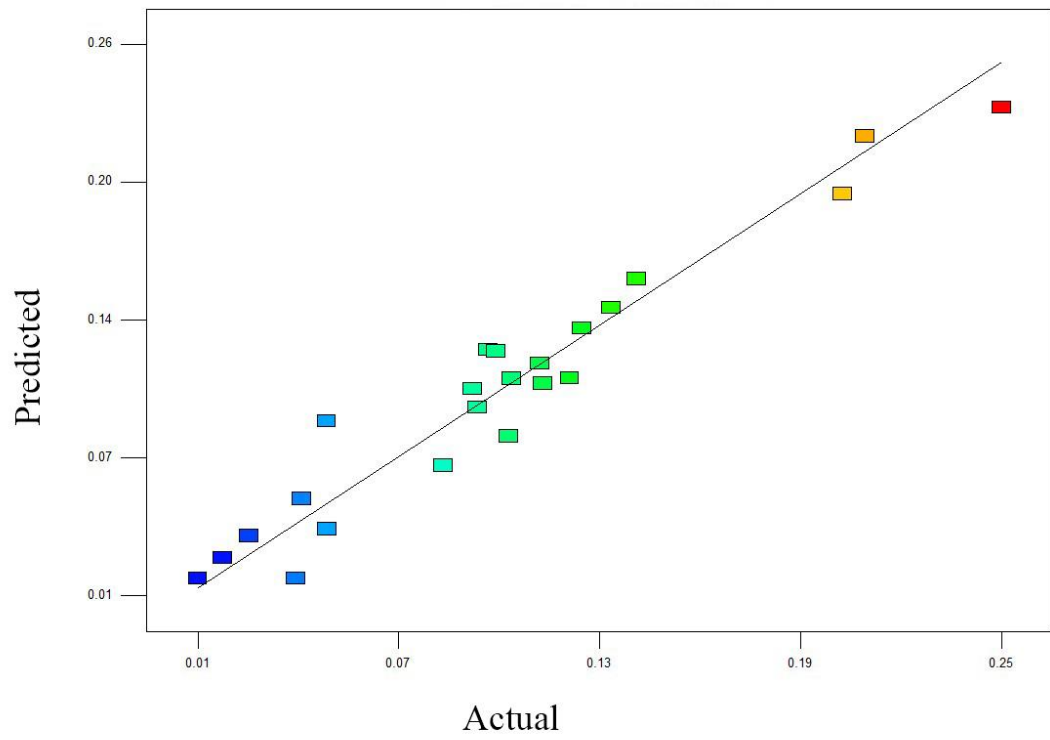


Figure 17 Diagnostic plots for assumption of ANOVA: predicted vs. actual for response R1

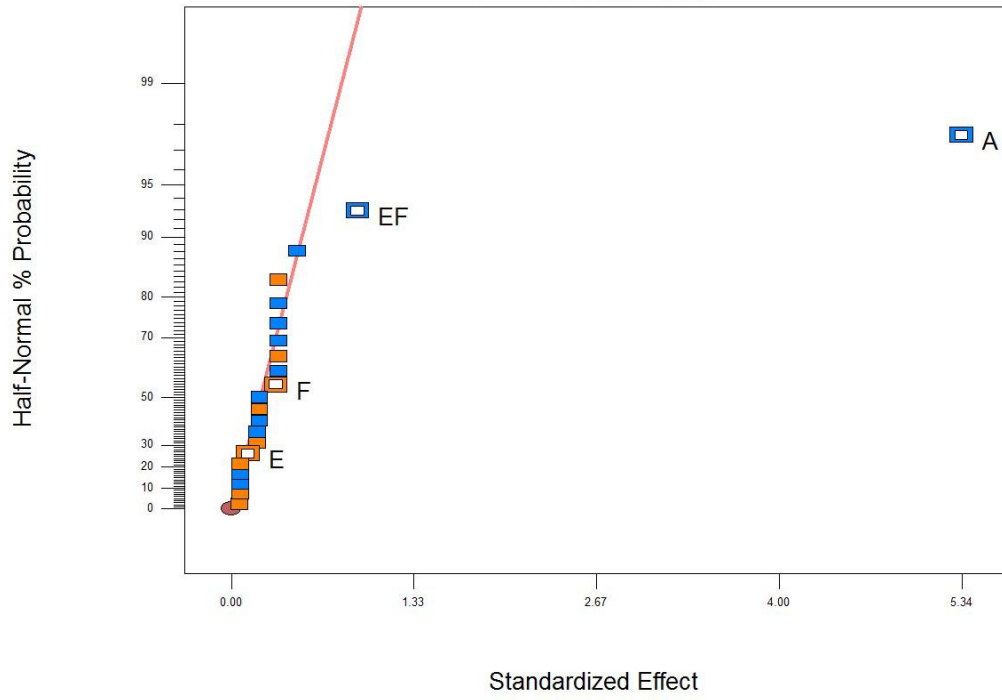


Figure 18 Half-normal probability plot for response R2

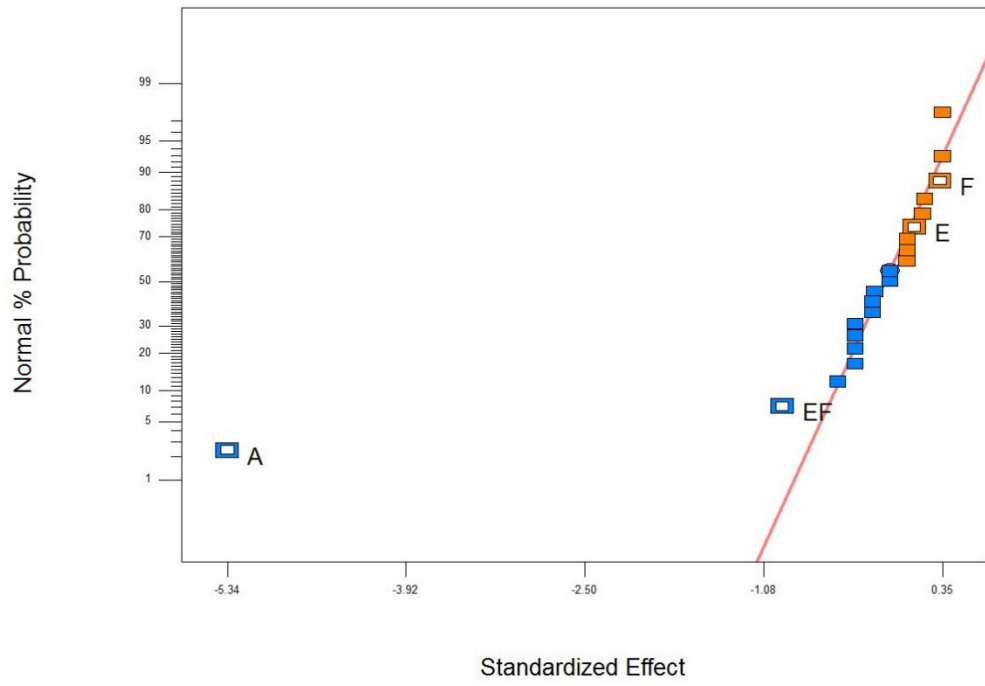


Figure 19 Normal probability plot for response R2

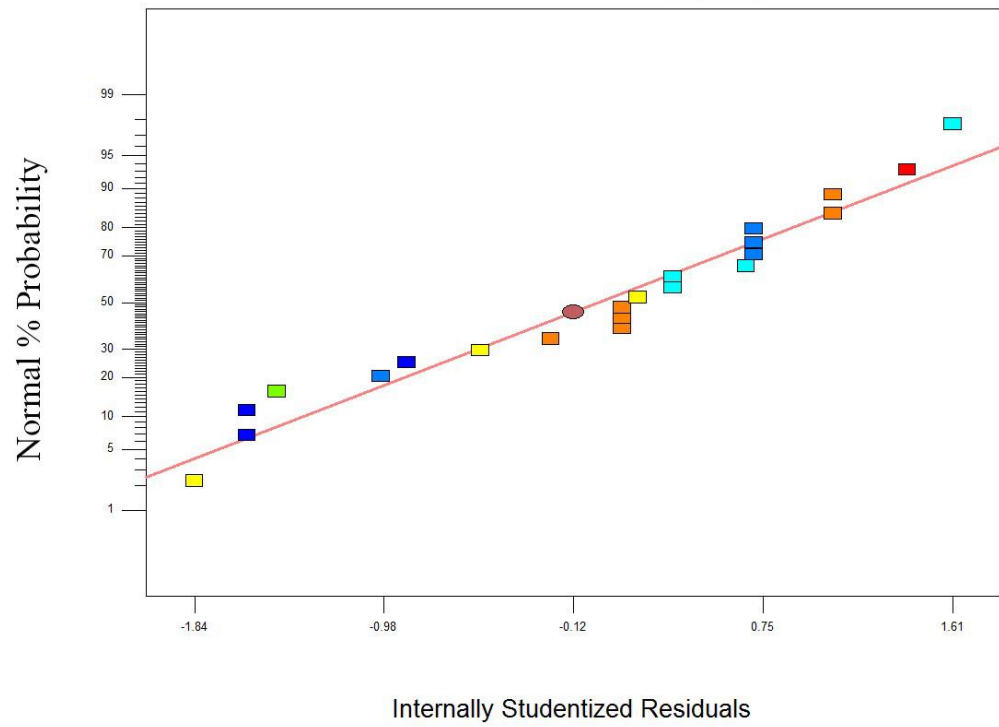


Figure 20 Diagnostic plots for assumption of ANOVA: normal probability of residuals for response R2

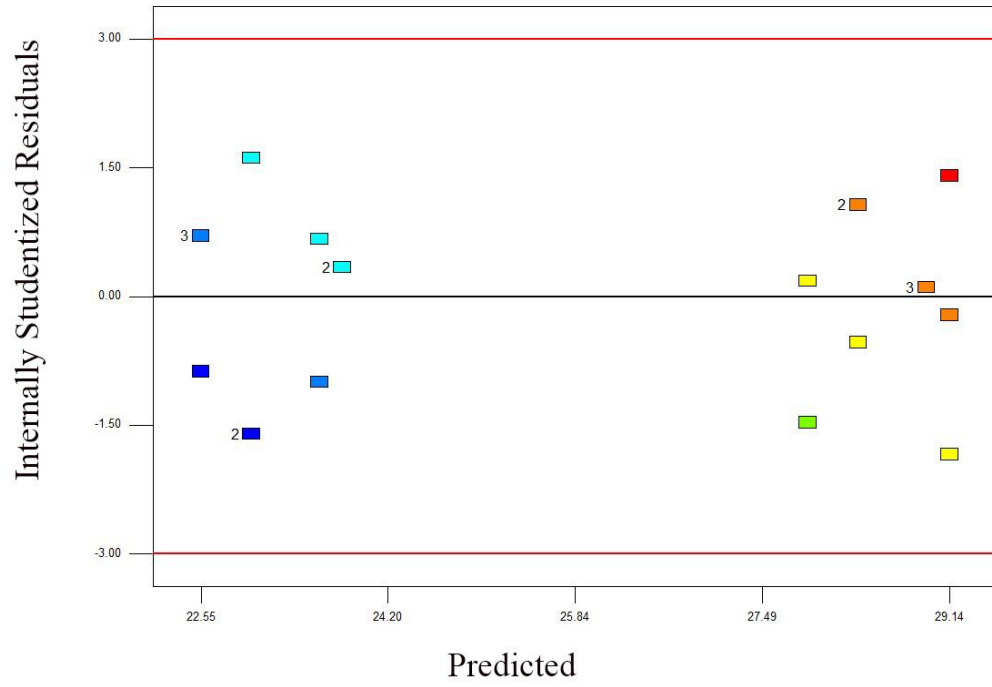


Figure 21 Diagnostic plots for assumption of ANOVA: residuals vs. predicted for response R2

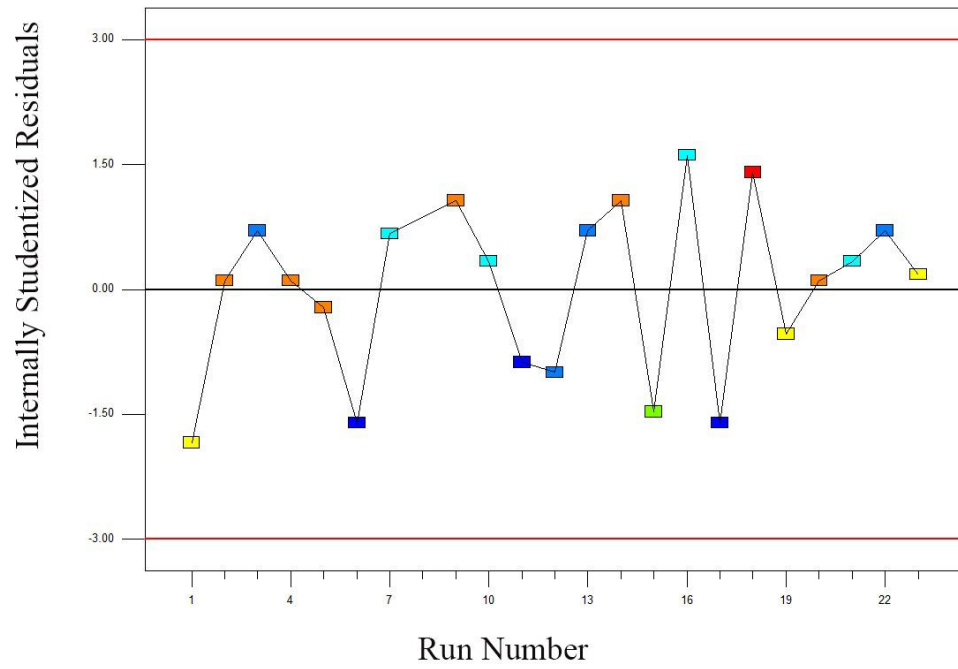


Figure 22 Diagnostic plots for assumption of ANOVA: residuals vs. run for response R2

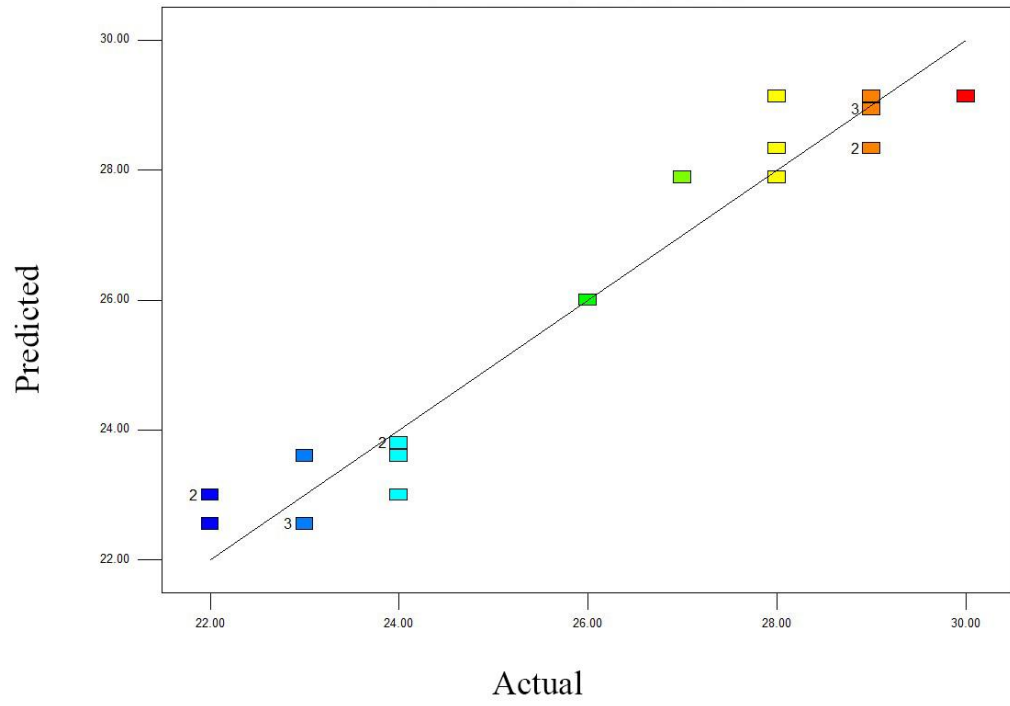


Figure 23 Diagnostic plots for assumption of ANOVA: actual vs. predicted for response R2

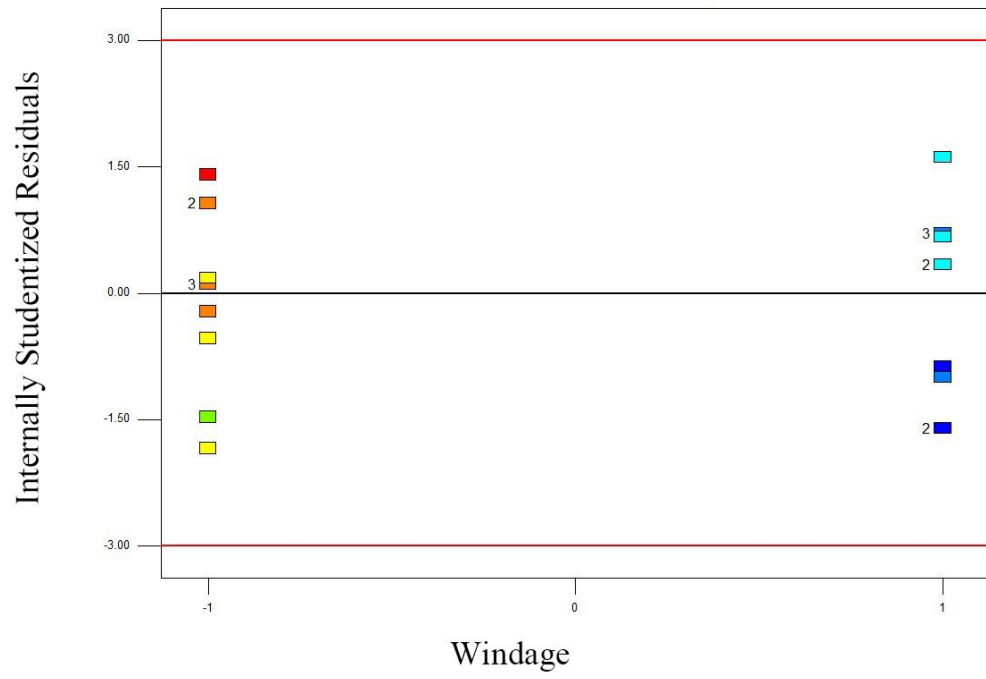


Figure 24 Diagnostic plots for assumption of ANOVA: residuals vs. windage for response R2

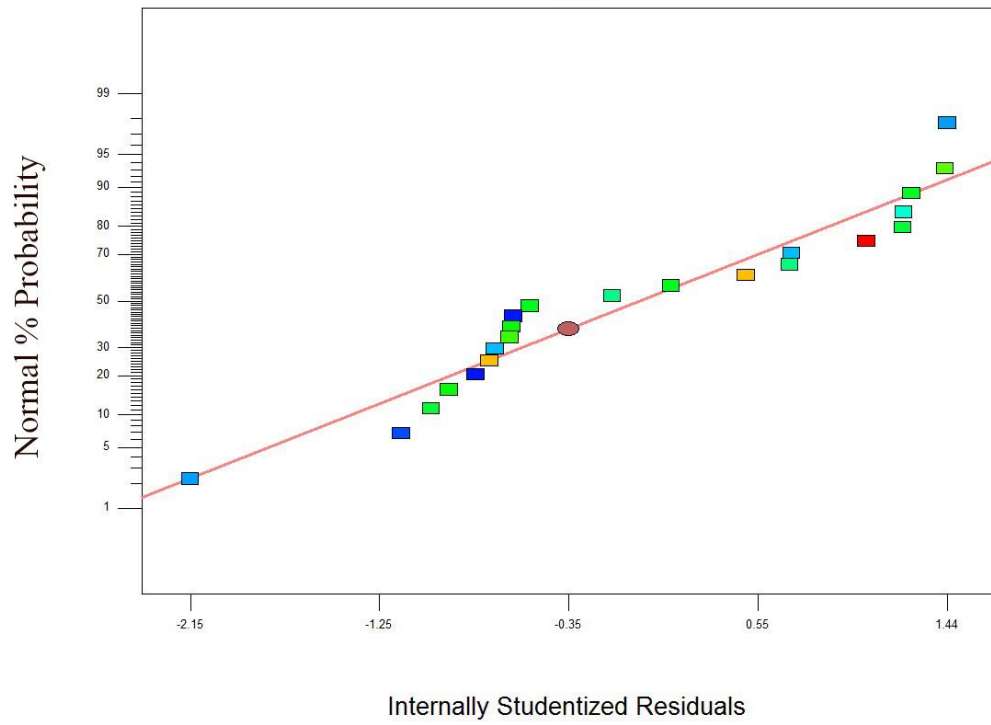


Figure 25 Diagnostic plots for assumption of ANOVA: normal probability of residuals for response R2

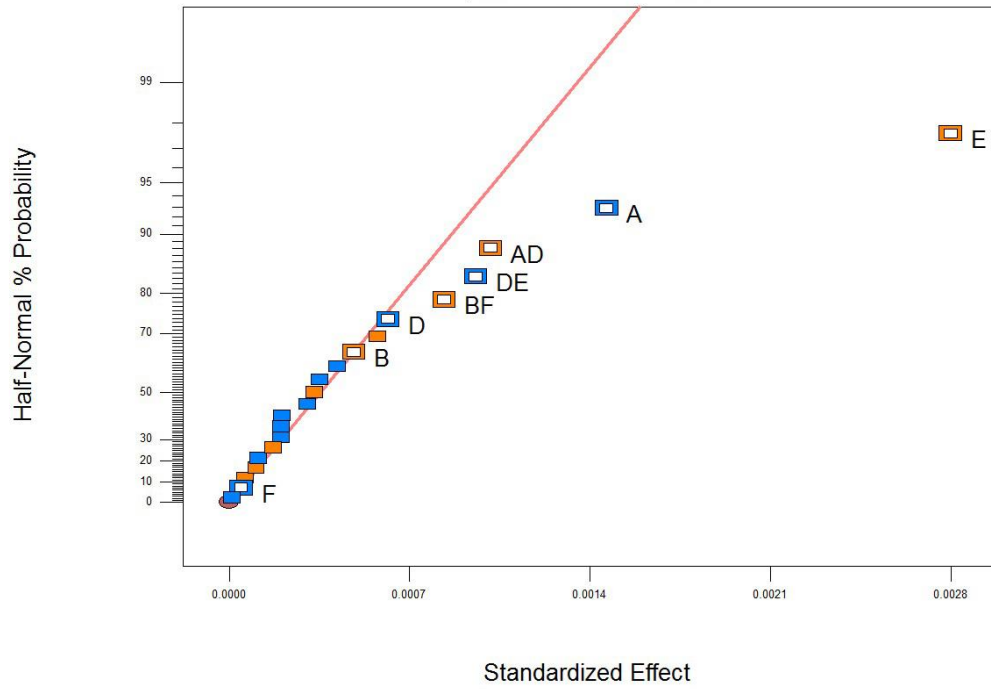


Figure 26 Half-normal probability plot for response R3

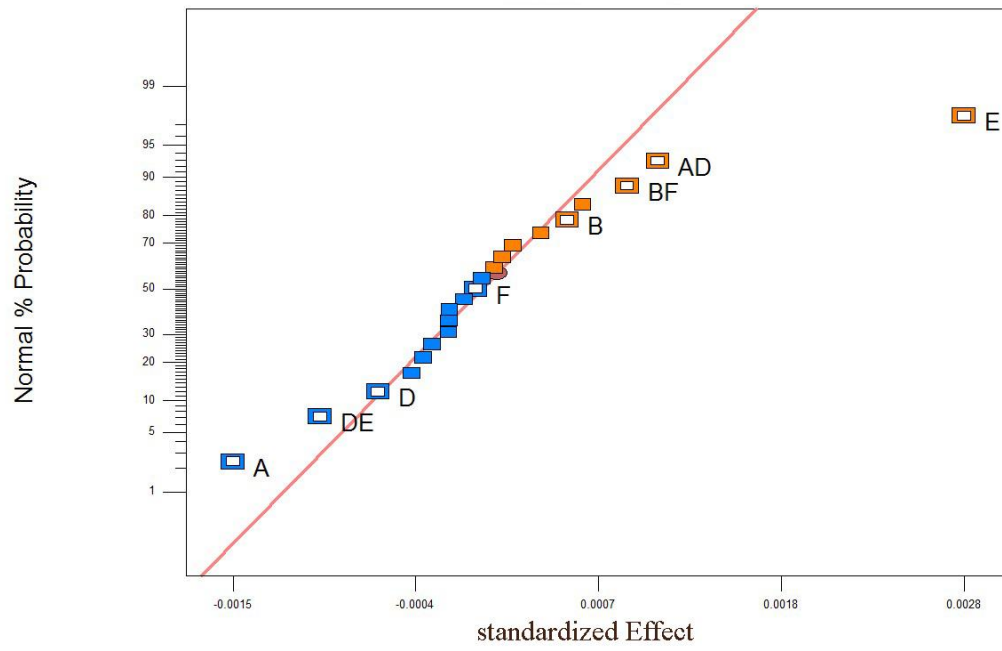


Figure 27 Normal probability plot for response R3

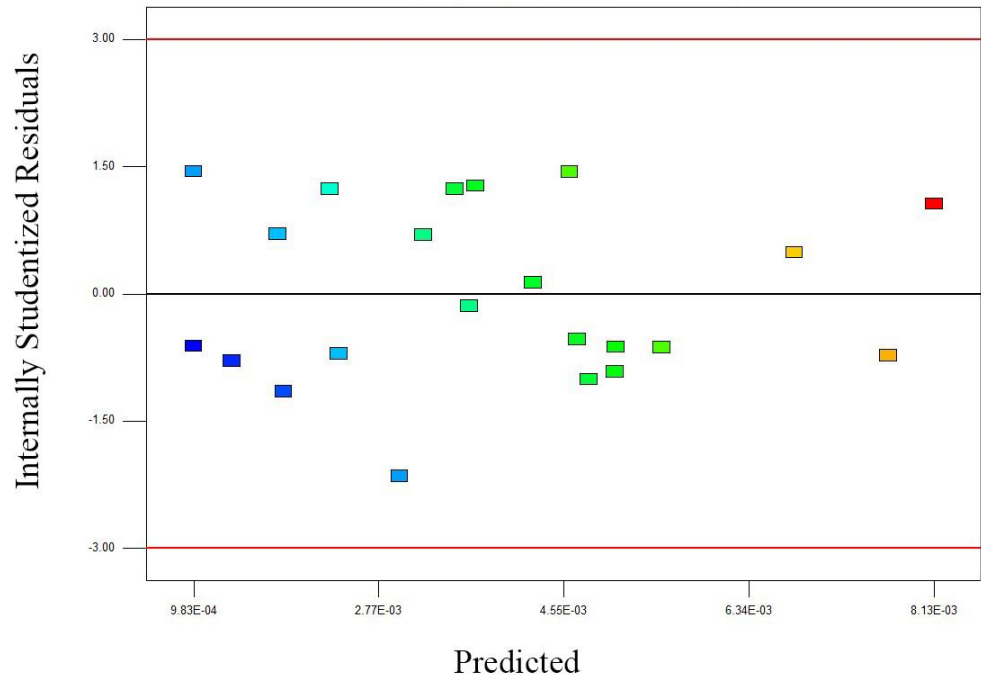


Figure 28 Diagnostic plots for assumption of ANOVA: residuals vs. predicted for response R3

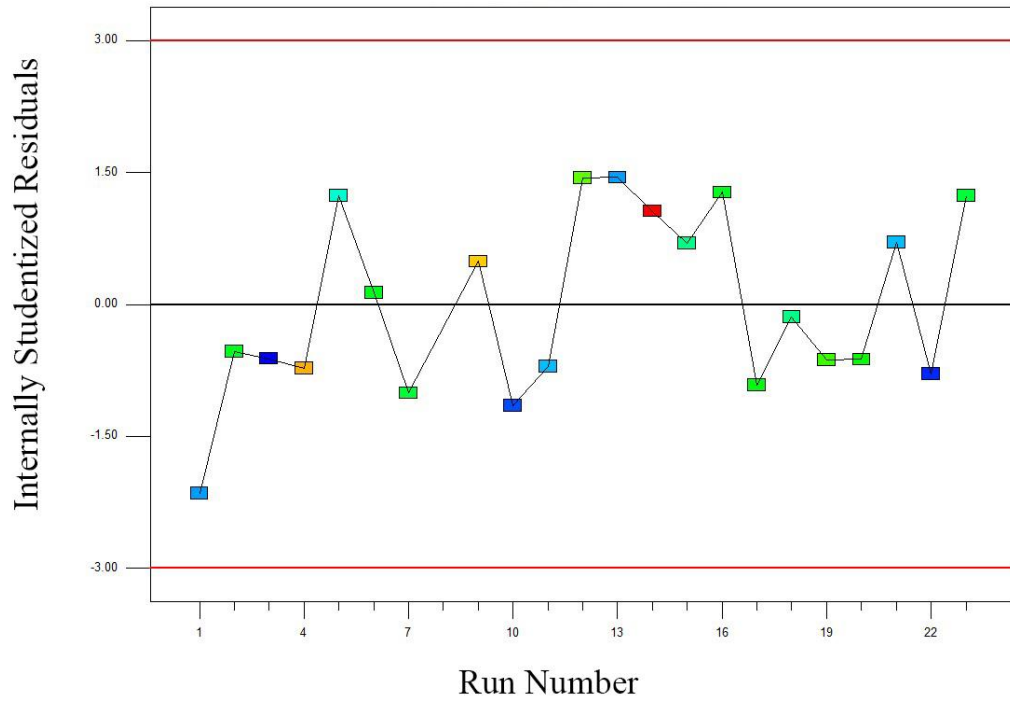


Figure 29 Diagnostic plots for assumption of ANOVA: residuals vs. run for response R3

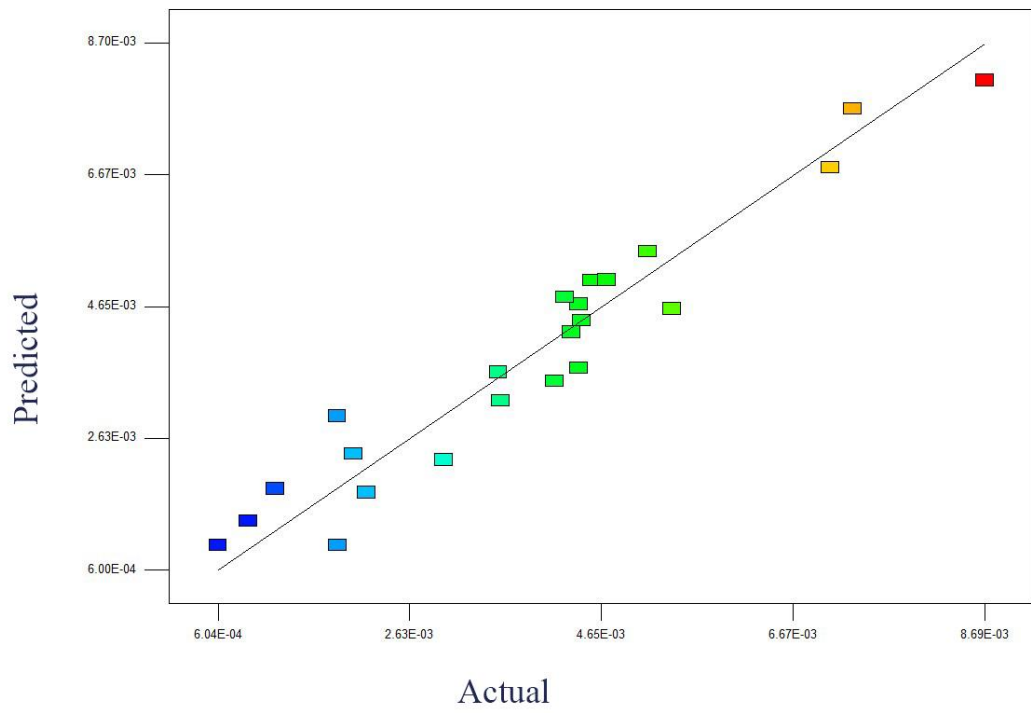


Figure 30 Diagnostic plots for assumption of ANOVA: actual vs. predicted for response R3

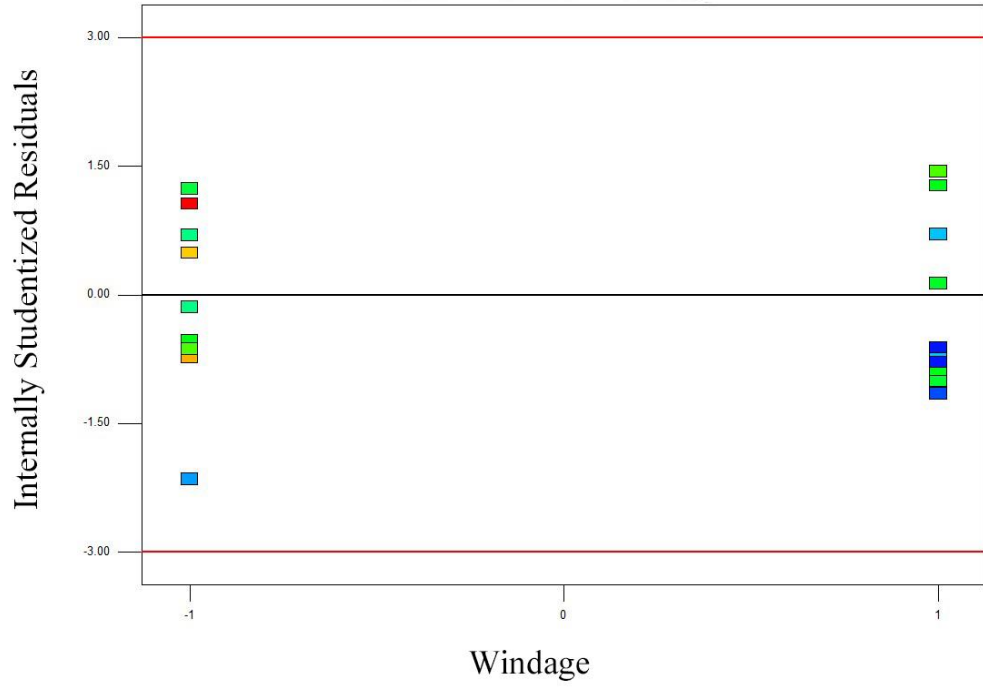


Figure 31 Diagnostic plots for assumption of ANOVA: residuals vs. windage for response R3

Viewed from Fig. 14, all the residuals were close to the diagonal line; therefore, the normal distribution assumption was satisfied. In Fig. 15, because all the residual points were scattered randomly all over the graph within the upper and lower bounds instead of accumulating in the other areas, the assumption of homoscedasticity was fulfilled. Fig. 16 indicated that all the residual points were spread within upper and lower bounds, showing no patterns. This plot approves that the independence assumption was satisfied. In Fig. 17, all the points were close to the diagonal line, showing that the “predicted vs. actual” plot was satisfactory and the model fitted well with the observation. Therefore, all the diagnostic plots indicated that all the required assumptions of ANOVA were met. Similarly, viewed from Figs. 18-31, responses R2 and R3 also met all the required assumptions of ANOVA. It was indicated that the DOE aided method can meet the requirement of parameters analysis of oil spill simulation results derived from GNOME.

Figs. 32-34 show the 3D surface model graphs of the interactions of significant parameters. It clearly shows that to obtain the highest R1 value, the maximum values for “Along current uncertainty” (B), “Wind direction scale” (E), “diffusion coefficient” (F), and the minimum values for “Windage” (A) and “Wind speed scale” (D) were preferred. Fig. 35 shows the interaction between “Wind direction” and “diffusion” when R2 as the response. We can noticed that either the uncertainties of wind direction or the diffusion can lead to the negative effect to the value of R2 (with further distance), but when the uncertainties of both were large enough, the effect became positive. The figs. 36-38 show that R3 had the similar trend of interactions of the important parameters with those of R1, which meant coverage showed a stronger effect than the distance if considered both values in the response R3. So

in the simulation of oil spill, the performance of shape and location of oil slick is more important than the distance between simulated and observed results. Once the information were collected from DOE process, prediction could be conducted to check the accuracy of this response model.

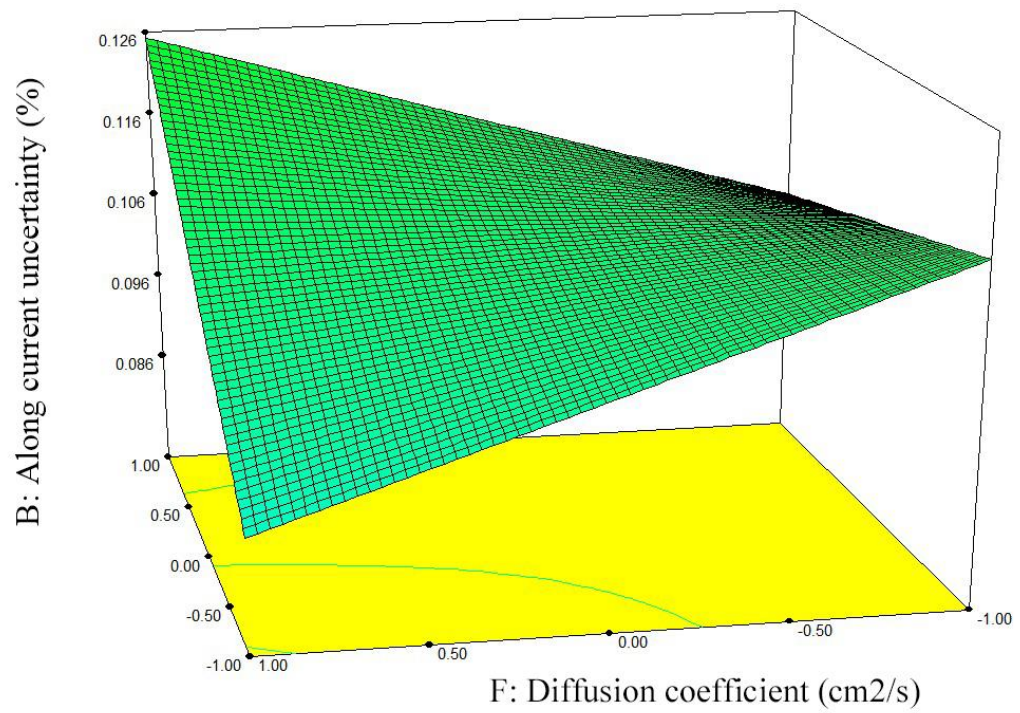


Figure 32 Three dimensional surface graph of interaction between factors B and F for response R1

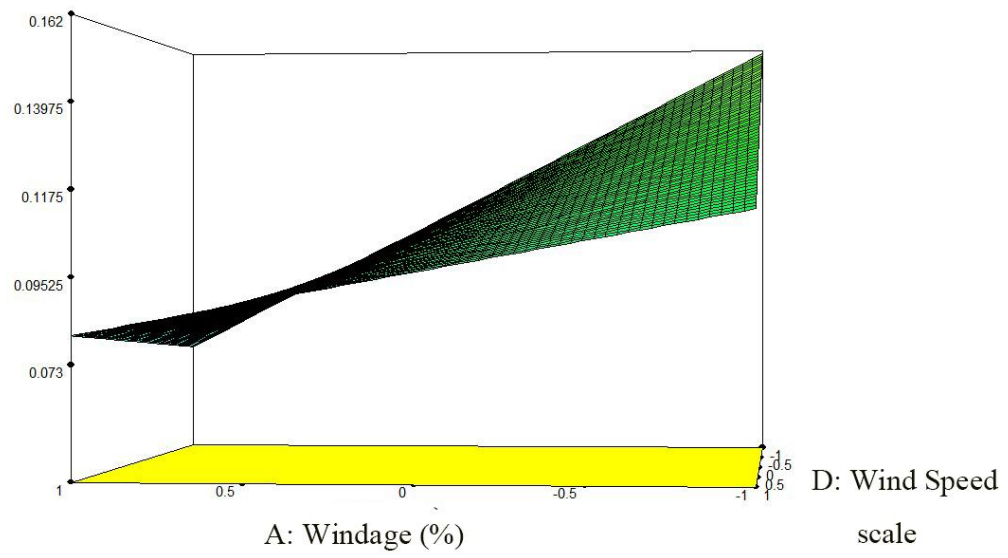


Figure 33 Three dimensional surface graph of interaction between factors A and D for response R1

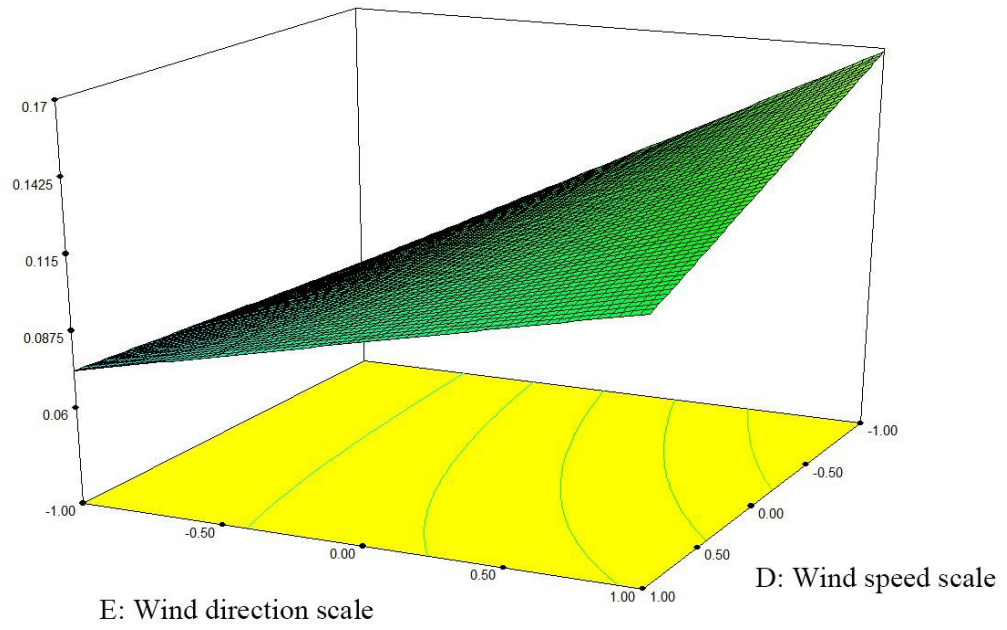


Figure 34 Three dimensional surface graph of interaction between factors E and D for response R1

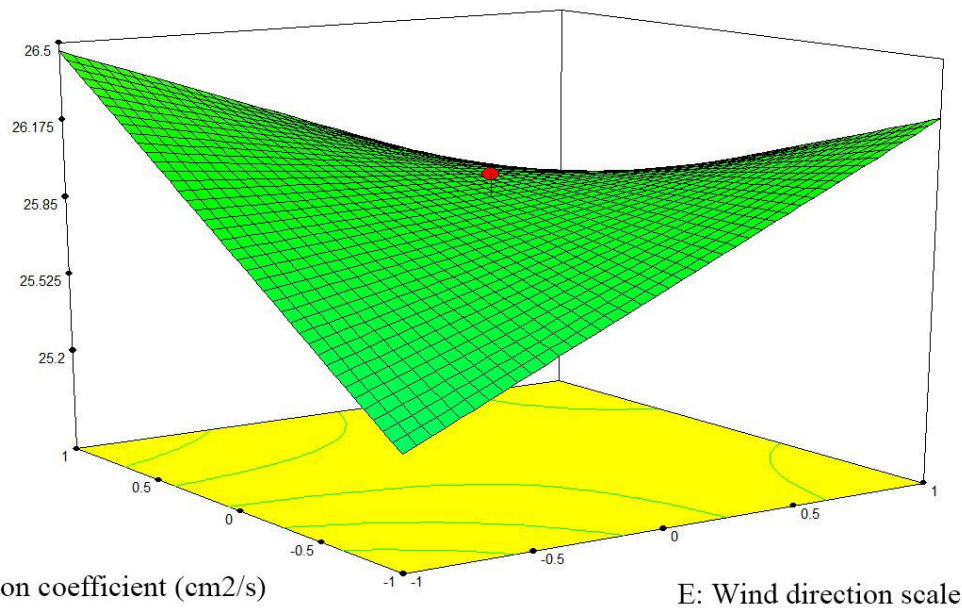


Figure 35 Three dimensional surface graph of interaction between factors E and F for response R2

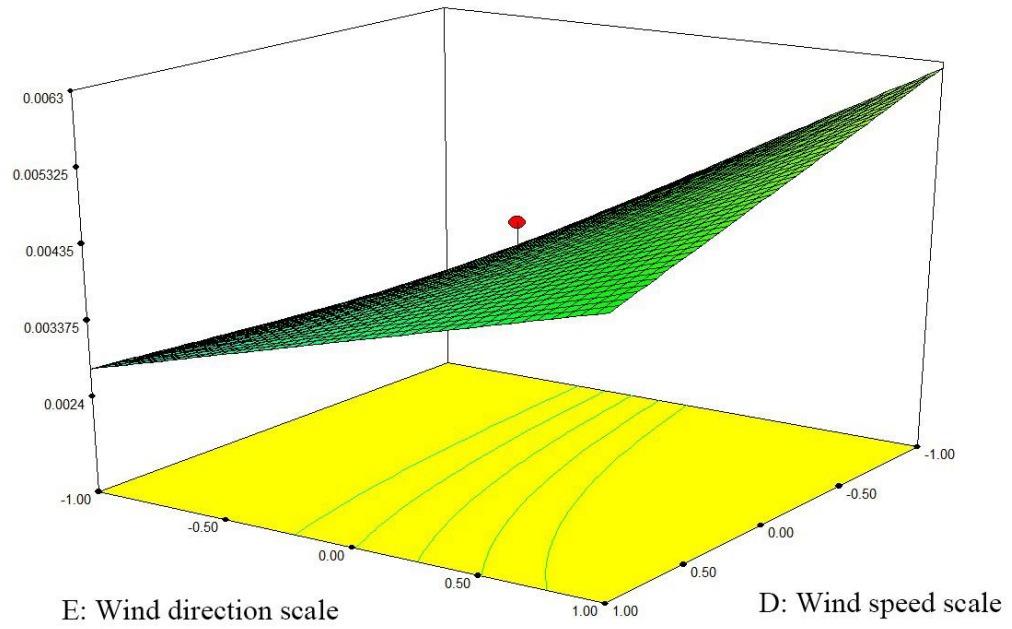


Figure 36 Three dimensional surface graph of interaction between factors E and D for response R3

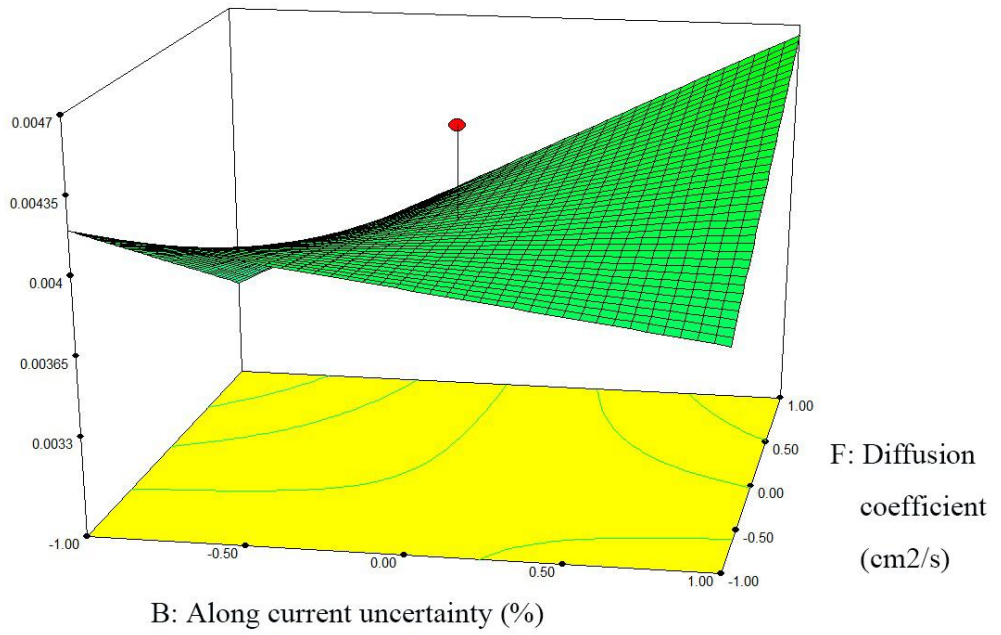


Figure 37 three dimensional surface graph of interaction between factors B and F for response R3

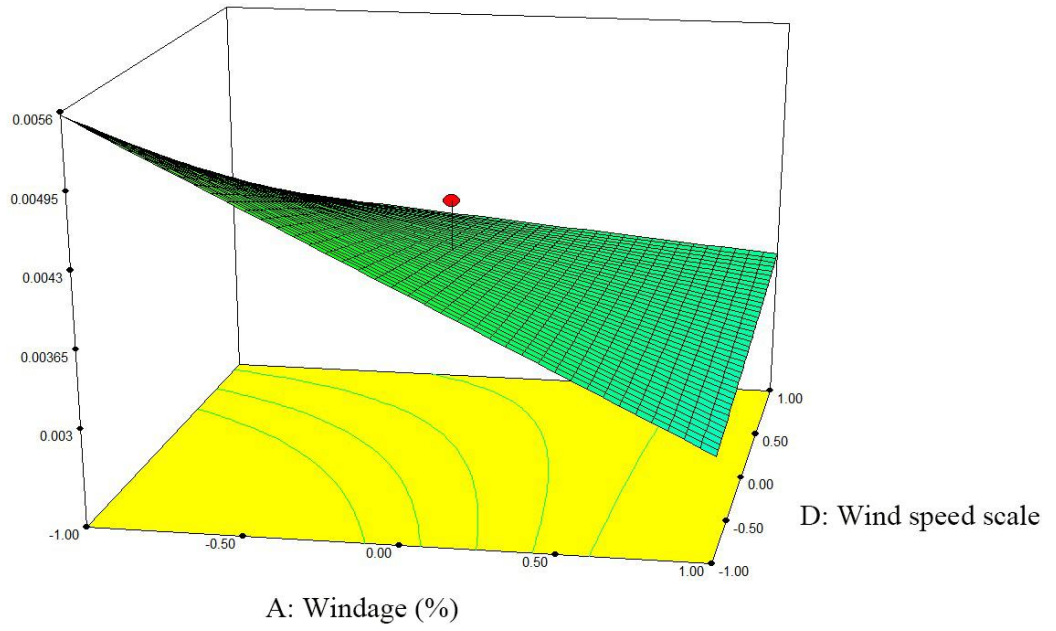


Figure 38 Three dimensional surface graph of interaction between factors A and D for response R3

4.4.2 Calibration and validation

The predicted regression equations for responses R1, R2 and R3 in terms of coded factors are given as follows:

$$R1 = 0.11 - 0.030 * A + 7.466 * 10^{-3} * B - 0.010 * D + 0.037 * E - 9.930 * 10^{-4} * F + 0.014 * A * D + 0.012 * B * F - 0.014 * D * E \quad (4 - 4)$$

$$R2 = 25.91 - 2.67 * A + 0.061 * E + 0.16 * F - 0.46 * E * F \quad (4 - 5)$$

$$R3 = 4.004 * 10^{-3} - 7.420 * 10^{-4} * A + 2.437 * 10^{-4} * B - 3.069 * 10^{-4} * D + 1.417 * 10^{-3} * E - 2.340 * 10^{-5} * F + 5.187 * 10^{-4} * A * D + 4.289 * 10^{-4} * B * F - 4.893 * 10^{-4} * D * E \quad (4 - 6)$$

Similar to the previous conclusion based on the ANOVA analysis in Section 4.4.1, the highest R1 value was derived by taking the maximum values for “Along current uncertainty”, “diffusion coefficient” and “Wind direction scale”, the minimum values for “Windage” and “Wind speed scale”. The optimized results were further verified by using Lingo® through linear optimization for eq. (4-4). To validate the predicted maximum R1, these values combined with other parameters using their original values were set as the new input data for the GNOME model. The new simulation results showed that the R1 for the new setting was 0.252, which was close to the R1 value of 0.231 as predicted by the minimum resolution V response model.

The simulated data were also used to calculate the R2 and R3. R2 with the new setting was 22, which was close to the R2 value of 22.55 as predicted by the minimum resolution V response model. R3 with the new setting was 0.0087, which was close to the R3 value of 0.0081 as predicted by the minimum resolution V response model. It demonstrated that the

proposed DOE aided parameterization method was capable of and effective in determining the optimal combination of parameters in the GNOME model in order to improve the performance of oil spill simulation. In this case, the minimum resolution V response model could adequately represented the relationship between key parameters and the three responses calculated from both observation and simulation from the GNOME model.

The coefficient list and the final equations obtained from ANOVA of minimum resolution V response model were very useful to investigate the contribution of different parameters and to help researchers evaluate the uncertainties of parameters in the oil spill modeling. The coefficient list of responses R1, R2 and R3 are shown in Tables 5-7.

Table 5 Coefficient list of the significant terms for response R1

Factor	Coefficient	df	Standard	95% CI	95% CI	VIF
Intercept	0.11	1	4.336E-003	0.097	0.12	
A: Windage	-0.030	1	4.460E-003	-0.040	-0.020	1.09
B: Along	7.466E-003	1	4.438E-003	-2.121E-	0.017	1.08
D: Wind speed	-0.010	1	4.385E-003	-0.020	-9.132E-	1.06
E: Wind	0.037	1	4.460E-003	0.027	0.047	1.09
F: Diffusion	-9.930E-004	1	4.438E-003	-0.011	8.594E-	1.08
AD	0.014	1	4.524E-003	4.285E-	0.024	1.11
BF	0.012	1	4.557E-003	2.286E-	0.022	1.13
DE	-0.014	1	4.524E-003	-0.024	-4.619E-	1.11
Center Point	8.644E-003	1	0.020	-0.036	0.053	1.00

Table 6 Coefficient list of the significant terms for response R2

Factor	Coefficient	df	Standard	95% CI	95% CI	VIF
Intercept	25.91	1	0.15	25.59	26.22	
A: Windage	-2.67	1	0.15	-2.99	-2.35	1.05
E: Wind	0.061	1	0.15	-0.26	0.38	1.02
F: Diffusion	0.16	1	0.15	-0.16	0.48	1.02
EF	-0.46	1	0.15	-0.78	-0.14	1.04
Center Point	0.094	1	0.72	-1.42	1.61	1.00

Table 7 Coefficient list of the significant terms for response R3

Factor	Coefficient	df	Standard	95% CI	95% CI	VIF
Intercept	4.004E-003	1	1.546E-004	3.670E-	4.338E-	
A: Windage	-7.420E-004	1	1.590E-004	-1.085E-	-3.986E-	1.09
B: Along	2.437E-004	1	1.582E-004	-9.804E-	5.855E-	1.08
D: Wind speed	-3.069E-004	1	1.563E-004	-6.446E-	3.076E-	1.06
E: Wind	1.417E-003	1	1.590E-004	1.073E-	1.760E-	1.09
F: Diffusion	-2.340E-005	1	1.582E-004	-3.651E-	3.184E-	1.08
AD	5.187E-004	1	1.613E-004	1.703E-	8.671E-	1.11
BF	4.289E-004	1	1.625E-004	7.798E-	7.799E-	1.13
DE	-4.893E-004	1	1.613E-004	-8.377E-	-1.409E-	1.11
Center Point	4.337E-004	1	7.301E-004	-1.144E-	2.011E-	1.00

Table 5 shows the estimated coefficient for each significant factor, which came from the regression analysis. The positive coefficient means the factor has the positive effects on the response. In this case, the positive effect indicated when the value of that particular factor was increasing, the R1 value would be higher, which meant to obtain better model performance. As it was shown in Table 5, the main factor (B) “Along current uncertainty” (7.466E-003), (E) “Wind direction scale” (0.037), interaction (AD) of “Windage” and “Wind speed scale” (0.014), and interaction (BF) of “Along current uncertainty” and “Diffusion coefficient” (0.012) have positive effects to the R1. On the other hand, the main factor (A) “Windage” (-0.030), (D) “Wind speed scale” (-0.010), (F) “Diffusion coefficient” (-0.930E-004) and interaction (DE) of “Wind speed” and “Wind direction” (-0.014) showed the negative effects to R1. Therefore, according to these coefficients, the (E) “Wind direction scale” (0.037) had the greatest positive impact on the final response and the (A) “Windage” (-0.030) had greatest negative effect. This means when considering coverage as response, among the parameters, the windage and wind direction affect the simulation modeling at the largest scale. And low value of windage and high value of wind direction scale can improve the performance of simulation in this case study.

It is interesting to note that the main factors (A) “Windage” and (D) “Wind speed scale” both had negative effects on R1, but the interaction (AD) showed a positive effect. The main factor (B) “Along current uncertainty” had a positive effect and (F) “Diffusion coefficient” (-0.930E-004) had a negative effect, but the interaction (BF) had a positive effect, which means (B) “Along current uncertainty” showed a more positive effect than we thought.

The interaction between “Windage” and “Wind speed scale”, (AD), showed a significant effect in the simulation. When considering the wind drift in oil spill simulation, 3% of wind speed was always added to the oil slick movement according to the manuals and literatures. In some other studies, 1-4% of windage was considered as a proper range. The interaction between “Along Current” and “Diffusion”, (BF), showed a negative effect. Compared with the current fields from the HYCOM model, the currents moved mainly from the south to north direction around the spill area. The interaction between “Along Current” and “Diffusion” explained how the oil slicks were diffused with the movement of ocean currents. However, the interaction of “Wind Speed” and “Wind Direction” showed that the wind fields had more significant effect on the movement of oil slick than the current fields. The case study also indicated that the choice of parameters and their values during calibration was critical since they could affect the simulation result significantly. This also disclosed the value of the proposed method.

Just adjusting the main factor to optimize the response might not be the most efficient way in some cases. Interactions between factors might lead to an opposite way, and cause missing the desired response. Therefore, to efficiently obtain the optimal response, the sensitivity of a factor should be evaluated by taking the collective effects of that both the factors and the interactions into account.

In the validation and prediction of maximum responses R1 and R3, the same set of parameters was chosen for GNOME model. And the results showed that R1 and R3 for the new settings were both close to the predicted values. But R2 showed the result which was

not good enough. We noticed that the windage played a major role in all the three responses and the interaction of wind speed and direction was also showed effect when the distance was considered as response. Windage, which was one of the most important factors in oil spreading and advection, showed a significant effect in the numerical oil trajectory modelling. Ideally, when the simulated result had the best overlap with the observed oil coverage, the distance was supposed to be the shortest. But in the calibration, optimal parameters were selected in the presence of trade-offs, so the optimal solutions could not be achieved for responses R1 and R2 at the same time. As indicated by the results, the DOE predicted responses well fitted the results with the optimized parameters in the simulation model. Meanwhile, complicated interactions between the parameters in the oil trajectory model were found.

4.5 Summary

This chapter presented a study for gaining a better understanding of the oil spill simulation and particularly the impacts of uncertainties in parameters, and a new DOE aided parameterization method for improving simulation performance. The DOE method was combined into the GNOME model for the parameters calibration, sensitivity analysis, and their interaction analysis in the oil spill model. A set of responses was also proposed for facilitating the calibration process. A real case study based on the Terra Nova 2004 oil spill was carried out for testing and demonstration.

It was found that the DOE aided parameterization method could efficiently identify the key parameters and their interactions for the oil spill simulation models. After developing and optimizing the regression equations predicted by DOE, the results showed that obtained responses closely matched with those achieved from simulations of the numerical models. The impacts of individual parameters on the model and the interactions between parameters were further discussed.

Due to the incapability of revealing the interactions between parameters, traditional OFAT method could ignore the potentially significant variables and their interactive impacts. The proposed method which could analyze the interactions between parameters and the corresponding responses showed the high value and was strongly recommended for the oil spill simulation.

More parameters, such as temperature, salinity, tides and application of dispersants, can be considered in the future oil spill modeling studies. The application of the proposed method could also be potentially extended to different fate and transport models, in which parameter uncertainties and interactions need to be quantified in an efficient way.

During the spill events happened away from the coastlines and under harsh environmental conditions, more dynamic and effective decision making schemes considering limited access time, equipment and man power are much desired. With the application of oil spill models, parameters need to be calibrated with historical weather data. This could cost the precious recovery time, and affect the accuracy of oil slick movement prediction. In order

to shorten the process of preparation and calibration, the choosing of proper simulation models and best set of modeling parameters are critical. This study could be of great value for oil spill events in the Grand Banks in terms of improving the simulation and prediction, and for the researchers and responders in dealing with more efficient spill response in the future.

CHAPTER 5: CONCLUSION AND RECOMMENDATIONS

5.1 Summary

In the past decades, marine oil spills have led to a growing concern about the increasing contamination of oceans and shoreline areas. The petroleum industry worldwide maintained a rapid growth due to the continuous exploration of new offshore oil and gas fields and technological advancement in drilling and production even in deep waters. The close association between oil industry development and economic needs has resulted in the increase of offshore petroleum and maritime transit activities, which have increased environmental risks posed by potential oil-related accidents. Oil spill modeling for response management has been well recognized as a powerful and necessary means. Therefore, the development and improvement of spill modeling capability for supporting better response decision making are in great demand.

To understand and quantify the physical and chemical processes when oil spills occur in harsh marine environments, many studies have been conducted. The presence of low temperature, high wave, and strong wind present key challenges for oil spill observation and simulation. The oceanic and atmospheric physical variables and chemical and physical processes can affect the oil fate and transport significantly.

In the last three decades, the transport and fate processes of oil spills have been well studied, and various oil spill models have been developed. No matter where the spill occurs, the spill model can be used for the prediction of where the oil is most likely to become and go, based on information of ocean currents, winds, and other environmental variables.

However, the success of the application depends not only on the weathering and spreading formulations in the model, and also on the preparation of input data from the numerical models or observation data, and the handling of key parameters and their values. Due to the unavoidable errors or inaccuracy in the input data such as wind, wave and currents information, parameter uncertainties should be considered more carefully. Therefore, parameter calibration, and uncertainty and sensitivity analysis are critical to minimize the discrepancy between simulated and observed data and improve modeling performance and reliability.

In this research, two widely used oil spill modeling systems, GNOME/ADIOS2 and OSCAR, were first compared and evaluated. An oil spill event from the Terra Nova FPSO in the Grand Banks in November 2004 was used as a case study. The ocean current fields from HYCOM and wind data from NCDC were used to support the modeling efforts. The comparison indicated the better results of oil slick transport simulation by GNOME than that of OSCAR. On the other hand, more accurate weathering simulation results derived from the OSCAR than that of GNOME/ADIOS2. In the harsh environment conditions, it was clear that the wind field played a more important role in driving the movement of the spilled oil. Consequently, in this case, GNOME/ADIOS2 showed a better overall performance than OSCAR.

A DOE aided parameterization method was developed and combined into the GNOME model for the parameters calibration, sensitivity/uncertainty analysis, and their interaction analysis in the oil spill modeling process. The results of this method and validation process showed a good agreement with the observation by using the Terra Nova spill as case study.

The DOE method was proved as a feasible and effective calibration tool for the oil spill models. With the DOE method, better understanding of the impacts of modeling parameters and their interactions, and improved performance of spill simulation were obtained by using the proposed method.

In this study, DOE aided method had been proven with the capability of identifying key parameters and their interactions for oil spill simulation models efficiently. With the development and optimization of regression equations predicted by DOE, responses values which matched well with those achieved from numerical modeling simulation could be obtained. With the introduction of the DOE aided approach, analyzing uncertainties associated with the modeling parameters during offshore oil spill simulation was fulfilled. The interactions between wind speed and direction, and the currents analyzed and the effects of their interactions were studied. The interactions between parameters, more parameters, like temperature, salinity, tides and the application of dispersants could be further studied with field trials and field experimental measurements in the future. The proposed DOE aided parameterization method could also be potentially extended to different oil spill models.

In order to shorten the process of preparation and calibration processes in real oil spill case happened in certain areas, the choosing of models and modeling parameters are critical. This study could be valuable for oil spills happened in the Grand Banks area with the improvement of the simulation and prediction processes for the researchers and decision makers in dealing with spill response.

5.2 Research contributions

This research has led to following major contributions:

- 1) The oil spill fate, transport and effect, as well as the modeling methods were reviewed in details leading to the discussion on modeling needs and challenges.
- 2) Two widely recognized modeling systems, GNOME/ADIOS2 and OSCAR, were introduced and compared. Especially through a real spill (Terra Nova spill in 2004) case study.
- 3) Through the comparison, the capabilities of the two modeling systems in simulating oil spills under harsh environmental conditions were evaluated in the first time. Providing valuable information for scientific researchers and practical responders when applying the models in the future.
- 4) A DOE aided parameterization method for analyzing uncertainties associated with modeling parameters during marine oil spill simulation was proposed to minimize the effects of errors in the input data which derived from the observation or meteorological and oceanographic models and the uncertainties in the modeling parameters, resulting in significant improvement of modeling performance.
- 5) The interactions between key parameters such as wind speed and direction, and currents were quantified and their effects on spill simulation were analyzed for better understanding of spill modeling mechanisms and influencing factors.

5.3 Publications

Paper under preparation

1. **Zheng X.**, and Chen B. (2017). Simulation of marine oil spills and models comparison by a case study in the Newfoundland offshore area. *Marine Pollution Bulletin*. (Under preparation)
2. **Zheng X.**, Wu H.J., and Chen B. (2017). Design of Experiment Aided Uncertainty Analysis for Marine Oil Spill Modeling. In: *Proceedings of the 40th AMOP Technical Seminar on Environmental Contamination and Response*, June 6 to 8, 2017, Alberta, Canada. (Under review)
3. **Zheng X.**, Wu H.J., and Chen B. (2017). Marine oil spill simulation and uncertainty analysis- a case study in the Newfoundland offshore area. *Journal of Environmental Engineering*. (Under preparation)

Refereed Journal Publication

1. Li P., Chen B., Li Z.L., **Zheng X.**, Wu H.J., Jing L., and Lee K. (2014). A Monte Carlo simulation based two-stage adaptive resonance theory mapping approach for offshore oil spill vulnerability index classification. *Marine Pollution Bulletin*. 86(2): 434-442.

Other Refereed Publication

1. **Zheng X.**, Chen B. and Wu H.J. (2014). “Interpolation method and uncertainty analysis in oil spilling trajectory model”. *The International Society for Environmental Information Sciences (ISEIS) 2014 Annual Conference*, August 6-8, 2014, St. John’s, Canada.
2. Li P., Chen B., Jing L., Li Z.L. and **Zheng X.** (2013). “A Monte Carlo simulation-based two-stage adaptive resonance theory mapping model for site classification in offshore oil spill and leakage monitoring”, *Posters of 4th Annual Arctic Oil & Gas North America*, April 10-11, St. John’s, Canada.
3. Li P., Chen B., Jing L., Li Z.L. and **Zheng X.** (2014). An integrated simulation-based optimization approach for devices allocation and operation in offshore oil spill response. *Abstract for oral presentation in the 5th Annual Arctic Oil & Gas North America Conference*, March 25-27th, St. John’s, Canada.
4. Li P., **Zheng X.**, Chen B. and Zhang B.Y. (2015). A new simulation-optimization coupling approach for offshore oil spill responses. *Oral presentation in the 38th AMOP Technical Seminar on Environmental Contamination and Response*, June 2-4, Vancouver, Canada.
5. Chen B., Li Z.L., Ma Y.C. and **Zheng X.** (2013). “Carbon capture and storage: policies and technologies”, Technical report, prepared for the Green Development Programme, United Nations Development Programme (UNDP), August 31, 237 pages.

5.4 Recommendations

1. Three widely used marine oil spill models, namely GNOME, ADIOS2 and OSCAR, have been applied in the Terra Nova case to compare and evaluate their capabilities under the harsh marine environment. As we notice that different equations of spreading were applied in the GNOME and OSCAR, which might lead to the shifts in the simulation results. The effects of the different equations will be further studied in the future work.
2. A DOE aided parameterization method has been developed for analyzing uncertainties associated with the input and modeling parameters during offshore oil spill simulation. DOE method has been approved to be a useful tool in the uncertainty analysis and calibration in oil spill models. More oil spill models and real cases need to be applied to evaluate the capabilities of the proposed method.
3. Six parameters have been considered to be important in the calibration method. More parameters, such as temperature, salinity, tides and the application dispersants can be considered in the future's work with the proposed method.
4. More complicated oil spill cases, such as the ones with ice covered, with response process like booming and skimming, can be considered in the future work to improve the applicability and commonality of the proposed method.

References

- AAMO, O. M., REED, M. & DOWNING, K. (1997a). Oil spill contingency and response (OSCAR) model system: sensitivity studies. *International Oil spill conference*. American Petroleum Institute, 429-438.
- AAMO, O. M., REED, M. & LEWIS, A. (1997b). Regional contingency planning using the OSCAR oil spill contingency and response model. *ARCTIC AND MARINE OILSPILL PROGRAM TECHNICAL SEMINAR*. MINISTRY OF SUPPLY AND SERVICES, CANADA, 289-308.
- ABASCAL, A. J., CASTANEDO, S., MENDEZ, F. J., MEDINA, R. & LOSADA, I. J. (2009). Calibration of a Lagrangian transport model using drifting buoys deployed during the Prestige oil spill. *Journal of Coastal Research*, 80-90.
- AL-RABEH, A., LARDNER, R. & GUNAY, N. (2000). Gulfspill Version 2.0: a software package for oil spills in the Arabian Gulf. *Environmental Modelling & Software*, 15, 425-442.
- ALPERS, W. & ESPEDAL, H. A. (2004). Oils and surfactants. *Synthetic aperture radar marine user's manual*, 263-275.
- AMBJÖRN, C. (2006). Seatrack Web, forecasts of oil spills, a new version. *Institute of Electrical and Electronics Engineers US/EU Baltic International Symposium*. IEEE, 1-7.

- ASCE (1996). State-of-the-art review of modeling transport and fate of oil spills. ASCE Committee on Modeling Oil Spills, Water Resources Engineering Division. *Journal of Hydraulic Engineering*, 122, 594-609.
- AZWELL, T., BLUM, M. J., HARE, A., JOYE, S., KUBENDRAN, S., LALEIAN, A., LANE, G., MEFFERT, D., OVERTON, E. & THOMAS III, J. (2011). The Macondo blowout environmental report. *Deepwater Horizon Study Group Environmental Report*.
- BASAR, E., KOSE, E. & GUNEROGLU, A. (2006). Finding risky areas for oil spillage after tanker accidents at Istanbul strait. *International journal of environment and pollution*, 27, 388-400.
- BEEGLE-KRAUSE, C., BARKER, C., WATABAYASHI, G., LEHR, W. & BEEGLE, C. (2006). Long-term transport of oil from T/B DBL-152: Lessons learned for oils heavier than seawater. *Proceedings of the AMOP 2006*, 6-8.
- BEEGLE-KRAUSE, C. & O'CONNOR, C. (2005). GNOME data formats and associated example data files. *Seattle: NOAA Office of Response and Restoration, Hazardous Materials Response Division. Seattle, Washington*.
- BEEGLE-KRAUSE, J. (2001). General NOAA oil modeling environment (GNOME): a new spill trajectory model. International Oil Spill Conference. American Petroleum Institute, 865-871.
- BERGUEIRO, J., MARCH, R. R., GONZÁLEZ, S. G. & SOCÍAS, F. S. (2007). Simulation of oil spills at the Casablanca platform (Tarragona, Spain) under different environmental conditions. *Journal of Maritime Research*, 3, 55-71.

- BERRY, A., DABROWSKI, T. & LYONS, K. (2012). The oil spill model OILTRANS and its application to the Celtic Sea. *Marine pollution bulletin*, 64, 2489-2501.
- BLOKKER, P. (1964). *Spreading and evaporation of petroleum products on water*, publisher not identified.
- BLY, M. (2011). *Deepwater horizon accident investigation report*, Diane Publishing.
- BOARD, O. S. & BOARD, M. (2003). *Oil in the sea III: inputs, fates, and effects*, national academies Press.
- BOUFADEL, M. C., ABDOLLAHI-NASAB, A., GENG, X., GALT, J. & TORLAPATI, J. (2014). Simulation of the Landfall of the Deepwater Horizon Oil on the Shorelines of the Gulf of Mexico. *Environmental science & technology*, 48, 9496-9505.
- BRANDVIK, P. J., SØRHEIM, K., SINGSAAS, I. & REED, M. (2006). Short state-of-the-art report on oil spills in ice-infested waters. *JIP report*.
- BREKKE, C. & SOLBERG, A. H. (2005). Oil spill detection by satellite remote sensing. *Remote sensing of environment*, 95, 1-13.
- CARRACEDO, P., TORRES-LÓPEZ, S., BARREIRO, M., MONTERO, P., BALSEIRO, C., PENABAD, E., LEITAO, P. & PÉREZ-MUÑUZURI, V. (2006). Improvement of pollutant drift forecast system applied to the Prestige oil spills in Galicia Coast (NW of Spain): Development of an operational system. *Marine Pollution Bulletin*, 53, 350-360.
- CHAO, X., SHANKAR, N. J. & WANG, S. S. (2003). Development and application of oil spill model for Singapore coastal waters. *Journal of hydraulic engineering*, 129, 495-503.

- CHASSIGNET, E. P., HURLBURT, H. E., SMEDSTAD, O. M., HALLIWELL, G. R., HOGAN, P. J., WALLCRAFT, A. J. & BLECK, R. (2006). Ocean prediction with the hybrid coordinate ocean model (HYCOM). *Ocean weather forecasting*. Springer.
- CHENG, Y., LI, X., XU, Q., GARCIA-PINEDA, O., ANDERSEN, O. B. & PICHEL, W. G. (2011). SAR observation and model tracking of an oil spill event in coastal waters. *Marine pollution bulletin*, 62, 350-363.
- COPPINI, G., DE DOMINICIS, M., ZODIATIS, G., LARDNER, R., PINARDI, N., SANTOLERI, R., COLELLA, S., BIGNAMI, F., HAYES, D. R. & SOLOVIEV, D. (2011). Hindcast of oil-spill pollution during the Lebanon crisis in the Eastern Mediterranean, July–August 2006. *Marine pollution bulletin*, 62, 140-153.
- COUNCIL, N. R. (2003). Oil in the sea III: inputs, fates, and effects.
- CSANADY, G. T. (2012). *Turbulent diffusion in the environment*, Springer Science & Business Media.
- CUCCO, A., SINERCHIA, M., RIBOTTI, A., OLITA, A., FAZIOLI, L., PERILLI, A., SORGENTE, B., BORGHINI, M., SCHROEDER, K. & SORGENTE, R. (2012). A high-resolution real-time forecasting system for predicting the fate of oil spills in the Strait of Bonifacio (western Mediterranean Sea). *Marine pollution bulletin*, 64, 1186-1200.
- CZITROM, V. (1999). One-factor-at-a-time versus designed experiments. *The American Statistician*, 53, 126-131.

- DALING, P. S., MOLDESTAD, M. Ø., JOHANSEN, Ø., LEWIS, A. & RØDAL, J. (2003). Norwegian testing of emulsion properties at sea—the importance of oil type and release conditions. *Spill Science & Technology Bulletin*, 8, 123-136.
- DALING, P. S. & STRØM, T. (1999). Weathering of oils at sea: model/field data comparisons. *Spill Science & Technology Bulletin*, 5, 63-74.
- DE DOMINICIS, M., PINARDI, N., ZODIATIS, G. & LARDNER, R. 2013. Medslik-II, a Lagrangian marine surface oil spill model for short-term forecasting—Part 1: Theory. *Geosci. Model Dev*, 6, 1851-1869.
- DELVIGNE, G. A. (1989). A sampler for the collection of dispersed oil droplets. International Oil Spill Conference. American Petroleum Institute, 567-568.
- DI PIETRO, N. & COX, R. (1979). The spreading of a very viscous liquid on a quiescent water surface. *The Quarterly Journal of Mechanics and Applied Mathematics*, 32, 355-381.
- DIETRICH, J., TRAHAN, C., HOWARD, M., FLEMING, J., WEAVER, R., TANAKA, S., YU, L., LUETTICH, R. A., DAWSON, C. & WESTERINK, J. (2012). Surface trajectories of oil transport along the northern coastline of the Gulf of Mexico. *Continental Shelf Research*, 41, 17-47.
- DROZDOWSKI, A., NUDDS, S., HANNAH, C., NIU, H., PETERSON, I. & PERRIE, W. (2011). Canadian Technical Report of Hydrographic and Ocean Sciences 274.
- DUAN, Q., SOROOSHIAN, S. & GUPTA, V. (1992). Effective and efficient global optimization for conceptual rainfall-runoff models. *Water resources research*, 28, 1015-1031.

- EDWARDS, K., WERNER, F. & BLANTON, B. (2006). Comparison of observed and modeled drifter trajectories in coastal regions: an improvement through adjustments for observed drifter slip and errors in wind fields. *Journal of Atmospheric and Oceanic Technology*, 23, 1614-1620.
- EL-TAHAN, M. & WARBANSKI, G. (1987). Prediction of short-term ice edge drift. Proc. Sixth Int. Offshore Mechanics and Arctic Engineering Symp. 1-6.
- ETKIN, D. S. (2001). Analysis of oil spill trends in the United States and worldwide. International Oil Spill Conference. American Petroleum Institute, 1291-1300.
- ETKIN, D. S. & WELCH, J. (1997). OIL SPILL INTELLIGENCE REPORT INTERNATIONAL OIL SPILL DATABASE: TRENDS IN OIL SPILL VOLUMES AND FREQUENCY¹. International Oil Spill Conference. American Petroleum Institute, 949-951.
- FANNELOP, T. K. & WALDMAN, G. D. (1972). Dynamics of oil slicks. *AIAA Journal*, 10, 506-510.
- FARZINGOHAR, M., Z IBRAHIM, Z. & YASEMI, M. (2011). Oil spill modeling of diesel and gasoline with GNOME around Rajae Port of Bandar Abbas, Iran. 10, 35-46.
- FAY, J. A. (1969). The spread of oil slicks on a calm sea. *Oil on the Sea*. Springer.
- FAY, J. A. (1971). Physical processes in the spread of oil on a water surface. International Oil Spill Conference. American Petroleum Institute, 463-467.
- FERRARO, G., MEYER-ROUX, S., MUELLENHOFF, O., PAVLIHA, M., SVETAK, J., TARCHI, D. & TOPOUZELIS, K. (2009). Long term monitoring of oil spills in European seas. *International Journal of Remote Sensing*, 30, 627-645.

- FINGAS, M. (2009). A new generation of models for water-in-oil emulsion formation.
- FINGAS, M. (2010). *Oil spill science and technology*, Gulf professional publishing.
- FINGAS, M., HOLLEBONE, B. & FIELDHOUSE, B. (2006). The density behaviour of heavy oils in freshwater: The example of the Lake Wabamun spill. *Emergencies Science and Technology Division, Environment Canada*.
- GALT, J. (1997). Uncertainty analysis related to oil spill modeling. *Spill Science & Technology Bulletin*, 4, 231-238.
- GALT, J., WATABAYASHI, G., PAYTON, D. & PETERSEN, J. (1991). Trajectory analysis for the Exxon Valdez: Hindcast study. International Oil Spill Conference. American Petroleum Institute, 629-634.
- GOEURY, C., HERVOUET, J.-M., BAUDIN-BIZIEN, I. & THOUVENEL, F. (2014). A Lagrangian/Eulerian oil spill model for continental waters. *Journal of hydraulic Research*, 52, 36-48.
- GRABER, H. C., DIXON, T. H. & EVANS, R. H. (2006). Center for Southeastern Tropical Advanced Remote Sensing (CSTARS). DTIC Document.
- GRUENDLING, T., GUILHAUS, M. & BARNER-KOWOLLIK, C. (2009). Design of Experiment (DoE) as a Tool for the Optimization of Source Conditions in SEC-ESI-MS of Functional Synthetic Polymers Synthesized via ATRP. *Macromolecular rapid communications*, 30, 589-597.
- HACKETT, B., BREIVIK, Ø. & WETTRE, C. (2006). Forecasting the drift of objects and substances in the ocean. *Ocean weather forecasting*. Springer.
- HACKETT, B., COMERMA, E., DANIEL, P. & ICHIKAWA, H. (2009). Marine pollution monitoring and prediction. *Oceanography*, 22, 168-175.

- HALLIWELL, G. R. (2004). Evaluation of vertical coordinate and vertical mixing algorithms in the HYbrid-Coordinate Ocean Model (HYCOM). *Ocean Modelling*, 7, 285-322.
- HEYDARIHA, J. Z. & GHIASSI, R. (2010). Oil Spill Simulation in Mouth of Persian Gulf. *Adv. Waste Manage*, 56-60.
- HOLVOET, K., VAN GRIENSVEN, A., SEUNTJENS, P. & VANROLLEGHEM, P. (2005). Sensitivity analysis for hydrology and pesticide supply towards the river in SWAT. *Physics and Chemistry of the Earth, Parts A/B/C*, 30, 518-526.
- HOULT, D. P. (1972). Oil spreading on the sea. *Annual Review of Fluid Mechanics*, 4, 341-368.
- HOWLETT, E. & JAYKO, K. (1998). COZOIL (Coastal Zone Oil Spill Model), Model Improvements and Linkage to a Graphical User Interface. Twenty-first Arctic and Marine Oilspill Program (AMOP) Technical Seminar. 19.
- HOWLETT, E., JAYKO, K. & SPAULDING, M. (1993). Interfacing real-time information with OILMAP.
- HU, C., LI, X., PICHEL, W. G. & MULLER-KARGER, F. E. (2009). Detection of natural oil slicks in the NW Gulf of Mexico using MODIS imagery. *Geophysical Research Letters*, 36.
- HUANG, J. C. (1983). A review of the state-of-the-art of oil spill fate/behavior models. International Oil Spill Conference. American Petroleum Institute, 313-322.
- HUNG, H., KALLENBORN, R., BREIVIK, K., SU, Y., BRORSTRÖM-LUNDÉN, E., OLAFSDOTTIR, K., THORLACIUS, J. M., LEPPÄNEN, S., BOSSI, R. & SKOV, H. (2010). Atmospheric monitoring of organic pollutants in the Arctic under the

- Arctic Monitoring and Assessment Programme (AMAP): 1993–2006. *Science of the Total Environment*, 408, 2854-2873.
- JHA, M. N., LEVY, J. & GAO, Y. (2008). Advances in remote sensing for oil spill disaster management: state-of-the-art sensors technology for oil spill surveillance. *Sensors*, 8, 236-255.
- JING, L. & CHEN, B. (2011). Field investigation and hydrological modelling of a subarctic wetland-the Deer River watershed. *Journal of Environmental Informatics*, 17, 36-45.
- JING, L., CHEN, B., ZHANG, B. & PENG, H. (2012). A review of ballast water management practices and challenges in harsh and arctic environments. *Environmental Reviews*, 20, 83-108.
- KARIMI, P., ABDOLLAHI, H., ASLAN, N., NOAPARAST, M. & SHAFAEI, S. (2010). Application of response surface method and central composite design for modeling and optimization of gold and silver recovery in cyanidation process. *Mineral Processing & Extractive Metallurgy Review*, 32, 1-16.
- KHELIFA, A. (2010). A summary review of modelling oil in ice.
- KIM, T.-H., YANG, C.-S., OH, J.-H. & OUCHI, K. (2014). Analysis of the contribution of wind drift factor to oil slick movement under strong tidal condition: Hebei spirit oil spill case. *PloS one*, 9, e87393.
- KLEMAS, V. (2010). Tracking oil slicks and predicting their trajectories using remote sensors and models: case studies of the Sea Princess and Deepwater Horizon oil spills. *Journal of Coastal Research*, 789-797.

- KOTOVA, L. & ESPEDAL, H. (1998). Oil spill detection using spaceborne SAR- A brief review. *Information for sustainability*, 791-794.
- KVENVOLDEN, K. & COOPER, C. (2003). Natural seepage of crude oil into the marine environment. *Geo-Marine Letters*, 23, 140-146.
- LARDNER, R., ZODIATIS, G., LOIZIDES, L. & DEMETROPOULOS, A. (1998). An operational oil spill model in the Levantine Basin (Eastern Mediterranean Sea). *Int. Symp. Mar. Pollut.* 5-9.
- LARGE, W. G. & YEAGER, S. G. (2004). *Diurnal to decadal global forcing for ocean and sea-ice models: the data sets and flux climatologies*, National Center for Atmospheric Research Boulder.
- LEHR, W., CEKIRGE, H., FRAGA, R. & BELEN, M. (1984). Empirical studies of the spreading of oil spills. *Oil and Petrochemical Pollution*, 2, 7-11.
- LEHR, W., JONES, R., EVANS, M., SIMECEK-BEATTY, D. & OVERSTREET, R. (2002). Revisions of the ADIOS oil spill model. *Environmental Modelling & Software*, 17, 189-197.
- LEHR, W. J. & SIMECEK-BEATTY, D. (2000). The relation of Langmuir circulation processes to the standard oil spill spreading, dispersion, and transport algorithms. *Spill Science & Technology Bulletin*, 6, 247-253.
- LEIFER, I., LEHR, W. J., SIMECEK-BEATTY, D., BRADLEY, E., CLARK, R., DENNISON, P., HU, Y., MATHESON, S., JONES, C. E. & HOLT, B. (2012). State of the art satellite and airborne marine oil spill remote sensing: Application to the BP Deepwater Horizon oil spill. *Remote Sensing of Environment*, 124, 185-209.

- LENHART, T., ECKHARDT, K., FOHRER, N. & FREDE, H.-G. (2002). Comparison of two different approaches of sensitivity analysis. *Physics and Chemistry of the Earth, Parts A/B/C*, 27, 645-654.
- LI, P., CHEN, B., LI, Z., ZHENG, X., WU, H., JING, L. & LEE, K. (2014a). A Monte Carlo simulation based two-stage adaptive resonance theory mapping approach for offshore oil spill vulnerability index classification. *Marine pollution bulletin*, 86, 434-442.
- LI, P., CHEN, B., ZHANG, B., JING, L. & ZHENG, J. (2014b). Monte Carlo simulation-based dynamic mixed integer nonlinear programming for supporting oil recovery and devices allocation during offshore oil spill responses. *Ocean & Coastal Management*, 89, 58-70.
- LI, X., LI, C., YANG, Z. & PICHEL, W. (2013). SAR imaging of ocean surface oil seep trajectories induced by near inertial oscillation. *Remote Sensing of Environment*, 130, 182-187.
- LIU, T. & SHENG, Y. P. (2014). Three dimensional simulation of transport and fate of oil spill under wave induced circulation. *Marine pollution bulletin*, 80, 148-159.
- LIU, Y., WEISBERG, R. H., HU, C. & ZHENG, L. (2011). Tracking the Deepwater Horizon oil spill: A modeling perspective. *Eos Trans. AGU*, 92.
- LONIN, S. A. (1999). Lagrangian model for oil spill diffusion at sea. *Spill Science & Technology Bulletin*, 5, 331-336.
- LOUGHLIN, T. R. (2013). *Marine mammals and the Exxon Valdez*, Academic Press.

- MACKAY, D., PATERSON, S. & NADEAU, S. (1908). Calculation of the evaporation rate of volatile liquids. Proc. 1980 National Conf. on Control of Hazardous Material Spills, Louisville, Ky.
- MARTA-ALMEIDA, M., RUIZ-VILLARREAL, M., PEREIRA, J., OTERO, P., CIRANO, M., ZHANG, X. & HETLAND, R. D. (2013). Efficient tools for marine operational forecast and oil spill tracking. *Marine pollution bulletin*, 71, 139-151.
- MASLO, A., PANJAN, J. & ŽAGAR, D. (2014). Large-scale oil spill simulation using the lattice Boltzmann method, validation on the Lebanon oil spill case. *Marine pollution bulletin*, 84, 225-235.
- MCGRATH, C. G. G. (2014). Preventing a Nationally-Significant Oil Spill on the Grand Banks of Newfoundland. International Oil Spill Conference Proceedings. American Petroleum Institute, 1226-1238.
- MCNUTT, M., CAMILLI, R., GUTHRIE, G., HSIEH, P. & LABSON, V. (2011). Assessment of flow rate estimates for the Deepwater Horizon/Macondo well oil spill. Flow rate technical group report to the national incident command, interagency solutions group, March 10.
- MIGLIACCIO, M., GAMBARDELLA, A. & TRANFAGLIA, M. (2007). SAR polarimetry to observe oil spills. *IEEE Transactions on Geoscience and Remote Sensing*, 45, 506-511.
- MIGLIACCIO, M., NUNZIATA, F., BROWN, C., HOLT, B., LI, X., PICHEL, W. & SHIMADA, M. (2012). Polarimetric synthetic aperture radar for transoceanic Deepwater Horizon oil accident monitoring. *Eos*, 16, 161-168.
- MONTGOMERY, D. C. (2008). *Design and analysis of experiments*, John Wiley & Sons.

- NIRCHIO, F., SORGENTE, M., GIANCASPRO, A., BIAMINO, W., PARISATO, E., RAVERA, R. & TRIVERO, P. (2005). Automatic detection of oil spills from SAR images. *International Journal of Remote Sensing*, 26, 1157-1174.
- NIU, H., YANG, R., WU, Y. & LEE, K. (2014). Modelling the Effects of Chemical Dispersant on the Fate of Spilled Oil: Case Study of a Hypothetical Spill near Saint John, NB. The International Conference on Marine and Freshwater Environments (iMFE 2014).
- ØKLAND GJØSTEEN, J., LØSET, S. & GUDMESTAD, O. (2003). The ability to model oil spills in broken ice. Proceedings of the International Conference on Port and Ocean Engineering Under Arctic Conditions.
- PAPADIMITRAKIS, J., PSALTAKI, M., CHRISTOLIS, M. & MARKATOS, N. (2006). Simulating the fate of an oil spill near coastal zones: The case of a spill (from a power plant) at the Greek Island of Lesbos. *Environmental Modelling & Software*, 21, 170-177.
- PARK, G.-J. (2007). Design of experiments. *Analytic Methods for Design Practice*, 309-391.
- PEETERS, L., PODGER, G., SMITH, T., PICKETT, T., BARK, R. & CUDDY, S. (2014). Robust global sensitivity analysis of a river management model to assess nonlinear and interaction effects. *Hydrology and Earth System Sciences*, 18, 3777-3785.
- PETERSON, I., PRINSENBURG, S. & HOLLADAY, J. (2008). Observations of sea ice thickness, surface roughness and ice motion in Amundsen Gulf. *Journal of Geophysical Research: Oceans*, 113.

- PIATT, J. F., LENSINK, C. J., BUTLER, W., KENDZIOREK, M. & NYSEWANDER, D. R. (1990). Immediate impact of the Exxon Valdez oil spill on marine birds. *The Auk*, 387-397.
- PRICE, J. M., JI, Z.-G., REED, M., MARSHALL, C., HOWARD, M., GUINASSO, N., JOHNSON, W. & RAINEY, G. B. (2003). Evaluation of an oil spill trajectory model using satellite-tracked, oil-spill-simulating drifters. OCEANS 2003. Proceedings. IEEE, 1303-1311.
- PRICE, J. M., REED, M., HOWARD, M. K., JOHNSON, W. R., JI, Z.-G., MARSHALL, C. F., GUINASSO, N. L. & RAINEY, G. B. (2006). Preliminary assessment of an oil-spill trajectory model using satellite-tracked, oil-spill-simulating drifters. *Environmental Modelling & Software*, 21, 258-270.
- RAMSEUR, J. L. Deepwater Horizon oil spill: the fate of the oil. (2010). Congressional Research Service, Library of Congress Washington, DC.
- REED, M., AAMO, O. & DALING, P. (1995a). Oscar, A Model System for Quantitative Analysis of Alternative Oil Spill Response Strategies. ARCTIC AND MARINE OILSPILL PROGRAM TECHNICAL SEMINAR. MINISTRY OF SUPPLY AND SERVICES, CANADA, 815-836.
- REED, M., AAMO, O. & DOWNING, K. (1996). Calibration and testing of IKU's oil spill contingency and response (OSCAR) model system.
- REED, M., AAMO, O. M. & DALING, P. S. (1995b). Quantitative analysis of alternate oil spill response strategies using OSCAR. *Spill Science & Technology Bulletin*, 2, 67-74.

- REED, M., DALING, P., LEWIS, A., DITLEVSEN, M. K., BRØRS, B., CLARK, J. & AURAND, D. (2004). Modelling of dispersant application to oil spills in shallow coastal waters. *Environmental Modelling & Software*, 19, 681-690.
- REED, M., DALING, P. S., BRAKSTAD, O. G., SINGSAAS, I., FAKSNESS, L.-G., HETLAND, B. & EKROL, N. (2000). OSCAR2000: a multi-component 3-dimensional oil spill contingency and response model.
- REED, M., GUNDLACH, E. & KANA, T. (1989). A coastal zone oil spill model: development and sensitivity studies. *Oil and Chemical Pollution*, 5, 411-449.
- REED, M., JOHANSEN, Ø., BRANDVIK, P. J., DALING, P., LEWIS, A., FIOCCO, R., MACKAY, D. & PRENTKI, R. (1999). Oil spill modeling towards the close of the 20th century: overview of the state of the art. *Spill Science & Technology Bulletin*, 5, 3-16.
- RUIZ, C. F. (2013). *Parasite component community of Gulf killifish, Fundulus grandis, in an oiled Louisiana saltmarsh*. Auburn University.
- SALTELLI, A. (1999). Sensitivity analysis: Could better methods be used? *Journal of Geophysical Research: Atmospheres (1984–2012)*, 104, 3789-3793.
- SAMUELS, W. B., AMSTUTZ, D. E., BAHADUR, R. & ZIEMNIAK, C. (2013). Development of a global oil spill modeling system. *Earth Science Research*, 2, 52.
- SAMUELS, W. B., HUANG, N. E. & AMSTUTZ, D. E. (1982). An oilspill trajectory analysis model with a variable wind deflection angle. *Ocean Engineering*, 9, 347-360.

- SARIKAYA, M. & GÜLLÜ, A. (2015). The Analysis of Process Parameters for Turning Cobalt-Based Super Alloy Haynes 25/L 605 Using Design of Experiment. Solid State Phenomena. Trans Tech Publ, 749-753.
- SEBASTIAO, P. & SOARES, C. G. (2006). Uncertainty in predictions of oil spill trajectories in a coastal zone. *Journal of Marine Systems*, 63, 257-269.
- SINGHA, S., VESPE, M. & TRIESCHMANN, O. (2013). Automatic Synthetic Aperture Radar based oil spill detection and performance estimation via a semi-automatic operational service benchmark. *Marine pollution bulletin*, 73, 199-209.
- SOLBERG, A. H. S. (2012). Remote sensing of ocean oil-spill pollution. *Proceedings of the IEEE*, 100, 2931-2945.
- SPAULDING, M., WARD, M. & ISAJI, T. (2004). Estimating heavy oil release rates from sunken vessels in deep marine waters.
- SPAULDING, M. L. (1988). A state-of-the-art review of oil spill trajectory and fate modeling. *Oil and Chemical Pollution*, 4, 39-55.
- STIVER, W. & MACKAY, D. (1984). Evaporation rate of spills of hydrocarbons and petroleum mixtures. *Environmental science & technology*, 18, 834-840.
- STOLZENBACH, K. D., MADSEN, O. S., ADAMS, E. E., POLLACK, A. M. & COPPER, C. (1977). Review and evaluation of basic techniques for predicting the behavior of surface oil slicks.
- SUMAILA, U. R., CISNEROS-MONTEMAYOR, A. M., DYCK, A., HUANG, L., CHEUNG, W., JACQUET, J., KLEISNER, K., LAM, V., MCCREA-STRUB, A. & SWARTZ, W. (2012). Impact of the Deepwater Horizon well blowout on the

- economics of US Gulf fisheries. *Canadian Journal of Fisheries and Aquatic Sciences*, 69, 499-510.
- TKALICH, P. (2006). A CFD solution of oil spill problems. *Environmental Modelling & Software*, 21, 271-282.
- TKALICH, P., HUDA, K. & HOONG GIN, K. Y. (2003). A multiphase oil spill model. *Journal of Hydraulic Research*, 41, 115-125.
- TRI, D. Q., DON, N. C. & CHING, C. Y. (2013). Trajectory modeling of marine oil spills: case study of Lach Huyen port, Vietnam. *Lowland technology international: the officisl journal of the International Association of Lowland Technology (IALT)/Institute of Lowland Technology, Saga University*, 15, 41-55.
- TURNER, M., SKINNER, J., ROBERTS, J., HARVEY, R. & ROSS, S. (2010). Review of offshore oil-spill prevention and remediation requirements and practices in Newfoundland and Labrador.
- VELIČKOVIĆ, A. V., STAMENKOVIĆ, O. S., TODOROVIĆ, Z. B. & VELJKOVIĆ, V. B. (2013). Application of the full factorial design to optimization of base-catalyzed sunflower oil ethanolysis. *Fuel*, 104, 433-442.
- VENKATESH, S., EL-TAHAN, H., COMFORT, G. & ABDELNOUR, R. (1990). Modelling the behaviour of oil spills in ice-infested waters. *Atmosphere-Ocean*, 28, 303-329.
- VIOLEAU, D., BUVAT, C., ABED-MERAÏM, K. & DE NANTEUIL, E. (2007). Numerical modelling of boom and oil spill with SPH. *Coastal Engineering*, 54, 895-913.

- VRUGT, J. A., GUPTA, H. V., BOUTEN, W. & SOROOSHIAN, S. (2003). A Shuffled Complex Evolution Metropolis algorithm for optimization and uncertainty assessment of hydrologic model parameters. *Water Resources Research*, 39.
- WANG, J., HU, H., MIZOBATA, K. & JIN, M. (2007). Sea Ice-Ocean-Oilspill Modeling System (SIOMS) for the Nearshore Beaufort and Chukchi Seas: Parameterization and Improvement (Phase II). *Annual Report No. 14*, 1001, 14.
- WEI, L., HU, Z., DONG, L. & ZHAO, W. (2015). A damage assessment model of oil spill accident combining historical data and satellite remote sensing information: A case study in Penglai 19-3 oil spill accident of China. *Marine pollution bulletin*, 91, 258-271.
- WILHELM, S. I., ROBERTSON, G. J., RYAN, P. C. & SCHNEIDER, D. C. (2006). An assessment of the number of seabirds at risk during the November 2004 Terra Nova FPSO oil spill on the Grand Banks. *Canadian Wildlife Service Technical Report Series*.
- WILHELM, S. I., ROBERTSON, G. J., RYAN, P. C. & SCHNEIDER, D. C. (2007). Comparing an estimate of seabirds at risk to a mortality estimate from the November 2004 Terra Nova FPSO oil spill. *Marine pollution bulletin*, 54, 537-544.
- WU, H., LYE, L. M. & CHEN, B. (2012). A design of experiment aided sensitivity analysis and parameterization for hydrological modeling. *Canadian Journal of Civil Engineering*, 39, 460-472.
- XU, Q., LI, X., WEI, Y., TANG, Z., CHENG, Y. & PICHEL, W. G. (2013). Satellite observations and modeling of oil spill trajectories in the Bohai Sea. *Marine pollution bulletin*, 71, 107-116.

- YANG, M., KHAN, F., GARANIYA, V. & CHAI, S. (2015). Multimedia fate modeling of oil spills in ice-infested waters: An exploration of the feasibility of fugacity-based approach. *Process Safety and Environmental Protection*, 93, 206-217.
- YIM, U. H., KIM, M., HA, S. Y., KIM, S. & SHIM, W. J. (2012). Oil spill environmental forensics: the Hebei Spirit oil spill case. *Environmental science & technology*, 46, 6431-6437.
- ZHENG, L., YAPA, P. D. & CHEN, F. (2003). A model for simulating deepwater oil and gas blowouts-Part I: Theory and model formulation. *Journal of Hydraulic Research*, 41, 339-351.